AN IMAGE-GUIDED PLATFORM FOR ON-THE-FLY MANDIBULAR RECONSTRUCTION SURGERY

by

MOLLY MURRAY STEWART

MEng University of Strathclyde, 2017

A THESIS SUBMITTED IN PARTIAL FULFILMENT OF

THE REQUIREMENTS FOR THE DEGREE OF

MASTER OF APPLIED SCIENCE

in

THE FACULTY OF GRADUATE AND POSTDOCTORAL STUDIES

(Biomedical Engineering)

THE UNIVERSITY OF BRITISH COLUMBIA

(Vancouver)

October 2021

The following individuals certify that they have read, and recommend to the Faculty of Graduate and Postdoctoral Studies for acceptance, the thesis entitled:

An Image-guided Platform for On-the-fly Mandibular Reconstruction Surgery

Submitted by Molly Stewart in partial fulfilment of the requirements for the degree of Masters of Applied Science in Biomedical Engineering

Examining Committee:

Antony Hodgson, Mechanical Engineering, UBC
Supervisor

Etian Prisman, Surgery, UBC
Supervisory Committee Member

Sidney Fels, Electrical and Computer Engineering, UBC
Supervisory Committee Member

Roger Tam, Biomedical Engineering, UBC
Supervisory Committee Member

Abstract

Mandible reconstruction surgery requires a surgeon to remove a section of the mandible bone affected by a tumor and recreate the curved contour of the jaw using a donor bone since the mandible is fundamental in helping the patient to eat, talk and breathe. The most common donor bone used is the fibula, and the surgery requires small fibula segments of a specific length and cut angle to be created which are then aligned to one another to form the desired curve. Currently surgeons During this lead time the tumor can grow, and pre-printed guides cannot be changed during surgery to accommodate this.

Our research has addressed these issues through the development of a fully image-guided mandible reconstruction workflow. The scope of this thesis was to develop the software required to integrate image guidance into this procedure, investigate methods to guide the fibula cuts, and perform proof-of-concept testing on the fully-integrated system. A user study on the fibular cutting process highlighted that using an image-guided cutting guide would be the most feasible method for guiding the fibula cuts in a surgical environment. This method was able to replicate the planned fibula cuts with an average deviation of -0.68±2.66 mm in segment length and 3.68±2.59˚in cut angle.

Bench testing of the integrated system's workflow demonstrated that we could successfully perform an on-the-fly simulation of the surgery without requiring any pre-surgical planning as the VSP is generated during the surgery and can be changed as required throughout. Proof-of-concept testing performed on five cadaver specimens further demonstrated successful execution of the workflow in a more realistic surgical setting. These tests resulted in accuracy metrics that are comparable to existing state-of-the-art systems using 3D-printed cutting guides such as an average Dice score of 0.81 and Hausdorff distance of 0.94 mm when compared to the VSP. By utilizing image guidance during all stages of the surgical workflow, including to

guide the fibula cuts, this system demonstrates that an on-the-fly surgical workflow is possible, which, once transferred to the operating room, would eliminate the lead time and inflexibility of the physical cutting guides.

Lay Summary

A surgeon may remove a portion of the lower jawbone to treat certain forms of cancer. The gap is often reconstructed used the smaller lower leg long bone, but this is a complex procedure as it requires creating the curved jawline with a straight bone. Currently, up to four weeks before surgery, a virtual preoperative plan is created, and patient-specific cutting guides are 3D-printed to replicate this plan intraoperatively. However, this technique requires significant lead time and is not flexible during surgery. We have developed a new surgical workflow that integrates optical tracking into this surgery. By eliminating the need for patient-specific guides the surgical plan can be generated in surgery and the optical tracking system guides the surgeon in replicating it. The accuracies achieved with this system during testing are comparable to those attained using the patient-specific guides.

Preface

This thesis is an original piece of work by the author, Molly Stewart. The work outlined in Chapter Two of this thesis was completed by Georgia Grzybowski and myself, under the supervision of Professor Antony Hodgson and Dr Eitan Prisman. I was solely responsible for creating all software modules described. Initial workflow testing was done in equal collaboration with Georgia Grzybowski.

Chapter Three outlines a study performed as part of the ISTAR group by Dr Eitan Prisman, Professor Antony Hodgson and myself. No Ethics approval was required for this study. I was responsible for generating the system to be tested, supervising participants whilst they tested the system, and analysing results. Through this study it was discovered that the accuracy of using an optically tracked saw or optically tracked cutting guide, is statistically comparable to using 3D printed cutting guides. Feedback from users also brought to light the safety concerns with using an optically tracked saw.

The study completed as part of Chapter Four (Assessing the Accuracy and Usability of Optical Tracking in Mandibular Reconstruction Surgery on a Cadaver Model) gained ethics approval from The UBC Clinical Research Ethics Board, certificate number H20-04052. This study was performed as part of the ISTAR group by Dr Eitan Prisman, Professor Antony Hodgson, Georgia Grzybowski, Tom Milner, Anat Bahat Dinur, Orla McGee and myself. The study preparation and results analysis were performed in equal collaboration with Georgia Grzybowski. During the study procedure, I was responsible for running the system software and recording time measurements. This proof-of concept study achieved accuracies on par with the current 3D printed cutting guide mandible reconstruction method with reduced ischemia time and marginal increases in surgical time.

Table of Contents

Abstract ..... **iii**

Lay Summary ..... **v**

Preface ..... **vi**

Table of Contents ..... **vii**

List of Tables ..... **x**

List of Figures ..... **xi**

Acknowledgements ..... **xviii**

1 Introduction and Background **1**

1.1 Mandibular Reconstruction Surgery *1*

1.1.1 Overview of Surgical Process 2

1.1.2 Current Mandible Reconstruction Techniques 4

1.2 Summary *10*

1.3 Research Objectives *11*

1.3.1 Overall Research Objectives 11

1.3.2 Research Objectives Covered in this Thesis 11

2 System Development and Integration **13**

2.1 Surgical Workflow *13*

2.1.1 Current Surgical Workflow 13

2.1.2 Proposed Alterations to Current Surgical Workflow 14

2.1.3 New Surgical Workflow 16

2.2 System Design *17*

2.2.1 System Hardware 18

2.2.2 Data Handling 19

2.2.3 Software System Design 21

2.3 Full System Integration and Workflow Testing 52

2.3.1 Segment Alignment Workflow Testing 52

2.4 Final Module Design and User Interface 63

3 Fibula Osteotomy Accuracy Study 81

3.1 Purpose of Study 81

3.2 Methods 82

3.3 Results 87

3.4 Discussion 93

4 Integrated System Validation Testing 96

4.1 Cadaver Trial Phase One – Evaluating Practicality in Surgically-Realistic Setting 96

4.1.1 Method 97

4.1.2 Results 105

4.1.3 Discussion 119

4.1.4 User Feedback 129

5 Discussion and Conclusions 134

5.1 Thesis Contributions 134

5.2 System Limitations 137

5.3 Future Studies 138

5.3.1 User Study Focused on Usability 139

5.3.2 Cadaver Trial Phase Two – Combined Assessment of Usability and Accuracy 140

5.4 Future Development and Testing 140

5.5 Concluding Remarks 141

Appendices 150

Appendix A: Image-guided Surgery Surgical Steps 151

A.1 Tool Set Up 151

A.2 Mandible Set Up and Registration....151

A.3 Mandible Osteotomies....152

A.4 Fibula Registration....152

A.5 Generate VSP....153

A.6 Fibula Osteotomies....153

A.7 Segment Alignment....154

Appendix B: Workflow Testing Observations and Associated Module Updates....155

Appendix C: Cadaver Trial Phase One Accuracy Results....157

C.1 General Accuracy Results....157

C.2 Fibula Osteotomy Accuracy Results....159

Appendix D: Detailed Time Map of New and Existing Surgical Workflows....164

D.1 Average Cadaver Study Time Map....164

D.2 Shortest Time Cadaver Study Time Map....165

D.3 Patient-Specific Guide Time Map....166

Appendix E: Suggested Module Updates....167

List of Tables

Table 1 – Project aims and assigned collaborators. 12

Table 2 - Average accuracy results for each segment alignment method (* calculated using the fibula segments only model).....60

Table 3 - Average length error, angle error, time per cut for each guidance methods (*absolute values) 92

Table 4 - Cadaver trial phase one surgical steps.....103

Table 5 - Average overall accuracy metrics and separated averages for each alignment tested 116

Table 6 - Comparison of results achieved in literature using the 3D-printed cutting guides and the results achieved in phase one of the cadaver trial.....119

List of Figures

Figure 1 - Schematic of mandibular reconstruction using fibula free flap 3

Figure 2 – Patient-specific 3D-printed mandible (left) and fibula (right) cutting guides 6

Figure 3 – Current VSP and patient-specific 3D-printed cutting guides surgical workflow containing the following steps: (1) define cut planes. (2) generate VSP, (3) create 3D-printed guides, (4) attach mandible cutting guide, (5) make mandible cuts, (6) attach reconstruction plate, (7) attach fibula cutting guide, (8) make fibula cuts, (9) position and secure fibula segments. 13

Figure 4 - Proposed image-guided surgical workflow highlighting the following steps: (1) calibrate tools, (2/5) register anatomy, (3) make mandible cuts, (4) digitise mandible cuts, (6) generate VSP, (7) connect Helping Hands, (8) make fibula cuts, (9) update VSP, (10/11) align and secure fibula segments with respect to each other, (12) align and secure reconstruction with respect to the native mandible. 16

Figure 5 - Hardware used when completing an image-guided mandibular reconstruction surgery 19

Figure 6 - Flow of information through the utilised software systems. 21

Figure 7 - Diagram of pivot calibration. 22

Figure 8 - Diagram Outlining Probe Calibration Transform Calculation 24

Figure 9 - Saw calibration fiducial placement diagram where coordinate frame S represents the coordinate frame of the saw marker array, P represents the coordinate frame of the probe marker array and U represent the coordinate frame at the tip of the probe. T_{PS} and T_{UP} are known transforms that allow fiducials (yellow x) to be placed at the probe tip. 25

Figure 10 - Saw blade calibration transform calculation diagram where coordinate frame S represents the coordinate frame of the saw marker array, and B’ represents the coordinate frame formed by the placed fiducials and B represent the coordinate frame at the tip of the blade. T_{BS} is calculated by first calculating $T_{B'S}$ and $T_{BB'}$. 26

Figure 11 - Digitising points for paired-point registration where M represents the coordinate frame of the mandible marker array, P represents the coordinate frame of the probe marker array and U represent the coordinate frame at the tip of the probe. T_{PM} and T_{UP} are known transforms that allow fiducials (yellow x) to be placed at the probe tip. The fiducials placed vertically on the anatomical model are represented by a green x. 27

Figure 12 - Paired-point registration transform calculation diagram where M represents the coordinate frame of the mandible marker array, J’’ represents the coordinate frame of the anatomical fiducials placed with the probe, and J’ represents the coordinate frame of the model fiducials placed using the mouse. $T_{J'J''}$ is calculated using and ITK Landmark Based Transform Initializer. The transform is then applied to M to create M’.....28

Figure 13 - Digitising points for surface registration where M represents the coordinate frame of the mandible marker array, M’ represents M transformed by $T_{J''J'}$ (Figure 12), P represents the coordinate frame of the probe marker array and U represent the coordinate frame at the tip of the probe. $T_{PM'}$ and T_{UP} are known transforms that allow fiducials (yellow x) to be placed at the probe tip as it is drawn across the surface. 29

Figure 14 - Surface registration transform calculation diagram (offset between S' and S is exaggerated for clarity) where M represents the coordinate frame of the mandible marker array, M’ represents M transformed by $T_{J''J'}$ (Figure 12), S’ represents the coordinate frame of the surface points placed with the probe, and S represents the coordinate frame of the anatomical model point clous generated from the 3D model. $T_{S'S}$ is calculated using an ICP algorithm in 3D slicer and then applied to M’ to create A.....30

Figure 15 - Mandible CT visualisation for defining the mandible cut planes.....31

Figure 16 - Digitise points on mandible cut planes where M represents the coordinate frame of the mandible marker array, A represents M transformed by $T_{J''J'}$ (Figure 12) and $T_{S'S}$ (Figure 14), P represents the coordinate frame of the probe marker array and U represent the coordinate frame at the tip of the probe. T_{PA} and T_{UP} are known transforms that allow fiducials (yellow x) to be placed at the probe tip on both mandible cut surfaces.....32

Figure 17 - Mandible cut planes transform calculation diagram where M represents the coordinate frame of the mandible marker array, A represents M transformed by $T_{J''J'}$ (Figure 12) and $T_{S'S}$ (Figure 14), and R and L represent the coordinate frames calculated based on the three fiducials placed on each of the mandible cut planes using the probe. 33

Figure 18 - Visualisation of mandible cuts after digitising cut planes to check the achieved margins. 33

Figure 19 - Comparison of equal segment length plan (left) and RDP plan (right). 35

Figure 20 - VSPs containing a step and rotated segments. 37

Figure 21 - VSP generated using updated algorithm with no steps or rotation between segments. 38

Figure 22 - Visual display for helping hand placement. 40

Figure 23 - Fibula segment tracking transform calculation diagram where F is the fibula marker array coordinate frame, A is this coordinate frame transformed by the initial and surface registration transforms, S is the coordinate frame of the fibula segment model, and H is the coordinate frame of the Helping Hand marker array. Using the know transforms shown in blue, the transform between the Hand marker array and the fibula segment T_{HS} can be calculated...41

Figure 24 - Fibula osteotomy guidance virtual display. 42

Figure 25 - Surgical saw axes of rotation. 43

Figure 26 - Updated resection planes for updating the VSP. 46

Figure 27 - Segment alignment guidance virtual display. 48

Figure 28 - Segment alignment in mandible transform calculation diagram where S1/S2 represent the coordinate frame of the fibula segment models and H1/H2 represent the coordinate frames of the Helping Hand marker array. The know transforms between the Hand and their associated segment (T_{S1H1}/T_{S2H2}), and the transform between the two hand marker array coordinate systems (T_{H1H2}), are used to calculate the transform between segment 1 and Hand 2's marker array.....49

Figure 29 - Hand two marker array orientations for aligning the segments with respect to each other (left) and in the mandible (right). 50

Figure 30 - Marker array orientation change transform calculation diagram where the transform between Hand two marker array in the fibula position (H2) and the mandible position (H') is calculated ($T_{H'H2}$) based on the know transforms between the Hand marker array coordinate system locations and the Hand virtual model coordinate system (C). 50

Figure 31 - Reconstruction alignment guidance virtual display. 51

Figure 32 - Potential segment alignment workflows. 54

Figure 33 - Workflow diagram of study using 3D-printed fibula segments including the following steps: (1) mandible registration, (2) perform mandible resection, (3) digitise mandible cut planes, (4) generate a VSP, (5) 3D-print planned fibula segments, then perform the guidance method.56

Figure 34 - Example of 3D models created of the full mandible reconstruction and of the aligned fibula segments. The yellow crosses represent the fiducials placed to calculate accuracy metrics. 57

Figure 35 - Width, projection and ICP error results for all three workflow study reconstruction sets 59

Figure 36 - Dice score results for all three workflow study reconstruction sets 59

Figure 37 - Mandible Workspace When Using the Guided Alignment at Mandible Workflow 63

Figure 38 - Set up user interface in 3D Slicer 65

Figure 39 - Attach X-Fix user interface in 3D Slicer 66

Figure 40 - Initial mandible registration user interface 3D Slicer 67

Figure 41 - Surface registration user interface in 3D Slicer 68

Figure 42 - Registration check user interface in 3D Slicer 69

Figure 43 - Contour check user interface in 3D Slicer 70

Figure 44 - Visualize mandible CT user interface in 3D Slicer 71

Figure 45 - Digitise mandible cut planes user interface in 3D Slicer 72

Figure 46 - Generate VSP user interface in 3D Slicer 73

Figure 47 - VSP output user interface in 3D Slicer 74

Figure 48 - Place Helping Hand user interface in 3D Slicer 75

Figure 49 - Fibula cut guidance user interface in 3D Slicer 76

Figure 50 - Digitise fibula cut plans user interface in 3D Slicer 77

Figure 51 - Visualize actual fibula segment and recalculate VSP user interface in 3D Slicer 78

Figure 52 - Fibula segment to segment alignment user interface in 3D Slicer 79

Figure 53 - Segment to mandible alignment user interface in 3D Slicer 80

Figure 54 - Saw bone model set up 83

Figure 55 - OTS (left) and OTG (right) cut guidance method set up 84

Figure 56 - 3D-printed cutting guides used in this study 85

Figure 57 – Segment length error sorted by cut guidance method 88

Figure 58 - Cut angle error sorted by cut guidance method 88

Figure 59 - Time per cut sorted by cut guidance method 89

Figure 60 - Segment length error sorted by participant 89

Figure 61 - Cut angle error sorted by participant 90

Figure 62 - Time per cut sorted by participant 90

Figure 63 - Segment length error sorted by segment 91

Figure 64 - Cut angle error sorted by segment 91

Figure 65 - Time per cut sorted by segment 92

Figure 66 - Holes in the mandible and fibula segmentations 98

Figure 67 - Mandible exposed for cadaver trial phase one 99

Figure 68 - Fibula exposed for cadaver trial phase one 100

Figure 69 - Placed fiducial locations and calculated width and projection diagram 104

Figure 70 - Width and projection results for each procedure 107

Figure 71 - Hausdorff distance results for each procedure 108

Figure 72 - Dice score results for each procedure 109

Figure 73 - Fibula segment length deviations from target segments 110

Figure 74 - Fibula segment length deviations from digitised segments 111

Figure 75 - Fibula segment angle deviations from target segments 112

Figure 76 - Fibula segment angle deviations from digitised segments.....113

Figure 77 - Mandible osteotomy displacement deviation from digitised cut plane.....114

Figure 78 - Mandible osteotomy angle deviation from digitised cut plane.....114

Figure 79 - Maximum distance between reconstructed mandible and mini plate 115

Figure 80 - Total time and ischemia time for each procedure.....117

Figure 81 - Time map of main surgical steps in current and proposed workflows.....118

Figure 82 - Trimmed fibula segments when using visual alignment method (Left – Visual 1, Right – Visual 2).....120

Figure 83 - Fibula segment tracking when reflective markers not visible transform calculation diagram.....123

Figure 84 - Fibula segment location when reflective markers not visible transform diagram....123

Figure 85 - Visual 2 Plate Segmentation and 3D Model at Maximum Plate to Bone Distance Location 127

Acknowledgements

I would like to thank all the faculty, staff and fellow students who have encouraged and inspired me though my studies at UBC. I am particularly grateful for the continued support guidance from Professor Antony Hodgson and Dr Eitan Prisman throughout the project and on many occasions giving up your free time to assist in studies and troubleshooting. Additionally, I am so grateful for all the help Edward Wang, Prash Pandey and, Linh Tran have given me over the course of the project working through software issues and being so patient with my questions. I would also like to show my appreciation to the funding sources for this project, a joint grant between Natural Sciences and Engineering Research Council of Canada (NSERC) and Canadian Institutes of Health Research (CIHR).

Throughout all the work we have performed in the lab, we have had help for people across many different groups through the STL lab, ISTAR, Dr Prisman's clinical group and CHHM staff. These people have been integral to our success in the project, and we couldn't have done it without them. Finally, to Georgia Grzybowski, thanks for volunteering to do all the dirty work whilst I operated the software! I have learned a lot from you not just through the project but about life in BC and Canada in general. We have worked together to achieve something to be proud off, and I have had a great time doing it. We started as strangers but finished friends, here's to us. Sláinte

1 Introduction and Background

In order to treat a patient who presents with a cancer in the mandible, one option is surgery (B. P. Kumar, 2016). The diseased section of the mandible is removed, and the gap is bridged with a donor bone, most commonly the fibula (Kokosis, 2016). This surgery is complex as it requires the surgeon to recreate the curved jaw line using a straight bone. In recent years, Virtual Surgical Planning (VSP) processes, supported by patient-specific 3D-printed cutting guides have been used in this type of surgery to try and combat some of these issues; however, these cutting guides require a significant lead time to design and create, are unadaptable once created, and are vulnerable to breaking before surgery. To combat these limitations, we have created a dynamic surgical navigation system that enables us to both generate the VSP and replicate it intraoperatively. This system completely replaces the previously used 3D-printed cutting guides with optical tracking, eliminating the extensive lead time required and giving the surgeon greater flexibility and adaptability during the procedure. We call this an “on-the-fly” technique. This thesis will outline the motivations for creating this system, the development of the software components, and the verification testing completed to evaluate its performance.

1.1 Mandibular Reconstruction Surgery

The mandible (lower jaw bone) is the largest bone in the human skull and is integral in helping us perform many of our daily tasks (Breeland, 2021). In addition to forming our lower jawline, the mandible also houses the lower teeth and helps us eat, speak and breath (Wilde, 2015).

If a patient presents with a benign or malignant tumour, osteomyelitis, or osteoradionecrosis in the mandible, then the affected section of the bone may need to be surgically removed (B. P. Kumar, 2016). The gap that is left behind must then be reconstructed. The most common epidemiology leading mandibular reconstruction is squamous cell carcinoma closely followed by

osteogenic sarcomas of the jaw (Disa, 2009). Although the second most common cause of a patient needing mandibular reconstruction surgery, osteogenic sarcomas is estimated to affect approximately 50,000 people worldwide each year (Chittaranjan, 2014). Therefore, it is of great interest to streamline the surgical workflow whilst still achieving the best surgical outcomes for patients.

1.1.1 Overview of Surgical Process

In mandibular reconstruction surgery, once the affected section of the mandible is removed, the patient is left with a gap in their mandible. There have been several different methods used to bridge this gap including: non-vascularized bone grafts such as the iliac or costochondral rib (B. P. Kumar, 2016); vascularized free flaps including the fibula, scapula or radial forearm (B. P. Kumar, 2016); reconstruction plate and soft tissue free flap (Lin, 2011); and tissue engineering approaches (Kakarala, 2018). However, the current gold standard approach is to use a vascularized free flap (Torroni, 2015), with the fibula being the donor bone most commonly used to bridge the gap (Lin, 2011). Thus, this method is used as the basis for the surgical approach outlined in this thesis.

When using this fibula free flap technique, the straight bone is sectioned in such a way that it approximates the curve of the resected mandible. These fibula segments are then held in place by a titanium reconstruction plate or mini plates (Kakarala, 2018). A virtual model of a mandible reconstruction using a fibula free flap technique is shown in Figure 1.

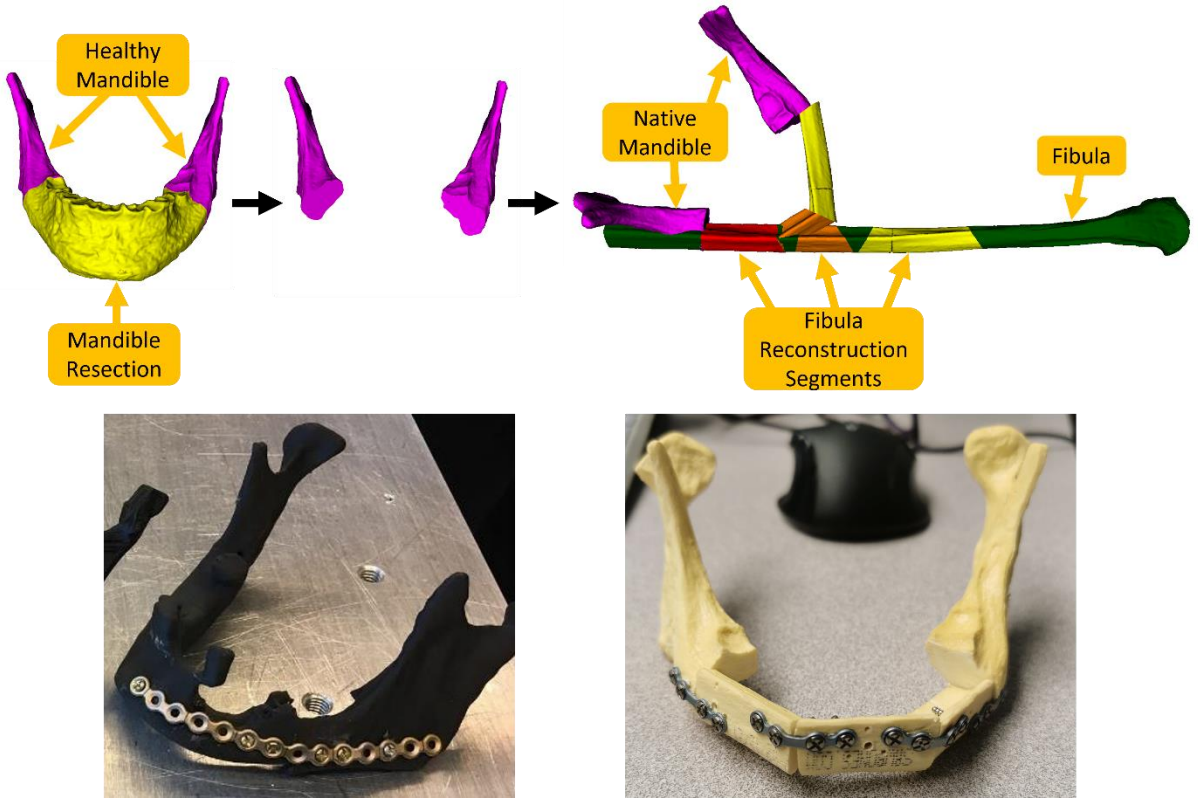

Figure 1 - Schematic of mandibular reconstruction using fibula free flap

When conducting this surgery, it is important for the surgeon to reconstruct an approximation of the premorbid healthy mandible contour to ensure the patient maintains a natural-looking jawline post reconstruction (B. P. Kumar, 2016). This is determined by the shape and size of the fibula segments used for the reconstruction.

The reconstruction is also required to reinstate the continuity of the mandible (Kakarala, 2018). Before resection, the mandible is one contiguous bone. However, when the affected section is removed that mandible becomes two independent bone segments. Re-establishing this continuity is vital to return much of its function such as assisting with mastication and speech (B. P. Kumar, 2016)(Lin, 2011). This is initially achieved via the titanium reconstruction plate; however, over time the native mandible and fibula segments begin to grow and fuse achieving bony union and restoring the continuity (May, 2021). One factor that influences the likelihood of the amount of bony union achieved postoperatively is the amount of bone-to-bone contact

between neighbouring segments (native mandible to fibula or fibula to fibula) during the procedure (May, 2021) (Kazanjian, 1952). The amount of bone-to-bone contact achieved is again determined by the shape and size of the fibula segments created. Consequently, the method used to determine the size and shape of the donor fibula segments and execute the fibula osteotomies can have a large impact on the patient's functional and aesthetic outcomes and thus the success of the mandible reconstruction.

1.1.2 Current Mandible Reconstruction Techniques

As discussed above, the size and shape of fibula segments used to reconstruct the mandible are important in determining the success of the surgery. There are several methods used today to undertake this process, each with their own advantages and disadvantages. The most common of these are discussed below. The most common of these are the freehand technique and Virtual Surgical Planning accompanied with patient-specific cutting guide technique. These, along with the use of reusable cutting guides and image guidance for this type of surgery, are discussed in more detail below.

1.1.2.1 Freehand Technique

The conventional method for creating these fibula segments is the freehand technique. After removing the section of mandible, the surgeon exposes the fibula, locates the appropriate blood supply to the bone (pedicle) and elevates the middle section of the fibula out of the leg (Hidalgo, 1989). The fibula segments are then created using measurements taken intraoperatively of the mandible gap and from x-rays and CT scans of the mandible and fibula (Hidalgo, 1989)(Nakayama, 2006)(S. Strackee, 2001). Sometimes these measurements are first used to create templates during surgery from different easily-altered materials such as plastic sheets, surgical sponges, thin metal plates, and balsa wood (Hidalgo, 1989)(Fernandes, 2007)(Moro,

2009)(Horowitz, 2019). These are then held over the fibula to help visualise and guide the fibula osteotomies more accurately.

Even whilst using these intraoperative templates, an optimised result with good bony contact can be difficult (Foley, 2013) and time consuming to achieve with one study finding the average surgical time of 10.5 hours (Hanasono, 2013). These problems, coupled with advances in technology, have motivated the development of alternative techniques to more accurately guide surgeons whilst creating these fibula segments.

1.1.2.2 Virtual Surgical Planning (VSP)

VSP is one such development. This technique involves using preoperative CT scans to create a virtual 3D model of the diseased mandible. The surgeon will then decide where to resect the mandible virtually and a reconstruction plan is created detailing length and angle of fibula segments along with their optimised position in the mandible. Depending on which system is used to undertake this virtual planning process, the fibula segments can be calculated using algorithms such as the Ramer–Douglas–Peucker contour simplification algorithm (RDP) (Luu, 2018), or they can be manually created by taking virtual fibula osteotomies and then fitting the virtual segments into the mandible gap in a trial and error process (W. H. Wang, 2013).

Once these plans are created, they then need to be replicated in the operating room, which can be done several different ways. In some cases, a 3D model of the resected mandible and repositioned fibular segments is manufactured and used as a visual reference during surgery (W. H. Wang, 2013). This model can also be used to guide pre-bending of the reconstruction plate to fit the planned reconstructed mandible contour rather than the original mandible contour (Hanasono, 2013).

1.1.2.3 3D-printed Cutting Guide Technique

Alternatively, patient-specific cutting guides can be created to more accurately guide the surgeon in replicating the VSP in the operating room (OR). These guides are made using 3D printing technology and then sterilised before being used in the OR. An example set of these cutting guides is shown below.

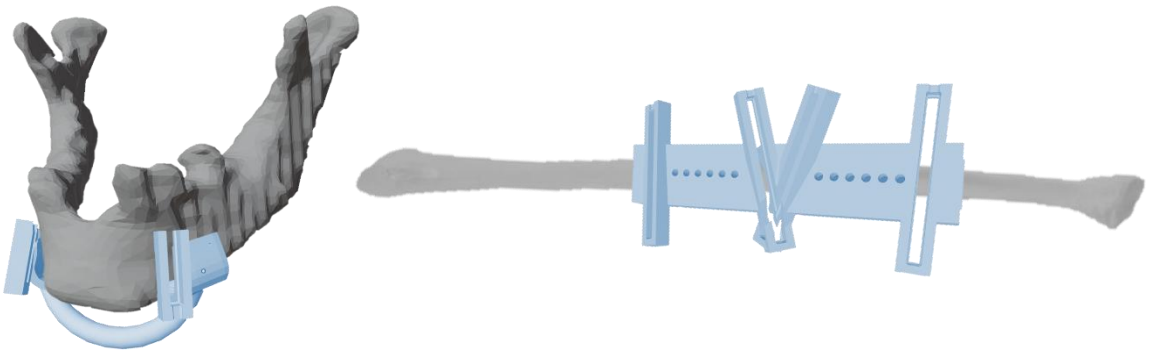

Figure 2 – Patient-specific 3D-printed mandible (left) and fibula (right) cutting guides

Several commercial companies offer this service. The surgical team would meet with an engineer to plan the reconstruction after which the company manufactures and sterilises the cutting guides which are then delivered to the surgical team ready to be used in surgery (Succo, 2014)(Shenaq, 2018). However, this process can take more than four weeks (Pietruski, 2019a) and can cost between $4000-$15,000 per case on top of the regular surgical cost (Luu, 2018).

Due to these limitations, several centres have created an inhouse workflow to not only create a VSP, but also to manufacture the cutting guides using 3D printers (Luu, 2018)(Numajiri, 2016)(Dupret-Bories, 2018). As everything is done inhouse, the surgeon has greater access to the planning process so can be fully involved in any decisions regarding generating the reconstruction plan and cutting guides. Additionally, planning and manufacturing inhouse reduces the cost to approximately $100-$200 (Luu, 2018) and lead in time to around one week (Dupret-Bories, 2018). The average accuracy in replicating the VSP osteotomies using the

inhouse cutting guides created at Vancouver General Hospital (the center this thesis was developed in collaboration with) for segment length and osteotomy angle are 1.91 ± 1.59 mm and 5.23 ± 5.21˚ respectively (E. Wang, 2020). However, this is not a suitable alternative to commercial options for all centres as they must have the expertise and equipment necessary inhouse to generate the VSP and manufacture the guides.

Another disadvantage of these guides (whether commercially made or inhouse) is that they do not allow for any flexibility in the VSP (Kirke, 2016). Once the plan is created and the guides are manufactured, the surgical plan is set. If, for example, on the day of surgery the surgeon needed to resect at different locations, or it is discovered that a different number of fibula segments would be optimal, the cutting guides could no longer be used, and the surgeon would have to revert to the freehand technique described above. If a larger mandible resection is required, the guides may still be viable used to make some of the fibula osteotomies with some manual alteration by either free handing an additional segment or just increasing the length of the final segment. However, this mat compromise some of the benefits gained from using the VSP such as increased bone to bone contact and a better replication of the healthy mandible contour.

Despite the drawbacks, VSP has been shown to reduce total surgical time and postoperative hospital stays which can offsets some of the additional cost from using VSP/cutting guides (E. Wang, 2020)(Y. Y. Wang, 2016)(Powcharoen, 2019). It also was found to reduce ischemia time (Y. Y. Wang, 2016)(Succo, 2014)(Zavattero, 2015). This has been shown in a number of studies to lead to fewer post-operative complications when reduced below 3-5 hours; however, further reducing the ischemia time below this threshold was shown to have no statistically significant effect on post-operative complications (S. Y. Chang, 2010)(Gürlek, 1997).

In addition to these benefits, VSP allows for a more optimised contour to be created leading to better aesthetic and functional outcomes for the patient (W. H. Wang, 2013)(Weitz, 2016). It has also been shown to reduce the likelihood of bony non-union by approximately 14% in one study (May, 2021) whilst achieving union in a shorter postoperative timeframe, 0.8 year compared to 1.4 years using the freehand method (May, 2021)(E. I. Chang, 2016)(Weitz, 2016).This study further linked the reduced rate on non-union to a reduced likelihood of free flap associated complications (May, 2021).

1.1.2.4 Reusable Guides

In order to reduce cost, lead time and lack of adaptability associated with the patient-specific cutting guide approach described above, a few reusable cutting guide systems have been developed. One such guide has been developed in a research setting that allows the mandible resection to be made during surgery using one jig, with the fibula osteotomies then determined by the shape of this mandible resection jig and guided using a second fibula jig (S. D. Strackee, 2004). Although this system eliminated any lead time and reduces cost, it only allows specific mandible resections to be made and restricts the number of fibula segments that can be used.

Another system which has been developed requires the surgeon to pre-plan the mandible resection and manually calculate the length and angle of each segment based on CT scans. The planned mandible resection is then replicated in surgery without any guidance with the developed jig being used to guide the fibula osteotomies only (S. D. Strackee, 2004). This system was shown to achieve similar accuracies (in terms of segment length and angle) at reproducing a pre-plan as the commercially available 3D-printed cutting guides (Meyer, 2020). It also somewhat increases the flexibility of the pre plan as the guide is not fixed, though changing the plan would require manually recalculating all subsequent fibula osteotomies, which may significantly increase surgical time.

One commercially-available system of reusable cutting guides has been developed by KLS Martin Group. When using this system, the surgeon makes the mandible resection at two of the four possible locations (which also have predetermined angles) on the jig. Based on which locations are chosen on the mandible jig, fibula osteotomies are guided using the corresponding fibula jig cutting slots (KLS Martin Group, 2019). Similar to the first reusable guide described, this system only allows the surgeon to resect the mandible in four discrete locations and allows no more than three fibula segments. This could prevent the system being used for certain cases or could force the surgeon to resect healthy mandible that may not have been needed to be removed.

1.1.2.5 Image Guidance Techniques

Another alternative to 3D-printed cutting guides is integrating image guided surgery (IGS) techniques into mandibular reconstruction surgery. For example, several studies have reported using optical tracking to guide the mandible resection based on a pre-plan (Bernstein, 2017)(Naujokat, 2017)(Hasan, 2020)(Pietruski, 2019b). IGS has also been used to check the location of the fibula segments once they have been placed in the mandible gap (X.-F. Shan, 2016). One paper compared the accuracy of placing the fibula segments freehand against using image guidance to check the placement of the segments against using a robot to place the segments (Zhu, 2016). The accuracy reported was the distance between a specific point on the pre and post operative CT scan when overlayed. The robot was the most accurate (1.221 mm), followed by the image guidance method (1.581 mm), followed by the freehand alignment method (2.313 mm), which is what is generally done when using the 3D-printed cutting guides.

Image guidance has also been used to guide the fibula osteotomies themselves, though this has only ever been done on artificial bone models in a lab setting (Pietruski, 2019a). Their accuracy at replicating the planned fibula osteotomies was 3.66° ± 3.60° of angular deviation

and 1.85 ± 0.99 mm linear deviation which is comparable to what has been reported in literature for 3D-printed cutting guides. This same group also used augmented reality with image guidance to try to enhance the accuracy and user experience of their system; however, this produced slightly lower accuracy results (Pietruski, 2019). The only other instance of using image guidance to make the fibula osteotomies used a robot arm to make the osteotomies; this was also tested on artificial bone models. This study achieved accuracies of 4.2 ± 1.78° of angular deviation and 1.3 ± 0.4 mm linear deviation which is similar to both the image-guided handheld saw study discussed previously and the 3D-printed cutting guides.

1.2 Summary

All the surgical methods discussed above have tried to reduce the complexity of performing a mandibular reconstruction surgery freehand. Segmenting a straight bone to recreate the curved mandible contour is a complex problem, especially since the quality of the reconstruction achieved can have such a drastic impact on the patient's quality of life post-surgery.

The VSP combined with patient-specific 3D-printed cutting guides is the most common alternative approach as this allows the surgeon to generate an optimised plan before surgery and helps them execute this plan in the operating room accurately. However, this method comes with its own problems including: the lead time required to complete the VSP, manufacture the guides and sterilise them ready for use in the operating room; the durability of the guide as they are known to have failed in use; and the lack of flexibility in the plan once the guides are manufactured.

The use of reusable guides tried to remedy these problems but limit the surgeon on how they can perform the reconstruction and may only be usable for certain cases. However, integrating image guidance into mandibular reconstruction surgery could eliminate the lead in time (as

there is no need to manufacture cutting guides) and allow maximum flexibility (by using a VSP system to generate the plan during the surgery). Additionally, the accuracy of these systems has been shown to be comparable to 3D-printed cutting guides. However, so far image guidance has only been used for single steps in the surgical workflow, with some of the steps not yet widely tested in a surgical setting.

1.3 Research Objectives

After evaluating all the methods described above, it was clear that creating a system that used image guidance through all stages in the mandibular reconstruction surgical workflow could eliminate the disadvantages of using 3D-printed cutting guides, achieve similar osteotomy accuracies to using 3D-printed cutting guides, and retain all the benefits of using VSP. Therefore, the aim of the project described in this thesis is to develop and test such a system.

1.3.1 Overall Research Objectives

This project is being developed as part of the Intraoperative Surgical Tools for Advanced Reconstruction (ISTAR) research group. ISTAR is comprised of members from across four departments at the University of British Columbia (UBC), mechanical, biomedical and electrical engineering, and the medical school (specifically the Department of Surgery). The collective aim of this group is to develop an optimisation-based method of virtual surgical planning integrated with a flexible and multidisciplinary surgical system.

1.3.2 Research Objectives Covered in this Thesis

Based on the arguments stated above, and within the global ISTAR aim, this thesis will focus on the following research objective:

Develop and test an optical tracking navigation system and associated devices to guide on-the-fly mandibular reconstruction surgery in a reliable, accurate, and time efficient way.

In order to complete this objective in full, the project has been undertaken in collaboration with another Master of Science candidate in the Biomedical Engineering department, Georgia Grzybowski. The project objective was split into the following five aims which were distributed equally between the two of us.

Aim One	Select and test an accurate and appropriate registration technique in order to register the patient anatomy, mandible cuts and surgical tools in surgery.	Georgia Grzybowski
Aim Two	Develop the associated supporting surgical devices that are needed in order to execute the reconstruction plan and track the mandible and fibula.	Georgia Grzybowski
Aim Three	Design a software system to guide the user through all stages of the surgery using the image guidance system and integrate this with all other aspects of the guidance system.	Molly Stewart
Aim Four	Evaluate the best approach to guide and execute fibula osteotomies using the image guidance system based on their accuracy and usability.	Molly Stewart
Aim Five	Perform validation testing of the full image-guided system to assess accuracy and usability on a cadaver model.	Georgia Grzybowski Molly Stewart

Table 1 – Project aims and assigned collaborators.

Aims Three, Four and Five will be covered in the remainder of this thesis. For further details related to Aims One and Two, please see Georgia Grzybowski's thesis (Grzybowski, 2021).

2 System Development and Integration

Developing a system that allows for mandible resection cuts to be made on-the-fly, without the need for any preplanning, by integrating optical tracking into the surgery will require a number of changes to the current surgical workflow. This chapter presents an overview of the principal components of the proposed workflow and the associated system required to implement it.

2.1 Surgical Workflow

2.1.1 Current Surgical Workflow

To better understand the requirements of the system, we must first understand the changes that integrating image guidance will have on the current surgical workflow. The current surgical workflow used when implementing the 3D-printed cutting guides technique is illustrated in Figure 3 below.

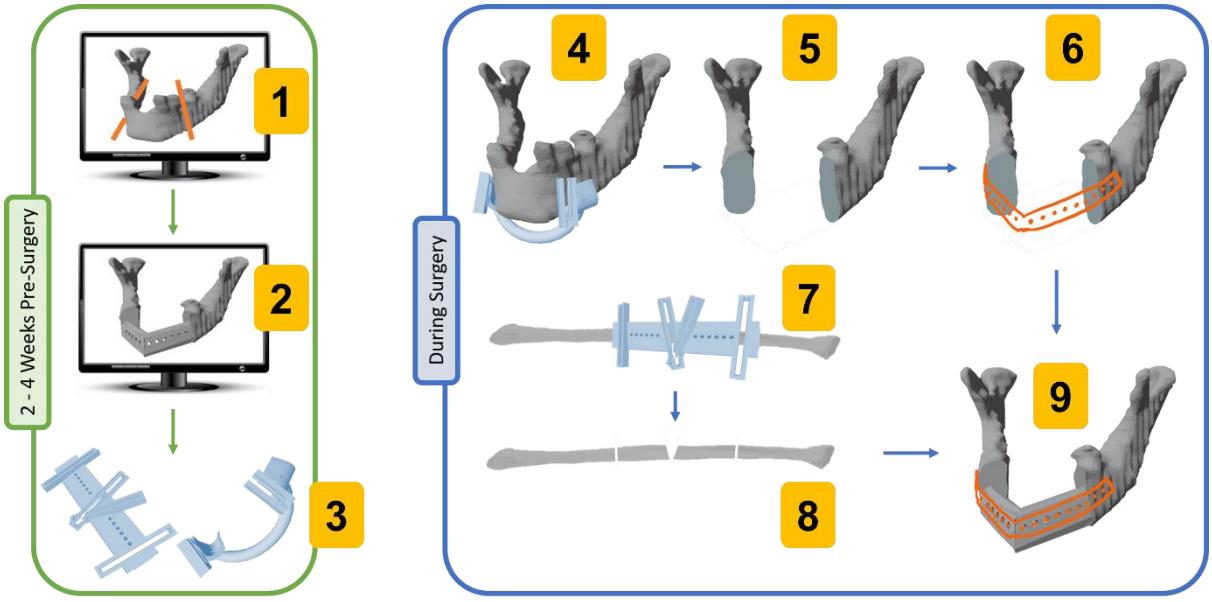

Figure 3 – Current VSP and patient-specific 3D-printed cutting guides surgical workflow containing the following steps: (1) define cut planes. (2) generate VSP, (3) create 3D-printed guides, (4) attach mandible cutting guide, (5) make mandible cuts, (6) attach reconstruction plate, (7) attach fibula cutting guide, (8) make fibula cuts, (9) position and secure fibula segments.

Steps 1 to 3 above are conducted a few weeks prior to the surgery. Based on visual inspection of the patient and preoperative CT scans, the surgeon, with the help of an engineer, determines the mandible osteotomy location on a virtual mandible model (Step 1). These cut planes are then used to generate a VSP and the engineer designs the patient-specific cutting guide (Step 2). These guides (along with a model of the full mandible reconstruction) are 3D-printed (Step 3). The printed reconstruction model is used to prebend the reconstruction plate which is then sterilised along with the cutting guides. During the surgery, the mandible is exposed, the mandible cutting guide is attached (Step 5), and the mandible osteotomies are made (Step 6). The reconstruction plate is then secured to the mandible fragments using the same screw holes as the mandible cutting guide (Step 7). In parallel to this, the fibula bone is expose, the cutting guide attached (Step 8), and the fibula osteotomies performed (Step 9). The pedicle is then cut and the fibula segments are brought into the mandible workspace where they are arranged in the resection gap and secured to the reconstruction plate (Step 10).

2.1.2 Proposed Alterations to Current Surgical Workflow

There are a number of steps within this workflow that will need to be adapted. The most significant of these is removing the preplanning step altogether. By using image guidance to guide the fibula cuts, we eliminate the lead time caused by preplanning and manufacturing physical cutting guides. This in turn will make the whole reconstruction more adaptable as it allows for the reconstruction plan to be generated based on decisions made during the surgery rather than prior to it. Subsequently, the plan can be continually changed throughout the surgery if required. This may be beneficial if, for example, an error is made during a previous fibula osteotomy which can then be corrected for in subsequent osteotomies, or the length of viable fibula used to build the reconstruction is less than expected so the number of segments used can be reduced.

However, not having a reconstruction plan generated before surgery means that less of the surgical workflow can be undertaken simultaneously. In the current surgical workflow shown above, all the steps done at the fibula (including all the fibula osteotomies) can be completed before the mandible is exposed, if needs be. This is because the plan is generated and the guides are manufactured before surgery begins, so all fibula osteotomies are already established. Unfortunately, this information would not be known with an image-guided on-the-fly approach. The plan could only be generating after the mandible resection has been completed in surgery. This then restricts the number of steps that can be completed before the VSP is generated.

There would also be several additional set-up steps associated with integrating optical tracking into mandibular reconstruction surgery. When using an optical tracking system one of the first steps that must be undertaken is to register the patient's anatomy to the virtual space. The optical tracking camera can only see the marker arrays, which are rigidly attached to the bones, so the user must tell the system how the anatomy is oriented with respect to these. This is done through a registration process which would need to be completed after the bone (both mandible and fibula) is exposed but before any resection/ fibula osteotomies are made.

Additionally, as there is no plan created before surgery, there is no model to prebend the reconstruction plate to. The plate could be bent in surgery, but this would have to be done to the unhealthy mandible contour which may result in significant gaps between the fibula segments and the plate. It also may be difficult to use the image-guided system with the large recon plate as there may not be enough space for everything to be in the mandible area. We therefore opted to develop a workflow based on using mini plates, which allow the surgeon to easily bend the plates to the fibula segments during surgery. These mini plates also only span from one segment to the next so should greatly reduce the interference between the image-guided system and the plates.

2.1.3 New Surgical Workflow

After integrating these changes and considering the issues outlined above, we developed a new image-guided on-the-fly workflow see Figure 4 below.

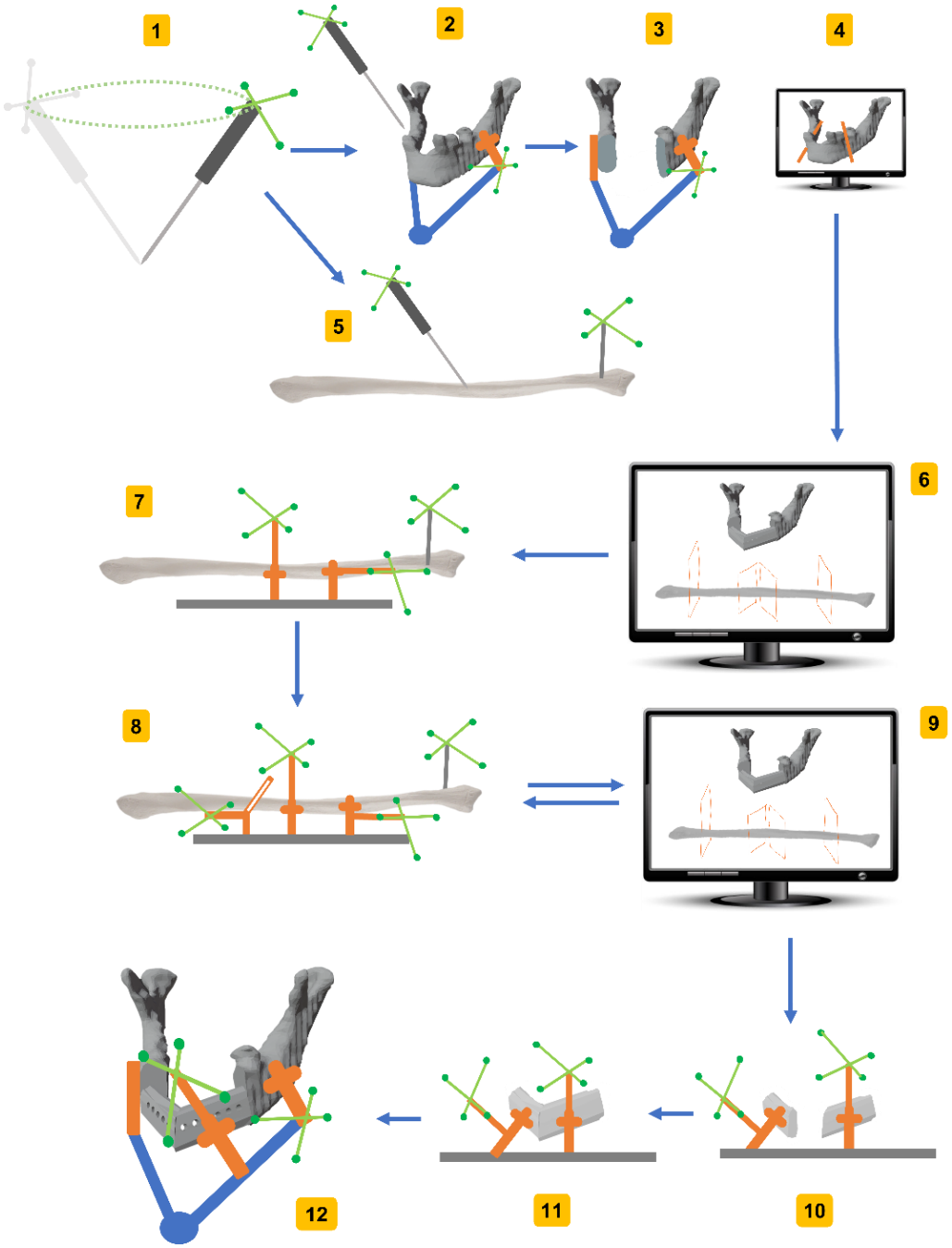

Figure 4 - Proposed image-guided surgical workflow highlighting the following steps: (1) calibrate tools, (2/5) register anatomy, (3) make mandible cuts, (4) digitise mandible cuts, (6) generate VSP, (7) connect Helping Hands, (8) make fibula cuts, (9) update VSP, (10/11) align and secure fibula segments with respect to each other, (12) align and secure reconstruction with respect to the native mandible.

In this new workflow, the only preoperative steps required are to obtain and segment a CT scan of the patient's mandible and fibula. Just prior to surgery the equipment can be arranged in the surgical space and the tools set up and calibrated (Step 1). Then, during the surgery, the mandible is exposed, and an external fixator is applied. The mandible registration is performed (Step 2), the mandible resection is made (Step 3), and the cut planes digitised (Step 4). The fibula can also be exposed and registered whilst these steps are being completed (Step 5). Following this, the VSP is generated (Step 6). To allow the segments to be guided, Helping Hands are rigidly connected to the fibula (Step 7) and the first segment osteotomies are made (Step 8). These cuts are then digitised and the VSP can be updated based on these (Step 9). This is repeated for each segment in the VSP. With the pedicle still attached to the leg, these segments are arranged and secured with respect to each other (Step 11). The pedicle is then cut, and the full reconstruction is then aligned in the resection gap and secured in place with mini plates (Step 12). A detailed description of the individual steps performed during this workflow is presented in 0. Each of these steps is described fully in the next section.

2.2 System Design

To implement the workflow outlined above, a set of components were developed. The basic image guided system uses an optical tracking camera that tracks passive reflective marker arrays connected to surgical tools and anatomy. This camera connects to a computer via a series of software packages allowing for a virtual representation of these tools and anatomy to be visualised. This visualisation is then used to guide the tools in all the steps required to generate and recreate the VSP in the operating room. As mentioned previously the hardware created for this system was developed by Georgia Grzybowski and is not described in this thesis.

2.2.1 System Hardware

The camera system we chose for this project was the Northern Digital Incorporated (NDI) Polaris Vega ST (Northern Digital Inc, Waterloo, Canada). This is an optical tracking camera which utilises near infrared light to track multiple marker arrays at once (Northern Digital Inc, 2020). It reports a volumetric root mean square (RMS) accuracy of 0.12 mm (Northern Digital Inc., 2020). Additionally, the camera itself has been approved for use in a clinical setting and is currently integrated into several different commercially available image-guided surgical systems.

We chose to use an optical tracking system over an electromagnetic tracking system due to the better accuracy of the optical tracking system (Kral, 2013). We also anticipated that many of the tools used for this procedure would be manufactured in metal which could affect the accuracy of an electromagnetic tracking system (Sorriento, 2020)(V. Kumar, 2017). The line-of-sight issues associated with optical tracking were considered when developing the system and surgical set up.

Passive spherical markers were used on both the NDI Probe tool and several 3D-printed mounts developed by a research group at Johns Hopkins University (Brown, 2018). A series of different groups of mounts (each group named after a fruit) were available within this package. All the mounts are compatible with the NDI system and all markers within the same group can be used simultaneously with the rest of that group. A total of seven marker arrays from the “Apple” group were used. This is the minimum required for our system when completing a three-piece reconstruction. These seven arrays connected to the hardware used in this system are shown in Figure 5.

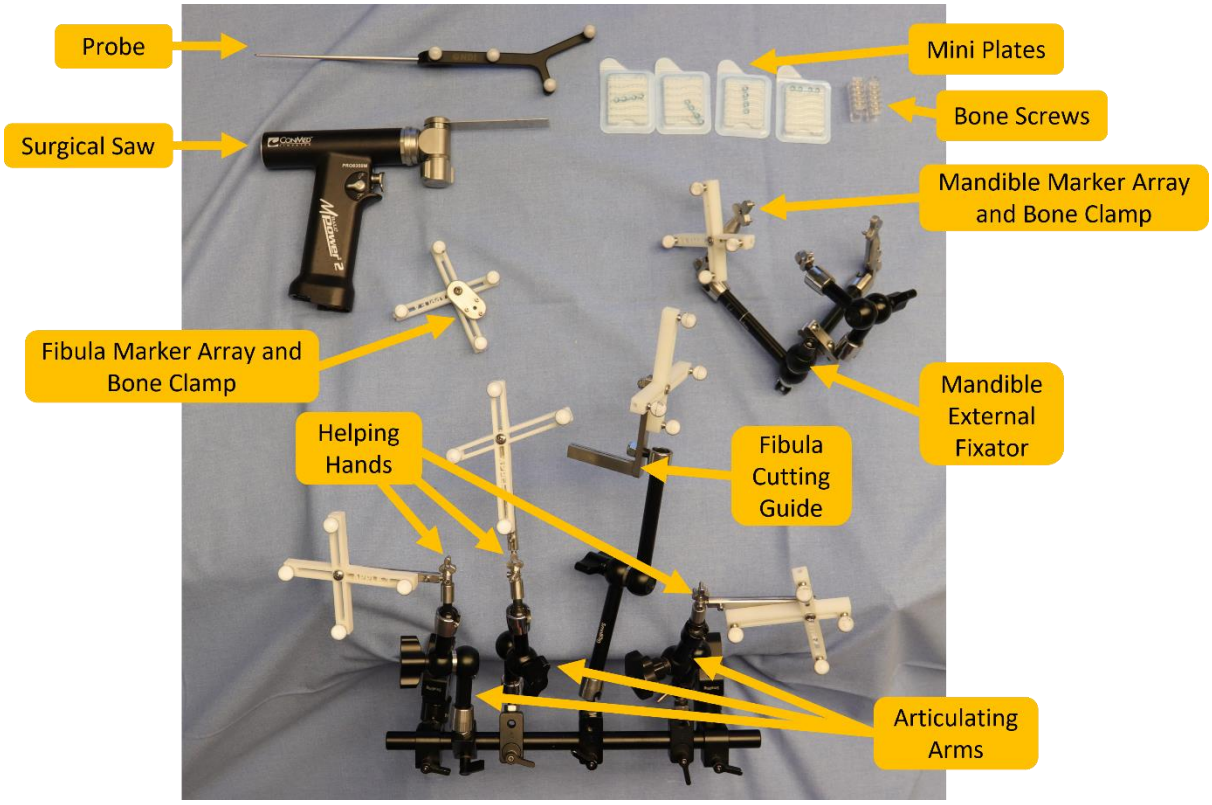

Figure 5 - Hardware used when completing an image-guided mandibular reconstruction surgery

As mentioned previously, the sourcing, design and manufacturing of these pieces was completed by Georgia Grzybowski (Grzybowski, 2021).

2.2.2 Data Handling

For each marker array, we created an associated Read-Only Memory (ROM) file using a software within the NDI Toolkit, 6D Architect. This file stores the relative position and normal of each marker on the array with respect to the others and allows the camera to distinguish between each marker array.

The optical tracking camera is connected, via an ethernet connection, to a computer unit through an open source toolkit called PLUS (Lasso, 2014). This allows for real time data acquisition from the camera by the computer and for each marker array to be associated with a specific tool or component of the system. For PLUS to associate each marker array with a

specific tool and output the transform between the specific marker array, a configuration file is written. This tags each file with an associated tool ID, identifies which tool IDs are to be tracked, and what transforms between tools are to be outputted.

These outputs are then read by an open source software, 3D Slicer (Fedorov, 2012)(*3D Slicer*, 2021). This is a modular platform that allows for the visualisation of medical images, segmentation of these images, and construction and manipulation of 3D models. The modular nature of the platform, along with the developer capabilities integrated into it, allow the user to create new modules for their unique application. These modules can be written using either C++ or Python scripting languages. We developed all the modules in Python 3.6.7.

Using an existing module within 3D Slicer, OpenIGTLinkIF (Tokuda, 2009), the outputs from Plus can be processed into a format which allows them to be manipulated within 3D Slicer whilst still being constantly updated as tools and marker arrays are moved in real space. The user written modules can then utilise these transforms, along with imported 3D models and DICOM files, to perform calculations or connect them to these 3D models to show tools moving in virtual space as they are moving in real space. The integration of these four software components with the optical tracking camera is shown in the diagram below.

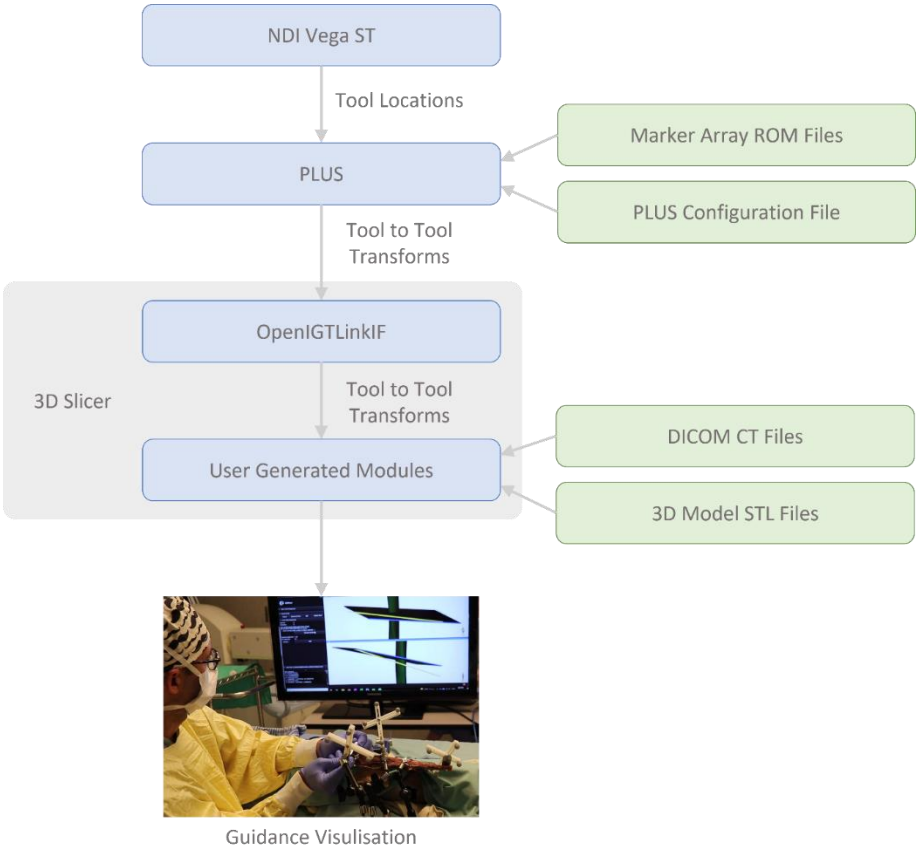

Figure 6 - Flow of information through the utilised software systems.

2.2.3 Software System Design

The user of this system is guided though every step in the updated surgical workflow shown in Figure 4. To do this, we developed a module in 3D Slicer for each step that provided descriptive instruction as well as allowed the user to interact with the image guidance system. These modules were designed to clearly outline what is required of the user at that step and how they are to perform that task, as well as provide a simple user interface and the associated coding required to visualise and complete that step. The next few subsections will outline the function, calculations and user interface developed to create each of these modules.

2.2.3.1 Tool Set Up (Step 1)

Before any steps in the surgical procedure can be undertaken, the tracked tools must be calibrated. This means telling the system how the tool is orientated with respect to the attached marker array. In this system there are two tools that need to be calibrated: the probe and the surgical saw.

Probe Calibration

The probe is calibrated using the pivot calibration technique provided by a built-in 3D Slicer Module, Pivot Calibration (Ungi, 2016). This process has the user place the point of the probe on a surface and move the head of the probe in a circle around this point as shown in Figure 7 below.

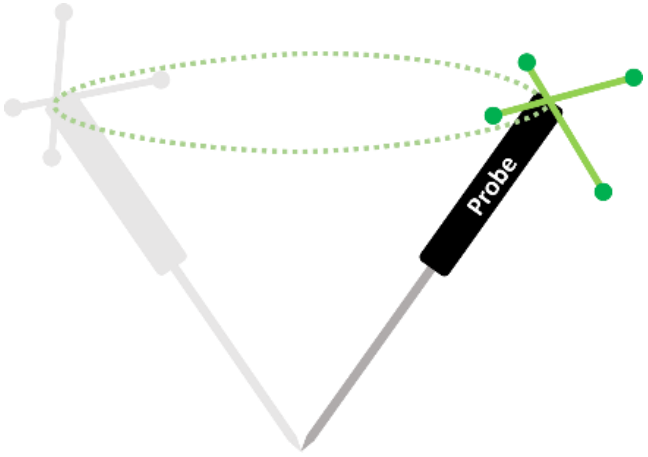

Figure 7 - Diagram of pivot calibration.

The marker array attached is tracked whilst the probe is pivoted over the course of 15 seconds. As visible in Figure 8, the transform $(T_{PF})_i$ between the probe marker array coordinate system (P) and the reference coordinate system (F) is known. Whilst pivoting, this transform is recorded and used to calculate the centre of rotation, i.e., the probe tip. This is done using the Algebraic One Step method (Yaniv, 2015) which uses the assumption that the probe is rotating round a single point. This means that for all time steps (i), U remains stationary and therefore T_{FU} is

constant. As the shaft of the probe is rigid, the transform between the probe tip coordinate frame (U) and the probe marker array coordinate system (P) also remains constant across all timesteps. This means that for each time step, the following equation can be created:

$$(T_{FP})_i T_{PU} = T_{FU}$$

The transform $(T_{FP})_i$ can be further broken down into its rotational (R_i) and translational (t_i) components and the above equation becomes:

$$R_i T_{PU} + t_i = T_{FU}$$

For a single time step this equation and be rearranged as shown below:

$$\begin{pmatrix} [R_i][-I] \end{pmatrix} \begin{pmatrix} [T_{PU}] \\ [T_{FU}] \end{pmatrix} = -t_i$$

When considering all time steps, this is then expanded to the following:

$$\begin{pmatrix} \\ [R_1][-I] \\ [R_2][-I] \\ \dots \\ [R_i][-I] \\ \dots \\ [R_n][-I] \end{pmatrix} \begin{pmatrix} [T_{PU}] \\ [T_{FU}] \end{pmatrix} = \begin{pmatrix} \\ -t_1 \\ -t_2 \\ \dots \\ -t_i \\ \dots \\ -t_n \end{pmatrix}$$

This forms Ax=b matrix equation that is solved using a pseudo-inverse for the optimal solution in terms of the least square between the calculated tip locations (U) when using the transform T_{FU} and when using the transforms $T_{FP}T_{PU}$. A diagram depicting this transform calculation is shown in Figure 8.

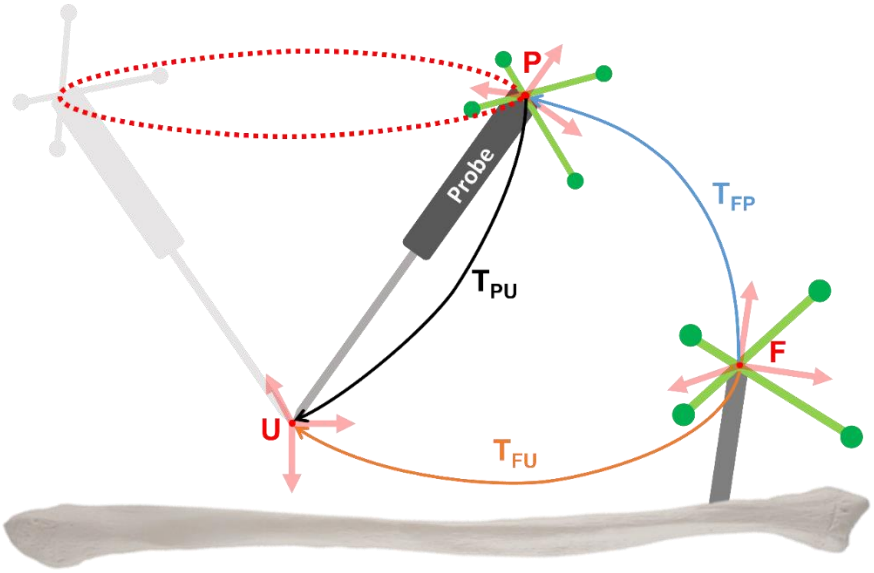

Figure 8 - Diagram Outlining Probe Calibration Transform Calculation

The module displays a calibration error achieved during the calibration process which was generally between 0.1 - 0.5 mm.

Surgical Saw Calibration

Once the probe is fully calibrated, it is then used to calibrate the tracked surgical saw. The user is asked to uses the pointer to indicate three points (fiducials) on the top surface of the saw blade within the saw marker array coordinate system (S). The first and last fiducial are placed on the front corners of the blade and the middle fiducial is placed in the centre at the back of the blade as shown in Figure 9.

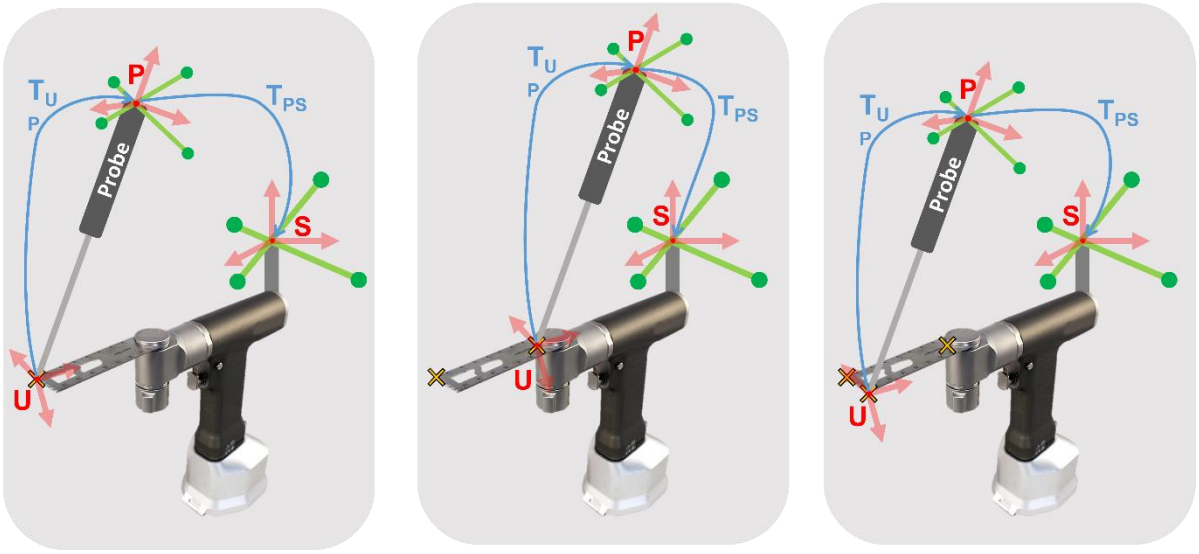

Figure 9 - Saw calibration fiducial placement diagram where coordinate frame S represents the coordinate frame of the saw marker array, P represents the coordinate frame of the probe marker array and U represent the coordinate frame at the tip of the probe. T_{PS} and T_{UP} are known transforms that allow fiducials (yellow x) to be placed at the probe tip.

Care must be taken not to bend the saw blade whilst the fiducials are being placed as this will result in a large error in this calibration step. These three fiducials form a plane in virtual space which corresponds to the plane of the top surface of the saw blade in real space. A new coordinate system (B') is then positioned at the center of this plane with axes corresponding to the plane normal and the vector connecting the middle fiducial to the first fiducial, with the last axis calculated by taking the cross product of these first two vectors. A transform ($T_{B'S}$) between the marker array coordinate system (S) and this new coordinate system on the saw blade (B') is then calculated. A second transform ($T_{BB'}$) is created and applied to B' to create an additional coordinate system (B) at the front and centre of the saw blade as shown in Figure 10.

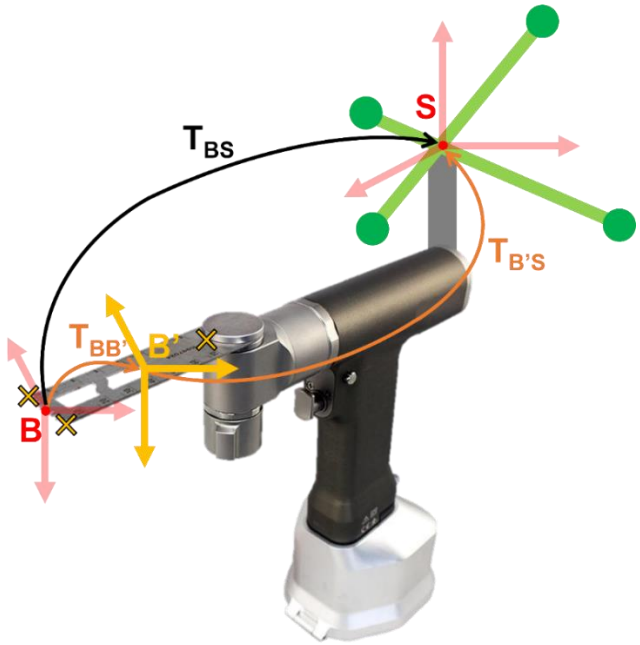

Figure 10 - Saw blade calibration transform calculation diagram where coordinate frame S represents the coordinate frame of the saw marker array, and B' represents the coordinate frame formed by the placed fiducials and B represent the coordinate frame at the tip of the blade. T_{BS} is calculated by first calculating $T_{B'S}$ and $T_{BB'}$.

2.2.3.2 Anatomy Registration (Step 2 and Step 5)

Similar to calibration, the system also needs to know where the patient's anatomy is with respect to the attached marker arrays. This process is called registration. There are a variety of methods used in literature to perform anatomy registration. We opted to use an initial paired-point registration followed by a surface registration (see detailed discussion of this choice in Georgia Grzybowski's thesis (Grzybowski, 2021)). The same registration technique was used for both the mandible and fibula.

Paired Point Registration

To perform the paired-point registration, the user first needs to identify three distinct points that can be located on both the patient's anatomy and on the virtual anatomical model. A fiducial is placed on these points virtually using the computer mouse. The same points are then collected in the same order using the calibrated probe. This is done by placing the point of the probe (T)

on the predefined location on the bone and then calculating its location with respect to the marker array attached to the anatomy (M) (Figure 11).

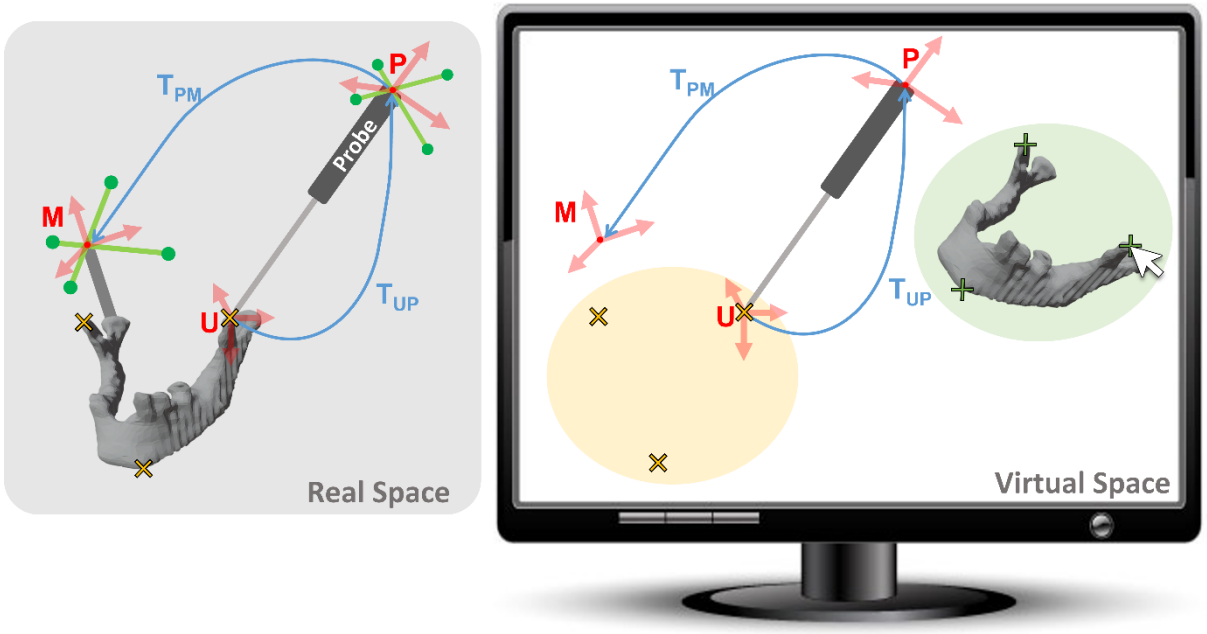

Figure 11 - Digitising points for paired-point registration where M represents the coordinate frame of the mandible marker array, P represents the coordinate frame of the probe marker array and U represent the coordinate frame at the tip of the probe. T_{PM} and T_{UP} are known transforms that allow fiducials (yellow x) to be placed at the probe tip. The fiducials placed vertically on the anatomical model are represented by a green x.

All three points are collected and then the transform between the coordinate frame of the points placed on the virtual model (J') and the coordinate frame of the points placed using the probe (J'') is calculated (Figure 12). This is done using the ITK Landmark Based Transform Initializer which maps the two sets of fiducials to minimise the least square distance between them. This transform ($T_{J''J'}$) is then applied to the mandible marker array coordinate frame (M) to create a new paired-point mandible coordinate frame (M'). In virtual space, M' represents the initial estimation of the location of the mandible marker array with respect to the mandible in real space.

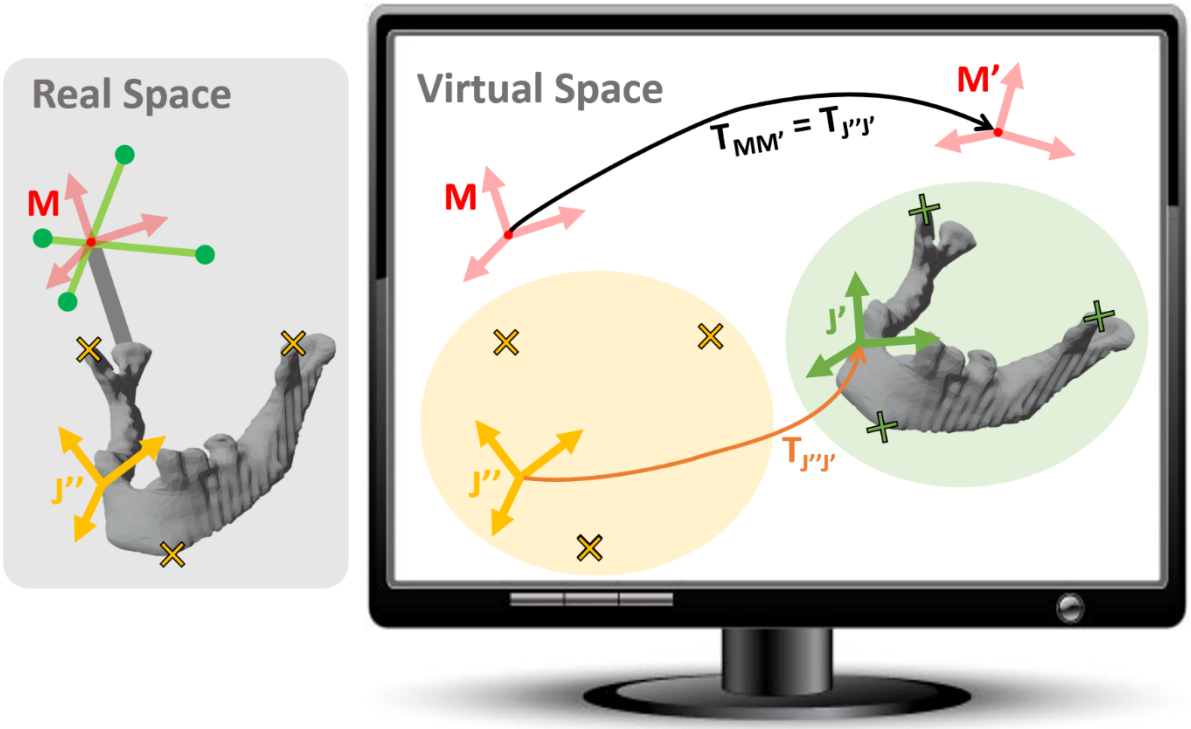

Figure 12 - Paired-point registration transform calculation diagram where M represents the coordinate frame of the mandible marker array, J'' represents the coordinate frame of the anatomical fiducials placed with the probe, and J' represents the coordinate frame of the model fiducials placed using the mouse. $T_{J'J''}$ is calculated using and ITK Landmark Based Transform Initializer. The transform is then applied to M to create M'.

This calculation is done by linking to a built in 3D Slicer Module, the Fiducial Registration Wizard (Ungi, 2016). This transform ($T_{J''J'}$) is then automatically applied to the live tool transforms to allow them to be visualised in the correct location on the anatomical models as they are moved around the patient anatomy in real space.

Surface Registration

Once this initial registration transform ($T_{J''J'}$) is applied to the live probe transform (T_{PM}), the surface registration can be calculated. Using the probe, the user performs a drawing motion over the surface of the bone and the system places a fiducial at the probe tip every 0.01seconds (see yellow crosses in Figure 13).

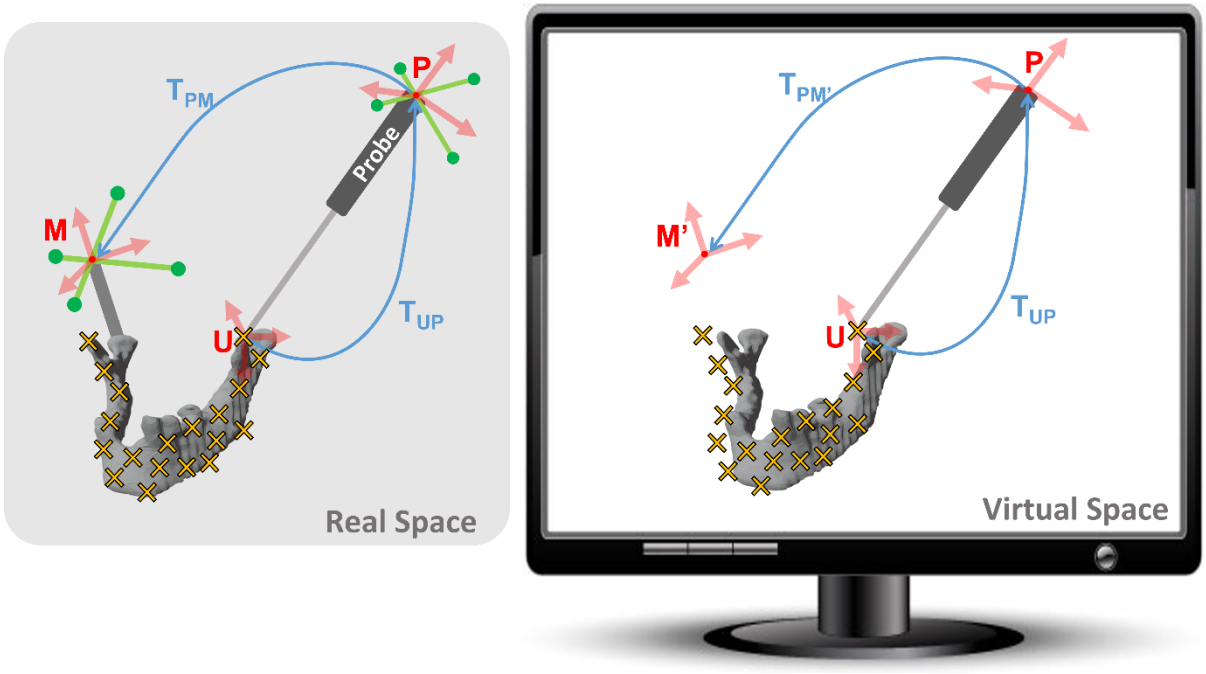

Figure 13 - Digitising points for surface registration where M represents the coordinate frame of the mandible marker array, M' represents M transformed by $T_{J'J'}$ (Figure 12), P represents the coordinate frame of the probe marker array and U represent the coordinate frame at the tip of the probe. $T_{PM'}$ and T_{UP} are known transforms that allow fiducials (yellow x) to be placed at the probe tip as it is drawn across the surface.

The process of collecting these points can be paused to allow the user to lift the probe off the surface of the bone to allow better access. It is important that no points are collected when the probe is not touching the surface of the bone as this will affect the accuracy of the registration. Once points are collected over all surfaces of the bone, the surface registration transform ($T_{S'S}$) can be calculated (Figure 14). This is the transform between the coordinate system of the anatomical model (S) and the coordinate system of all the surface points collected with the probe (S'). The system calculates this transform using an Iterative Closest Point (ICP) algorithm. This works by pairing each surface point collected with the probe with the closest point on the anatomical model. A transform is then estimated that will produce the biggest reduction in the mean square distance between the pairs. Each fiducial point is then re-paired with the new closest point and the system keeps estimating transforms until the maximum number of iterations is achieved and the final transform is outputted ($T_{S'S}$). The paired-point mandible coordinate frame (M') is then transformed by $T_{S'S}$ to generate a new coordinate frame (A)

corresponding to a more accurate representation of the location of the mandible marker array with respect to the mandible anatomy in real space.

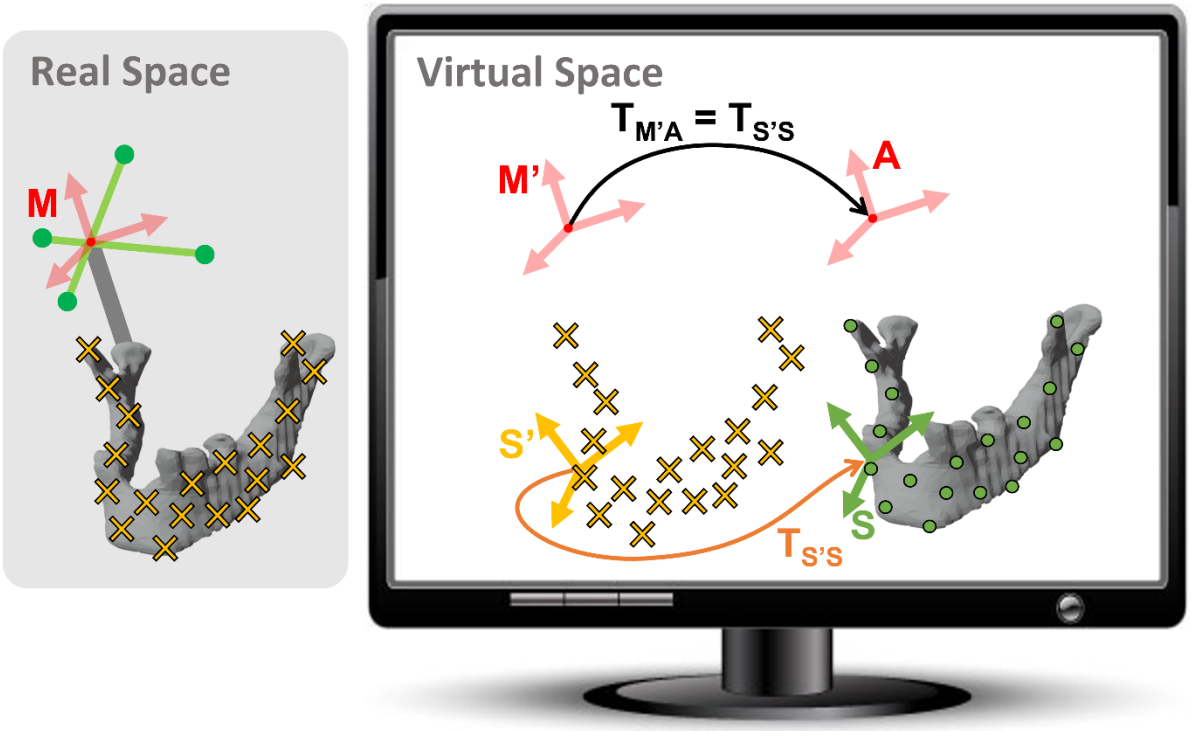

Figure 14 - Surface registration transform calculation diagram (offset between S' and S is exaggerated for clarity) where M represents the coordinate frame of the mandible marker array, M' represents M transformed by $T_{J'J'}$ (Figure 12), S' represents the coordinate frame of the surface points placed with the probe, and S represents the coordinate frame of the anatomical model point clous generated from the 3D model. $T_{S'S}$ is calculated using an ICP algorithm in 3D slicer and then applied to M' to create A.

This calculation is done by linking to a built in 3D Slicer Module, Fiducial-Model Registration (Ungi, 2016). This transform ($T_{S'S}$) is also applied to the live tool transforms and should improve the accuracy between the virtual and real space location of the tool on that anatomy.

2.2.3.3 Visualise and Register Mandible Resection (Step 4)

Once the mandible is registered, the surgeon needs to decide where to make the resection osteotomies on the mandible. This decision is based on visual inspection of the soft tissue and bone as well as using the preoperative CT scans.

Visualisation on Mandible CT

This module creates a visualisation of these CT scans and allows the surgeon to register the real time location of where the mandible resection osteotomies were made.

The surgeon uses the probe to create this visualisation. As the probe is moved across the surface of the mandible, the surgeon can see the CT slice at that point on the mandible parallel to the probe axis (Figure 15).

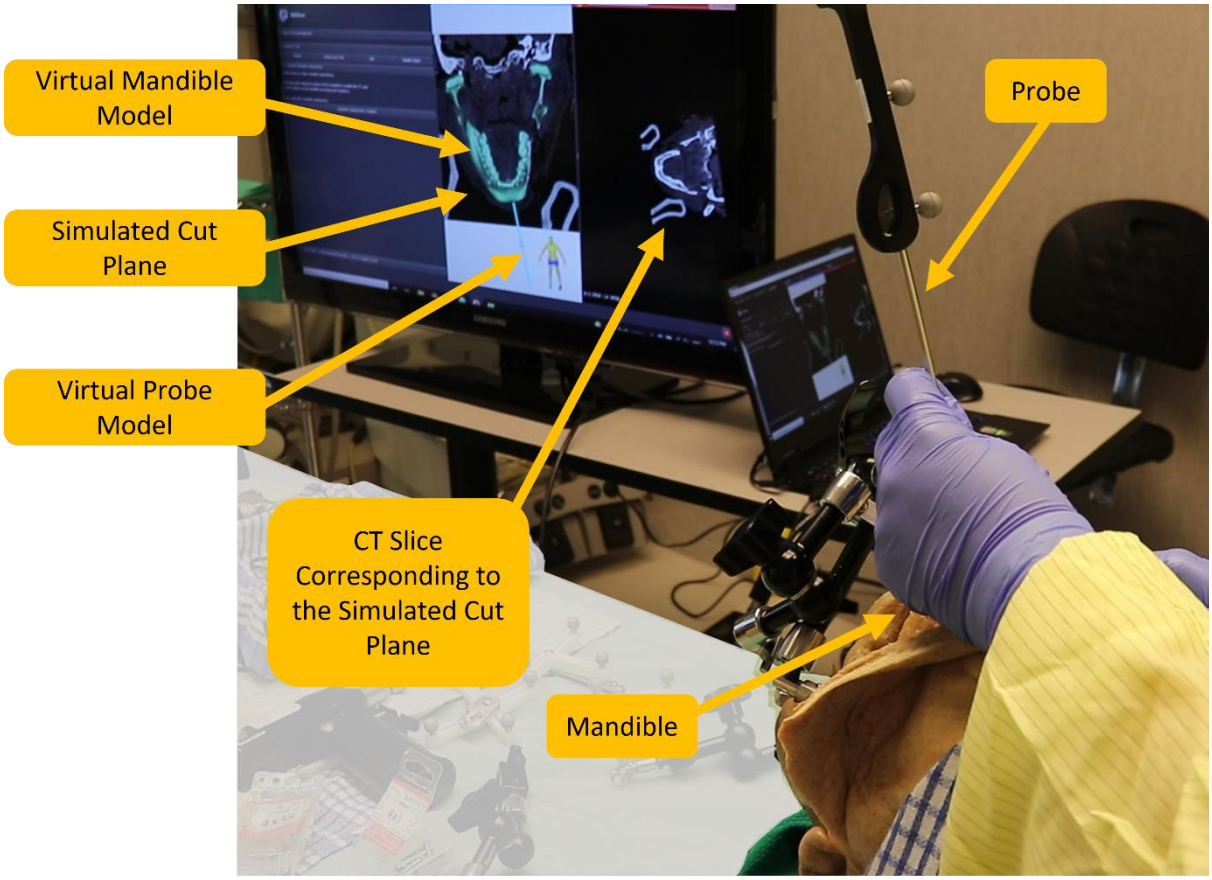

Figure 15 - Mandible CT visualisation for defining the mandible cut planes.

By rotating the probe, the user can view different views of the same location on the mandible. This visualisation can be used to help the surgeon see bony tumours and decide where to make the resection cuts. Once this decision is made, the user performs the osteotomies. This

contrasts with the current technique as these resections are made on-the-fly based on the intraoperative visual and CT inspections, not reliant on any preplanning.

These osteotomies then need to be registered so the system knows where they are with respect to the mandible marker array. This is done by using the probe to place three fiducials on the cut surface of the mandible (Figure 16).

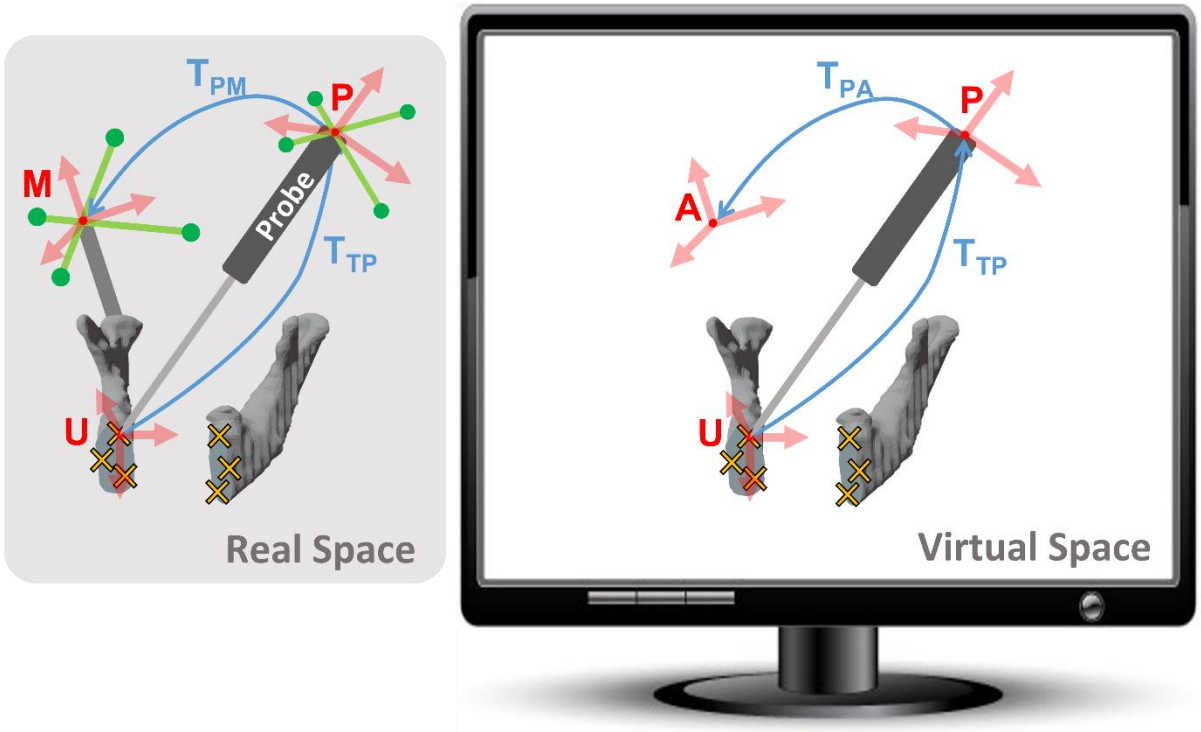

Figure 16 - Digitise points on mandible cut planes where M represents the coordinate frame of the mandible marker array, A represents M transformed by $T_{J''J'}$ (Figure 12) and $T_{S'S}$ (Figure 14), P represents the coordinate frame of the probe marker array and U represent the coordinate frame at the tip of the probe. T_{PA} and T_{UP} are known transforms that allow fiducials (yellow x) to be placed at the probe tip on both mandible cut surfaces.

Care must be taken at this point to ensure the tip of the probe is on the cortical bone to make certain the actual cut plane surface is registered. The system then calculates the transform (T_{RA}, T_{LA}) between the mandible marker array coordinate frame (A) and the coordinate frame created by each of the sets of three points place on the mandible cut surfaces (R, L) (Figure 17).

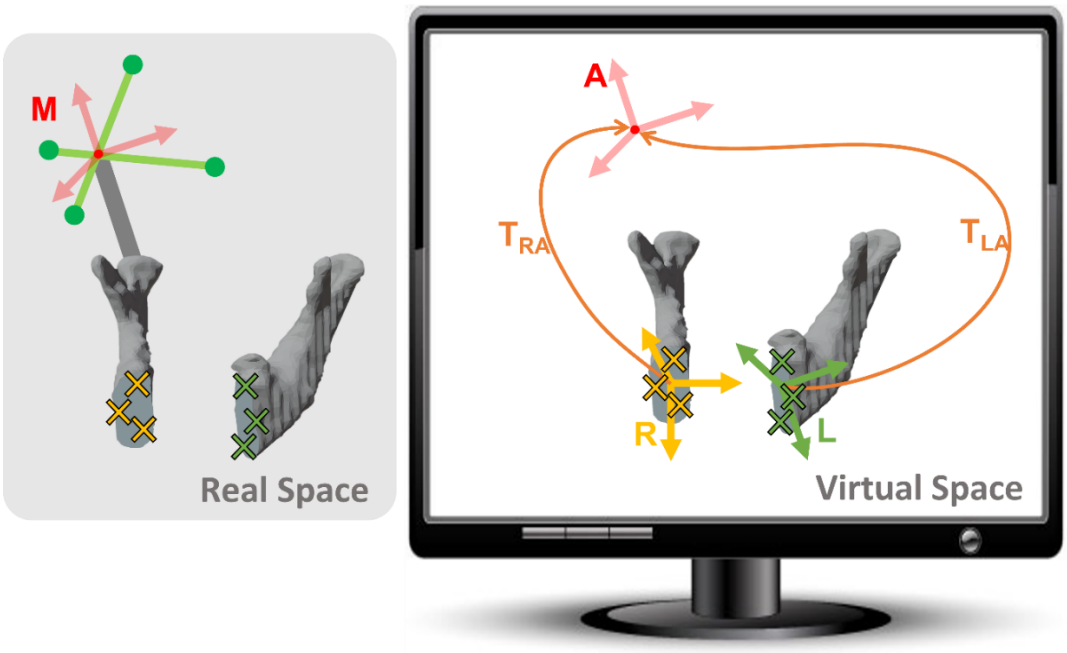

Figure 17 - Mandible cut planes transform calculation diagram where M represents the coordinate frame of the mandible marker array, A represents M transformed by $T_{J''J'}$ (Figure 12) and $T_{S'S}$ (Figure 14), and R and L represent the coordinate frames calculated based on the three fiducials placed on each of the mandible cut planes using the probe.

Once both planes are registered the CT slice for each is visible on the display, as well as the live slice at the probe's location shown in Figure 18.

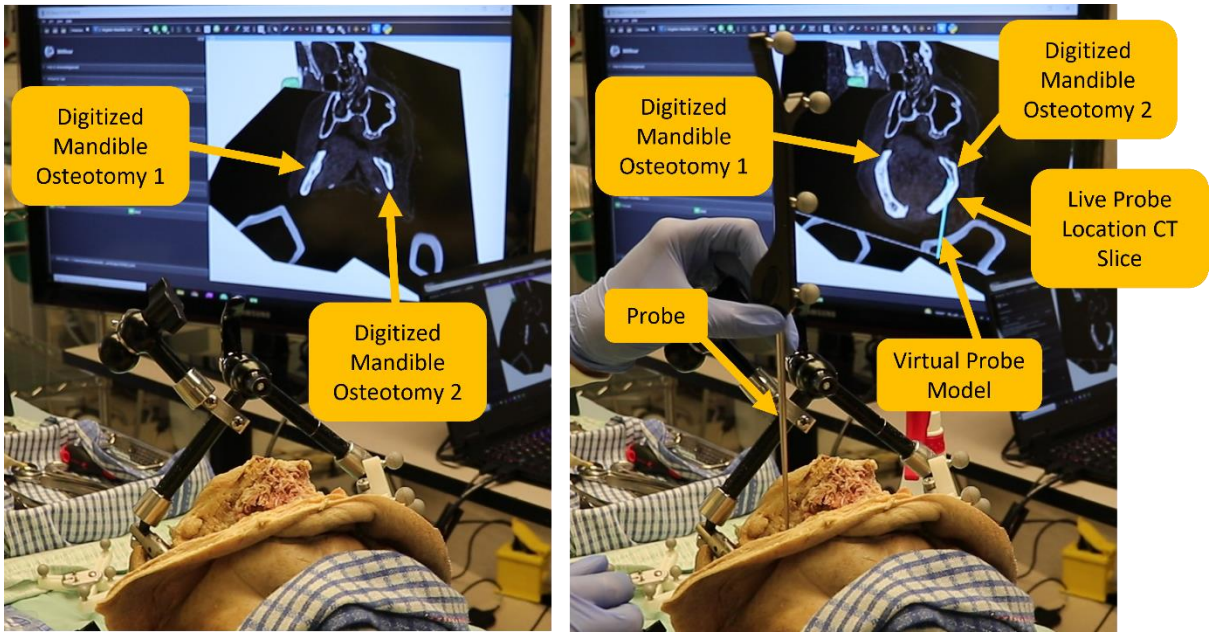

Figure 18 - Visualisation of mandible cuts after digitising cut planes to check the achieved margins.

This allows the user to check they have resected enough of the mandible to achieve the desired margins. These two mandible cut planes are then used to generate the VSP in the operating room.

2.2.3.4 Generate Reconstruction Plan (VSP) (Step 6)

This VSP generates a 3D model of the required fibula segments to bridge the resection gap as well as the fibula cut planes needed to create these segments and the optimal orientation of these segments in the native mandible. The base code used to generate the VSP in 3D Slicer was created by Edward Wang and was an early prototype of the system which is currently in use by Dr Eitan Prisman at Vancouver General Hospital to generate presurgical plans and patient-specific 3D-printed cutting guides (Luu, 2018). This early prototype was used, though a newer optimisation-based method of generating the VSP is currently under development but was not ready for use when these modules were being created.

The base code uses the RDP algorithm mentioned earlier which approximates the desired mandible contour (made up of a series of fiducial points) by a predetermined number of straight lines. The RDP algorithm works by first creating a straight line between the first and last point of the contour which are automatically marked as to be kept. The furthest point from this line is then calculated and if the distance to this line is greater than the user defined value of epsilon, two new lines are created between this point and the first and last point. This process is then repeated for each new line created. In our case the algorithm also considers the maximum number of fibula segments (number of lines created) and the minimum segment length (the length of the lines created). These are user-defined inputs on the module user interface that the surgeon will decide on before generating the VSP. This base code was altered to generate plans compatible with mini plates and the optical tracking system.

Segment Length Limitation

As the RDP algorithm determines the length of each fibula segment to reduce the distance between the straight line and the curved contour, it generally creates segments of varying lengths in a single reconstruction. This often meant that one segment was significantly smaller than the other two (assuming a three-piece reconstruction).

As mentioned above, the optical tracking system was designed to be used with mini plates. Due to the design of the mini plates that were available for testing, the minimum length of the segment was constrained to 28 mm to allow two screws to be secured onto each segment per plate. In order to test the system and devices fully, three-piece reconstructions were desired. To generate VSPs for these situations using the base code RDP algorithm, we simulated large resections to make sure the smallest segment in the reconstruction was above the minimum segment length due to the uneven segment lengths created. Therefore, we replaced the RDP algorithm by simply segmenting the mandible contour fiducials into equal groups based on the number of segments desired. A straight line is then generated for each group creating a plan with approximately equal length fibula segments (Figure 19).

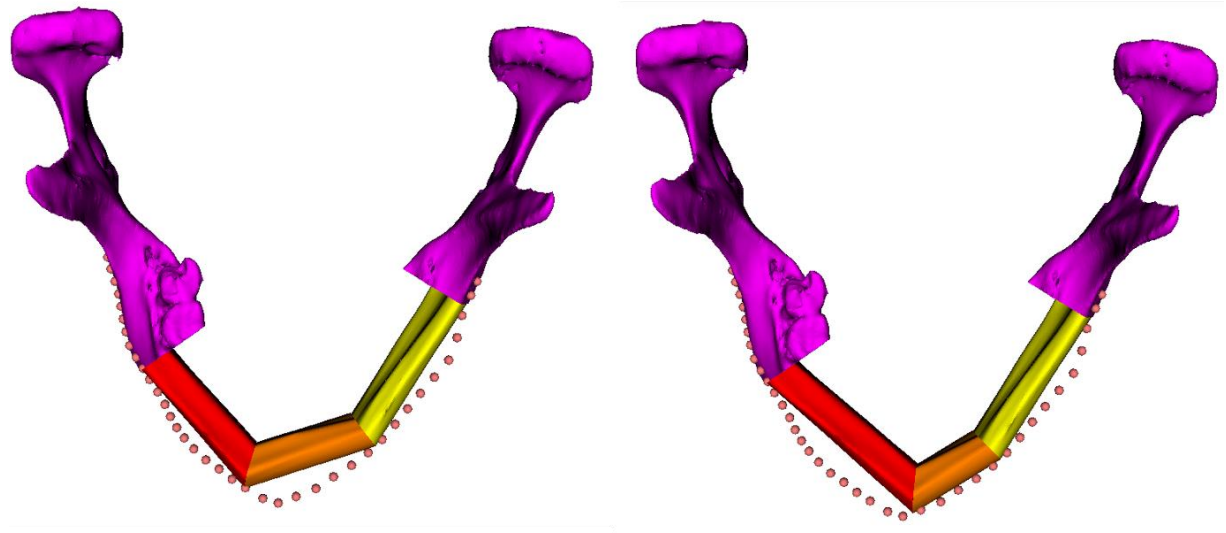

Figure 19 - Comparison of equal segment length plan (left) and RDP plan (right).

This does not produce as optimal a result as the RDP algorithm with respect to recreating the mandible contour as shown in Figure 19 above. However, this module is only intended for testing purposes, and will be replaced in due course by the newly developed optimisation system.

Segment Rotation Problem

Once the RDP lines are created for each fibula segment, they must be translated onto the fibula using landmark registration. To do this, we first defined the vector corresponding to the long axis of the fibula (fibula axis) within the base code. We defined the bounding box of the fibula model using the vtkOBBTree Class and extracted the axes characterizing the orientation of this bounding box. We manually placed a fiducial (initial fibula fiducial) at the distal end of the fibula on the lateral surface. We then used the fibula axis to project this initial fibula fiducial by the length of the current fibula segment and a second fiducial was automatically placed here (end fibula fiducial). We used the line created between the initial fibula fiducial and the end fibula fiducial (segment axis) for each fibula segment to align the segment in the resection gap by overlaying the segment axis and the RDP line created for that segment.

We also determined the rotation of the segment around the segment axis when it was placed in the resection gap using the segment axis. We achieved this by finding the closest point in the fibula model point cloud to this line periodically along the length of the segment axis. We then averaged the corresponding normal associated with each of these points to give the segment normal. We used the same method to determine the mandible normal, periodically sampling the closest point in the mandible model point cloud to the mandible contour polyline along the length of the RDP line and calculated the average normal. We then rotated the fibula segment around the segment axis to align these two normals.

Using this method to arrange these fibula segments in the mandible, the base code often had trouble ensuring the anterior (previously medial) face of the segment was flush with the anterior face of the native mandible and neighbouring fibula segments, and not rotated with respect to them. This is due to the shape of the fibula and the way the fibula axis is calculated. The fibula is approximately a triangular shape; however, there is a twist along the fibula axis. This means that using the fibula axis calculated from the bounding box axes to determine the segment axis could result in this axis projecting into the interior of the fibula. This means that when the segments are placed in the mandible there may be a step created between one segment and the next as shown in Figure 20. It also means that when calculating the segment normal, the closest point in the fibula point cloud may be a point on the interior of the fibula model and therefore, not reflecting the true segment surface normal. This would then cause the segments to be placed in the resection gap rotated with respect to each other also shown in Figure 20.

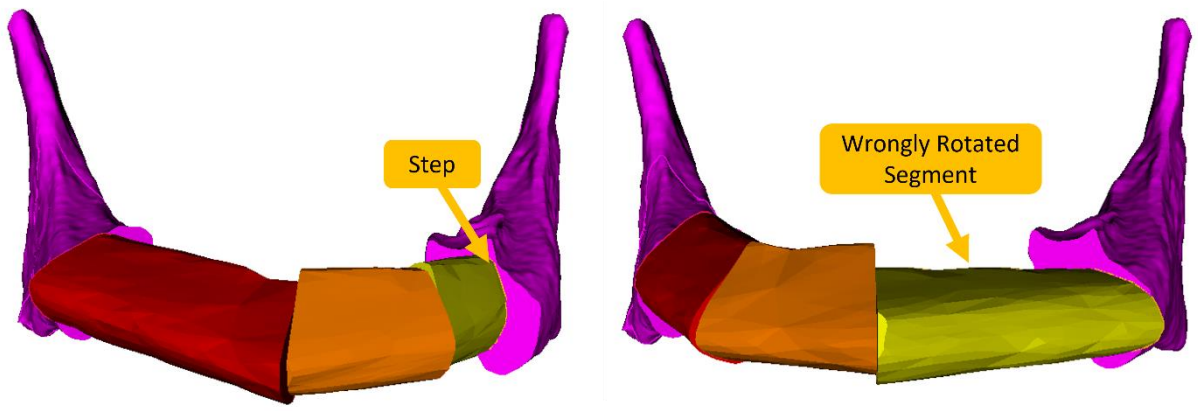

Figure 20 - VSPs containing a step and rotated segments.

Segment Rotation Fix

We addressed these issues by eliminating the need to use the fibula axis to calculate the segment axis. Instead, we manually placed two sets of fiducials periodically along the lateral face of the fibula model. We placed the first set in a line along the centre of this face. The software then calculated the segment axis separately for each segment based on the fiducials in

this set that were within the length of that segment. This prevents the segment axis from protruding below the surface of the fibula model and therefore removes the step between neighbouring segments or native mandible.

We placed the second set of fiducials across the entire lateral face of the fibula model. Again, we determined the fiducials in this set that are within the length of that segment and fitted plane to these fiducials. The normal of this plane is then calculated by the software and this becomes the segment normal. The software then rotates this around the segment axis to align with the mandible normal to determine the rotation of the segment in the resection gap. Using this method to determine the segment normal eliminated the error brought about by sampling the normal from the fibula model point cloud and ensures a flush intersection between fibula segment and native mandible. The outcome of these changes is shown in Figure 21 below.

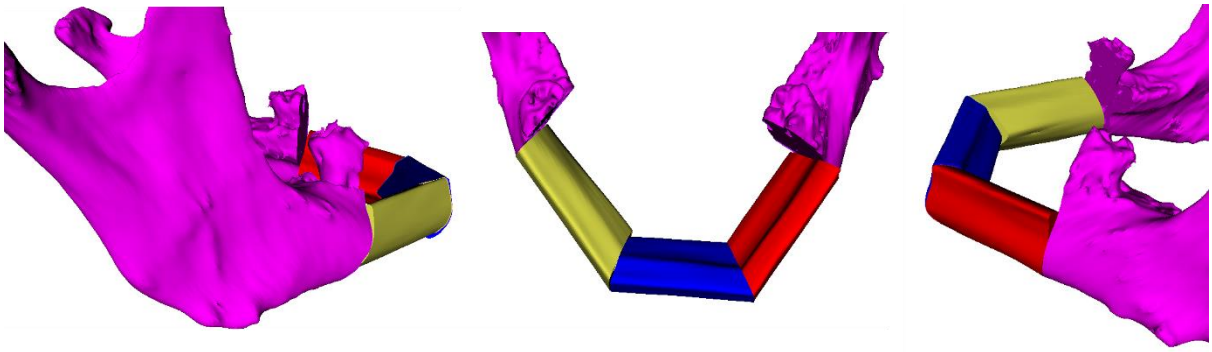

Figure 21 - VSP generated using updated algorithm with no steps or rotation between segments.

Although this method adds an additional manual step in the workflow, it is only intended as a temporary solution to allow for testing to be completed without a major overhaul of the VSP module. As mentioned previously, a new VSP system is under development that will eliminate these issues; however, this is not in the scope of this thesis.

Cut Plane Visualization

The method the base code uses to then generate the cut planes was not. However, we added additional code to allow for these cutting planes to be visualised. A square model is generated for each cut plane that is the same thickness as the saw blade used to make the cuts. The software then aligns this so that the saw blade thickness is on the outside of the fibula segment. So, for the first cut of each segment the software aligns the top of the model with the cut plane and for the second cut aligns the bottom of the model with the cut plane. Finally, the software generates a 3D model of the native mandible and fibula segments (both in the fibula and resection gap) based on these fibula cut planes and the digitised mandible cut planes. Again, the process of generating these models was not altered from the base code.

2.2.3.5 Segment Guidance Set Up (Step 7)

Following the generation of the VSP, the registration of the fibula is performed by the user. This follows the same process as outlined in section 2.2.3.1 producing the transform between the fibula marker array coordinate frame and the fibula model coordinate frame.

Helping Hand Placements

The helping hand devices must then be rigidly connected to each of the fibula segments by the user to allow the segments to be individually tracked. The software displays a virtual model of the fibula segments and the helping hands to allow the user to place them within the bounds of their associated segment as show in Figure 22.

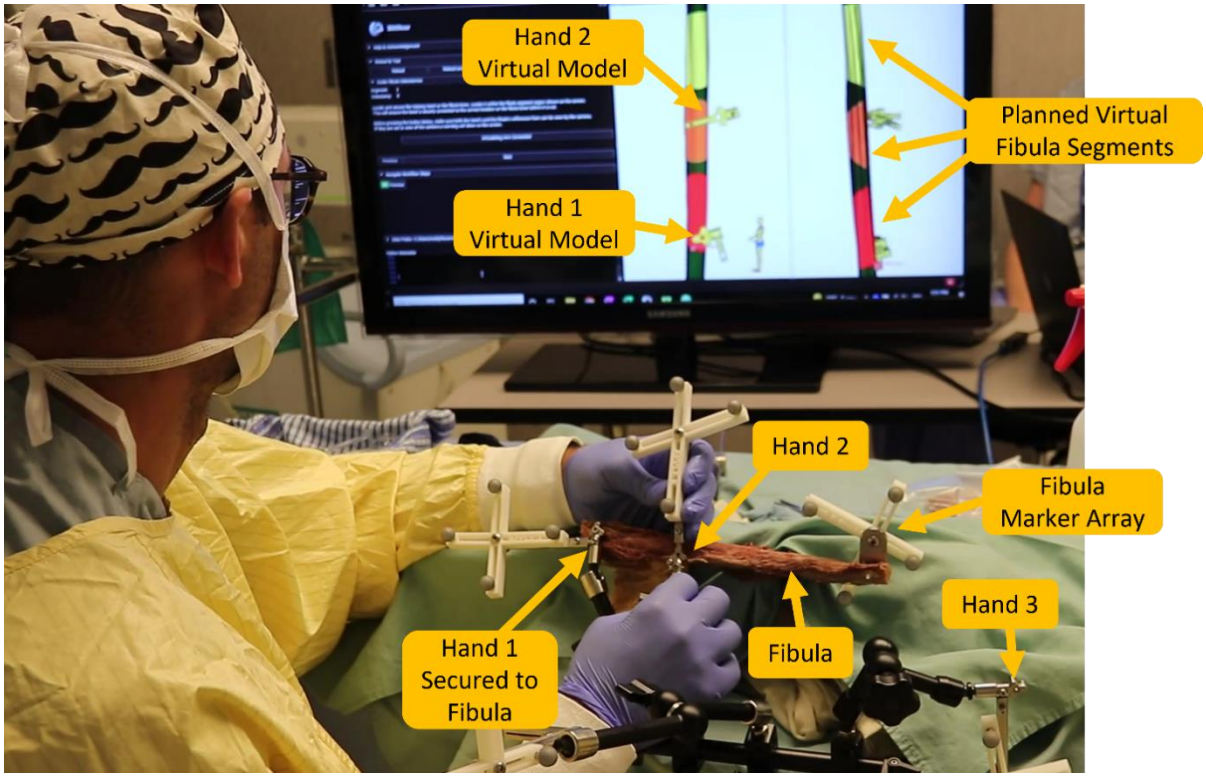

Figure 22 - Visual display for helping hand placement.

To reduce interference between the helping hand devices, we established recommended placement rules of thumb. For a three-piece reconstruction, the most distal hand should be placed at the distal end of its segment, the middle hand in the middle of its segment and the most proximal hand at the proximal end of its segment. We also articulated these rules on the user interface to remind the user how the hand should be placed.

Fibula Segment Tracking

Once the hands are rigidly secured to the fibula, the software calculates a transform between the fibula marker array coordinate frame and each helping hand's marker array coordinate frame. By calculating this transform before the segment is cut from the rest of the fibula (i.e., before it is no longer rigidly connected to the fibula marker array), it negates the need to individually register the segment to their helping hand reference frame. This transform from the hand marker array coordinate system to the segment model coordinate system can be

calculated using the previously defined fibula registration transform and fibula marker array to hand marker array transform as shown in Figure 23.

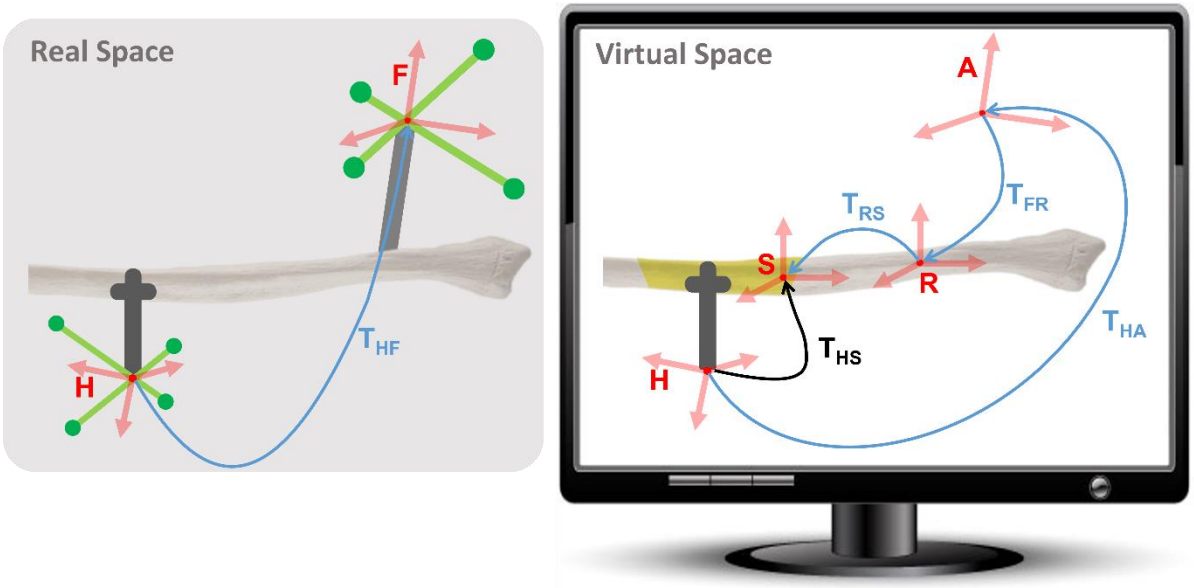

Figure 23 - Fibula segment tracking transform calculation diagram where F is the fibula marker array coordinate frame, A is this coordinate frame transformed by the initial and surface registration transforms, S is the coordinate frame of the fibula segment model, and H is the coordinate frame of the Helping Hand marker array. Using the know transforms shown in blue, the transform between the Hand marker array and the fibula segment T_{HS} can be calculated.

2.2.3.6 Fibula Osteotomy Guidance (Step 8)

Once this transform is calculated, the fibula segments can be created by guiding and making the fibula osteotomies. This may be done using a guided surgical saw or guided cutting guide.

Cutting Visualization

We created a visual display to guide the surgical saw/cutting guide into alignment with the planned cutting plane shown in Figure 24.

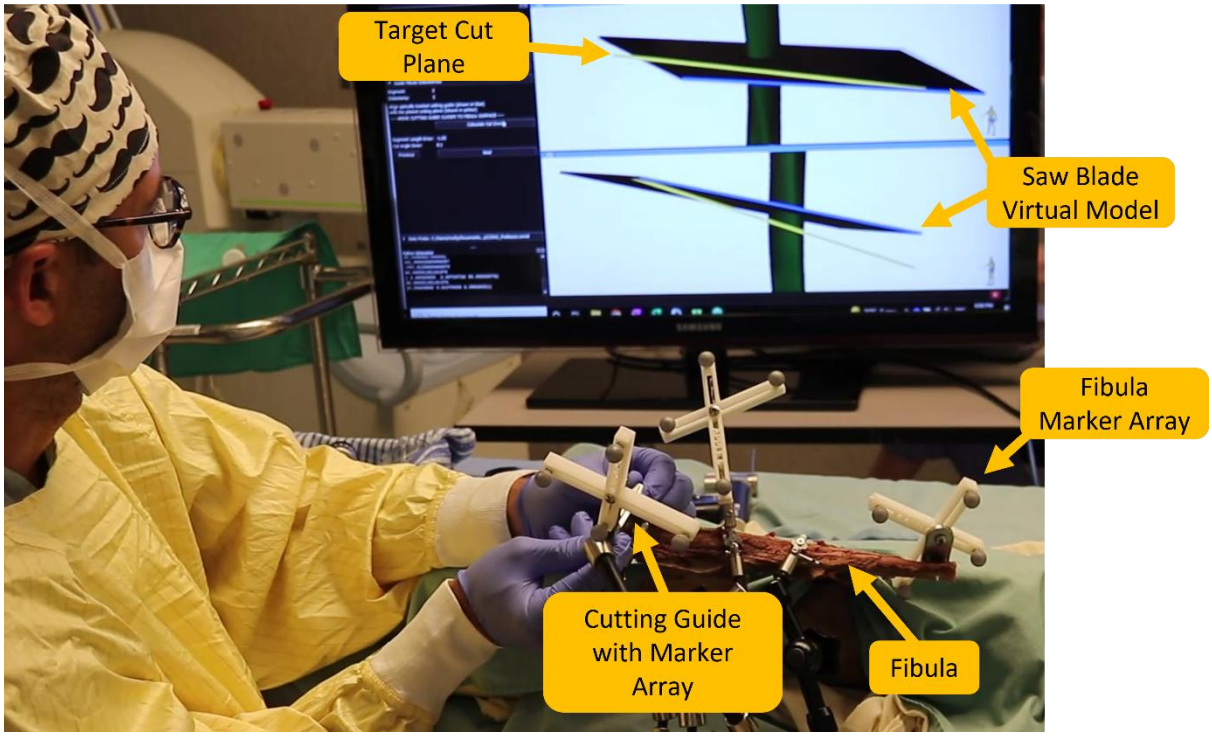

Figure 24 - Fibula osteotomy guidance virtual display.

The yellow/lime green model is the cut plane model created during the VSP and the blue model is the saw blade model. As the saw/cutting guide is moved by the user along the fibula, the software moves the blue model in virtual space. We programmed the software to show two views of the cut model, both looking perpendicular to the cut plane. However, one is rotated 90 degrees around the cut plane normal from the other resulting view one looking at the lateral edge of the cut plane and view two looking at the proximal edge. We showed these two views to allow the user to better visualise the alignment of the saw blade model and cut model in two (X and Y) of the three axes of rotation shown in Figure 25.

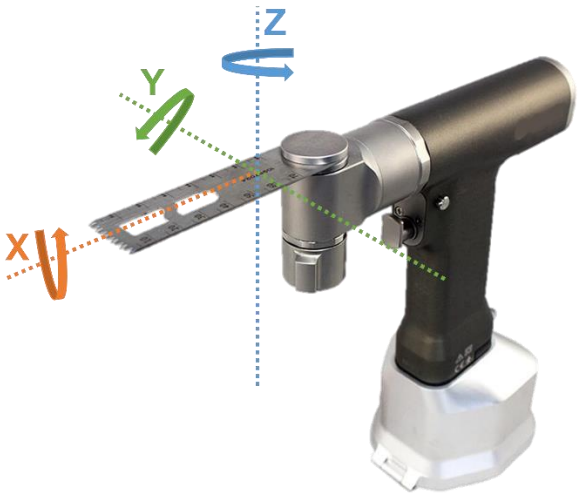

Figure 25 - Surgical saw axes of rotation.

The alignment of the third axis (z) does not need to be aligned using the visualisation as this will not affect the shape of the fibula segment and can be determined by the surgeon's preference. However, care should be taken by the user to ensure that the cut can be made without damaging the pedicle.

Numerical Error Display

Once the saw/cutting guide is positioned, the system can calculate the error between the location of the current saw blade cut plane and target cut plane. As the plane of the saw blade is known, the software compares the normal of the saw blade to the normal of the target cut plane to assess the angle error. However, as the cutting guide sits above the fibula, the length error cannot be calculated as the distance between the center of the planes. Instead, we achieved this by creating a new fibula segment model based on the current location of the saw blade model. The software then calculates the distance between the centre of the cut face of the new segment model and the target segment model. We included this segment length and cut angle deviation associated with this error in the user interface. At this point, the surgeon can decide whether this error is acceptable, and therefore either make the cut or decide if they need to

readjust the position of the saw/cutting guide. This error can then be recalculated by the software until the error is deemed acceptable and the cut is made.

Digitising Actual Fibula Cuts

This process is repeated by the user for the second cut to make the first fibula segment. Once the segment is created, the locations of the two cuts making that segment are digitised by the software. As with digitising the mandible cut planes, using the probe, three fiducials are placed on the cut surface of the fibula segment by the user with respect to the helping hand marker array. These points are then transformed into the fibula model coordinate frame by the software to allow an actual fibula segment model to be created and the VSP to be updated. We showed the actual and target segment models on the display, overlayed to visually show the error between them. The difference in length between this actual fibula segment and the target fibula segment, and the difference in angle of the proximal and distal ends of the segments are then calculated by the software and displayed in the user interface. These errors are calculated by first applying a plane to each set of three fiducials, transformed to the fibula model coordinate frame, placed on each end of the fibula segment. These planes are then used by the software to create an actual fibula segment model. The software then compares the normal of each plane to the normal of the target plane to give the angle error and calculates the distance between the centre of the cut surfaces of the actual and target fibula segment models to give the length error.

Depending on the size of these errors, it may be detrimental to update the plan based on the actual segment model. This is due to the fact that digitising the actual cut planes to create this model has an error associated with it, the size of which is dependent on the fibula registration error and the probe calibration error. Therefore, at this point the surgeon can decide whether

these errors are big enough to warrant updating the VSP to adjust the following segments to take account for these errors.

2.2.3.7 Update VSP to Incorporate Fibula Osteotomy Errors (Step 9)

Position Adjustment

If the plan is updated, the first step is to adjust the position of the actual fibula segment model in the resection gap so it is in contact with the native mandible or the previous fibula segment but there is no overlap between them. The software achieves this by incrementally moving the segment in virtual space along the segment axis calculated earlier until this overlap/gap is removed. Depending on whether the actual segment overlaps the mandible/previous fibula segment or there is a gap between them, the segment will be moved by the software in one direction or another along the segment axis. The software uses the Dice score to determine whether an overlap is present or not.

The alignment of the segment axis and the original RDP line is maintained by the software. This means that the angular error of the first osteotomy of each segment is not corrected for in the updated plan. Whilst maintaining the contour of the reconstruction, this method may reduce the bony contact between the fibula segment and native mandible/previous fibula segment. We adopted this method based on discussion with the supervising surgeon, the rationale being that as the expected angular error would be approximately three and a half degrees (based on literature (Pietruski, 2019a)), it was hypothesised that the maximum resulting gap between the native mandible/previous fibula segment and the actual segment would be sufficiently small to still permit bony union, and therefore alignment with the mandible contour was deemed to be a higher priority.

Recalculating VSP

Once the actual segment is repositioned, the remaining fibula segments are then recalculated by the software. We achieved this by rerunning the VSP module; however, the first resection plane is now moved from the right mandible osteotomy to align with the segment's second osteotomy actual cut plane as shown in Figure 26.

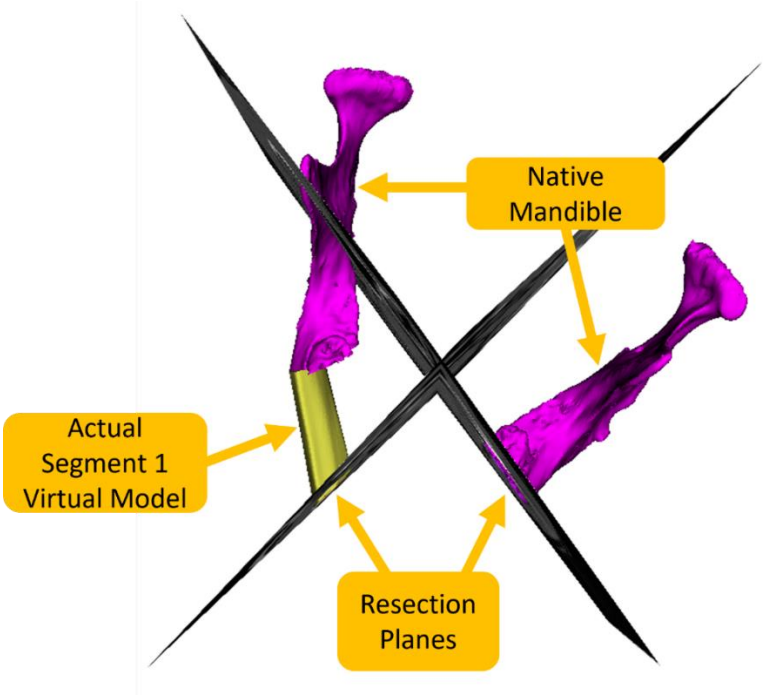

Figure 26 - Updated resection planes for updating the VSP.

By rerunning this module, the cut plane models, remaining fibula segment models, and their locations within the mandible are all updated by the software whilst maintaining the segment's alignment with the mandible contour and eliminating any step or rotation between the fibula segments and their neighbours.

These steps are repeated for each of the fibula segments in the VSP. After the final segment cut planes are digitised, the actual segment location in the resection gap is adjusted by the software as described above, but there are no further fibula segments to adjust. Therefore, no additional changes are made to the VSP. This will result in a slight overlap or gap between the last fibula

segment and the native mandible. The length of this final segment is increased by 0.5 mm during the creation of the VSP to try to ensure that once the segment is moved into its final placement, there is no gap between it and the mandible. This is because an overlap can be corrected with a freehand trim of the segment, but a gap cannot be corrected without shifting the native mandible segments with respect to each other. Following initial system testing, we will re-evaluated whether this increase to the final segment length will frequently be required.

2.2.3.8 Reconstruction Alignment

After cutting all the fibula segments, they must be aligned with respect to each other and placed in the mandible gap by the user. As described above, each of the segments can be tracked by the software using the rigidly connected helping hand marker arrays.

Segment to Segment Alignment (Step 11)

As shown in Figure 27, we illustrated the target location of all segments in the software as a partially transparent green model of the segments. We also made a second model of each of the segments (all a different colour and partially transparent) visible which will move in virtual space as the physical segment is move. We added an axis to each of the segment models to reduce the difficulty of aligning the target and actual models.

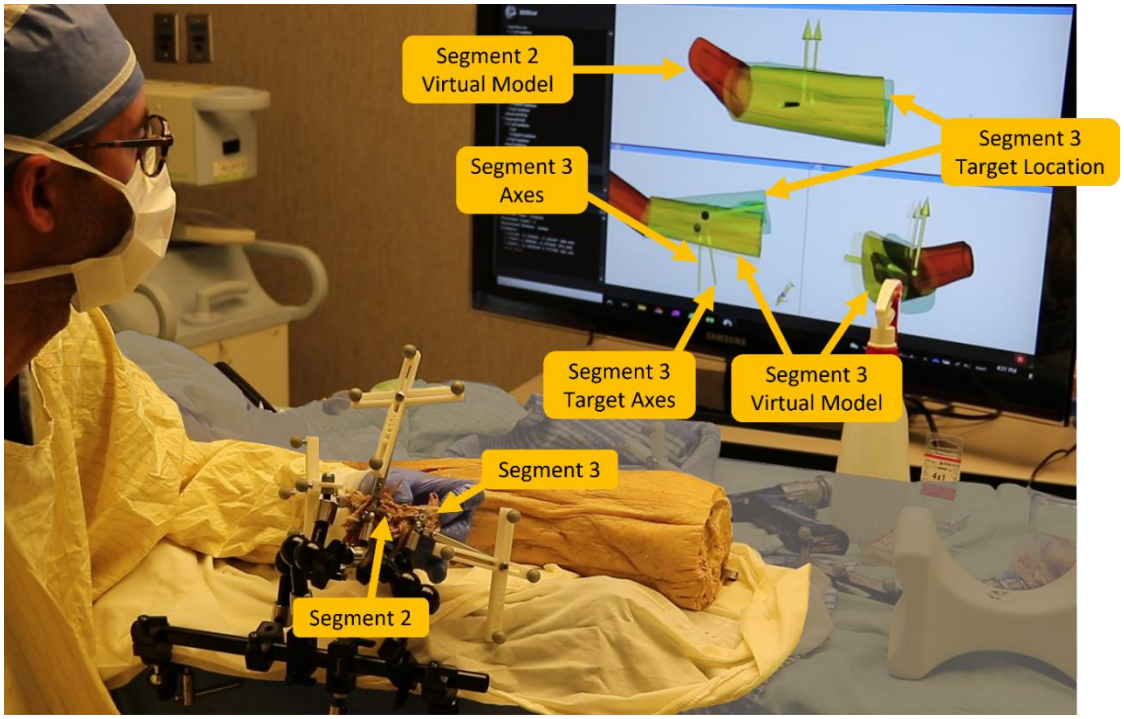

Figure 27 - Segment alignment guidance virtual display.

Th software tracks and aligns each segment with respect to segment two (the middle segment for a three-piece reconstruction). The surgeon will use the visualisation to align the segment based on the VSP but may decide to deviate from this plan if they consider it will improve the surgical outcome. However, as the segments are at this point away from the native mandible fragments, care must be taken by the user if deviating from the plan as this may cause the reconstruction to not fit in the resection gap. Once the user has aligned all the segments, they secure the segments to each other using mini plates so the segments become rigidly attached to each other. At this point only one marker array needs to be connected (Helping Hand Two's marker array) to continue tracking the reconstruction.

Segment to Segment Transform Calculation

Before removing any hands, the transform between hand two's marker array coordinate system (H2) and the other fibula segments model coordinate systems (S1) must be calculated by the software (T_{H2S1}). The software does this by utilising previously calculated transforms between

the individual hands marker array coordinate systems (H1) and their associated segment model coordinate systems (T_{S1H1}), and the live transform between the individual hands marker array coordinate system and hand two's marker array coordinate system (T_{H1H2}) (Figure 28).

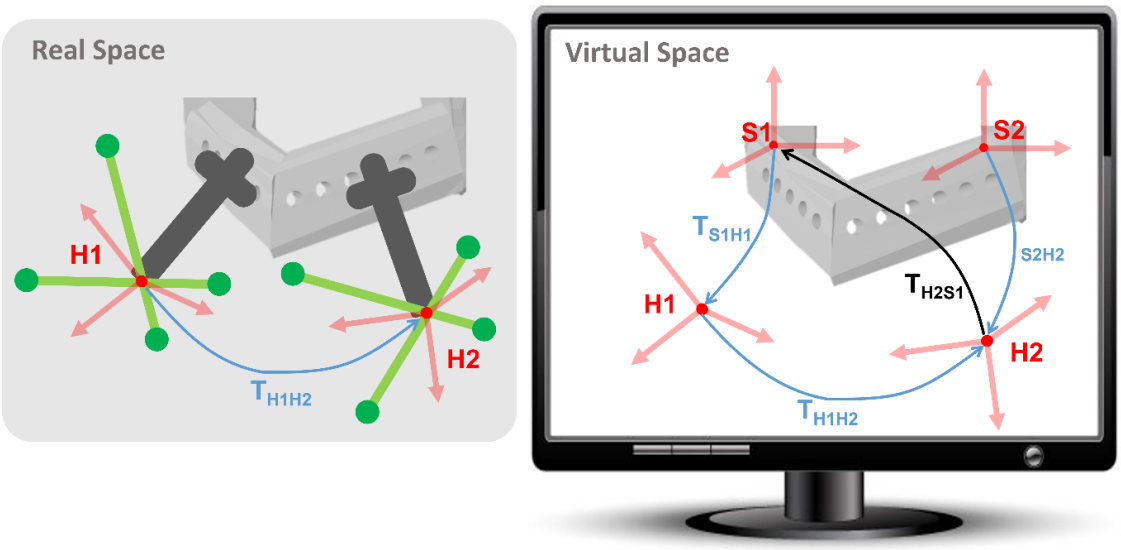

Figure 28 - Segment alignment in mandible transform calculation diagram where S1/S2 represent the coordinate frame of the fibula segment models and H1/H2 represent the coordinate frames of the Helping Hand marker array. The know transforms between the Hand and their associated segment (T_{S1H1}/T_{S2H2}), and the transform between the two hand marker array coordinate systems (T_{H1H2}), are used to calculate the transform between segment 1 and Hand 2's marker array.

Hand Two Marker Array Change

Once the software has calculated this, the excess helping hands can be removed by the user. To reduce interference between hand two's marker array and the patient's body, we designed it so the marker array could be attached in two distinct orientations as shown in Figure 29.

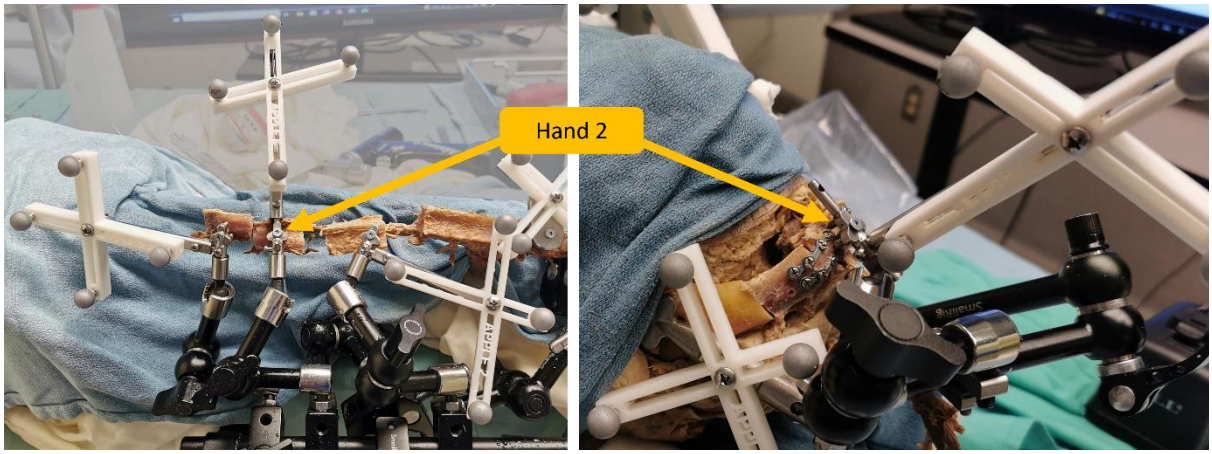

Figure 29 - Hand two marker array orientations for aligning the segments with respect to each other (left) and in the mandible (right).

Therefore, before aligning the reconstruction in the resection gap, the reconstruction models location must be updated by the software to account for this change in marker array orientation. As the transform between the Helping Hand virtual model coordinate system (C) and the hand two marker array orientation coordinate frames (H2 and H') from the Helping Hand set up, the transform between the two marker array coordinate frames can be calculated by the software as shown in Figure 30 below.

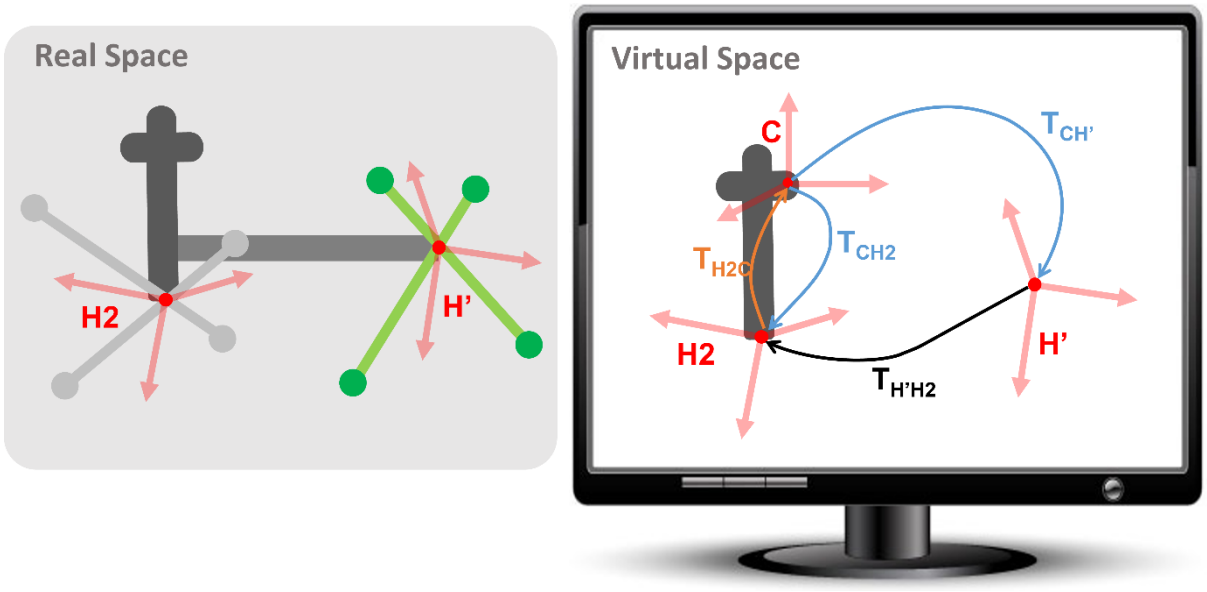

Figure 30 - Marker array orientation change transform calculation diagram where the transform between Hand two marker array in the fibula position (H2) and the mandible position (H') is calculated ($T_{H'H2}$) based on the know transforms between the Hand marker array coordinate system locations and the Hand virtual model coordinate system (C).

Reconstruction Alignment in Resection Gap (Step 12)

We used a similar visualisation as describe above to align the reconstruction in the mandible resection gap. However, we made the remaining mandible segment model visible (shown in Figure 31) and the segments are now tracked and aligned with respect to the mandible marker array. Again, this visualisation will guide the segment to align with the VSP, though the surgeon may opt to deviate from this if they expect it will improve surgical outcomes.

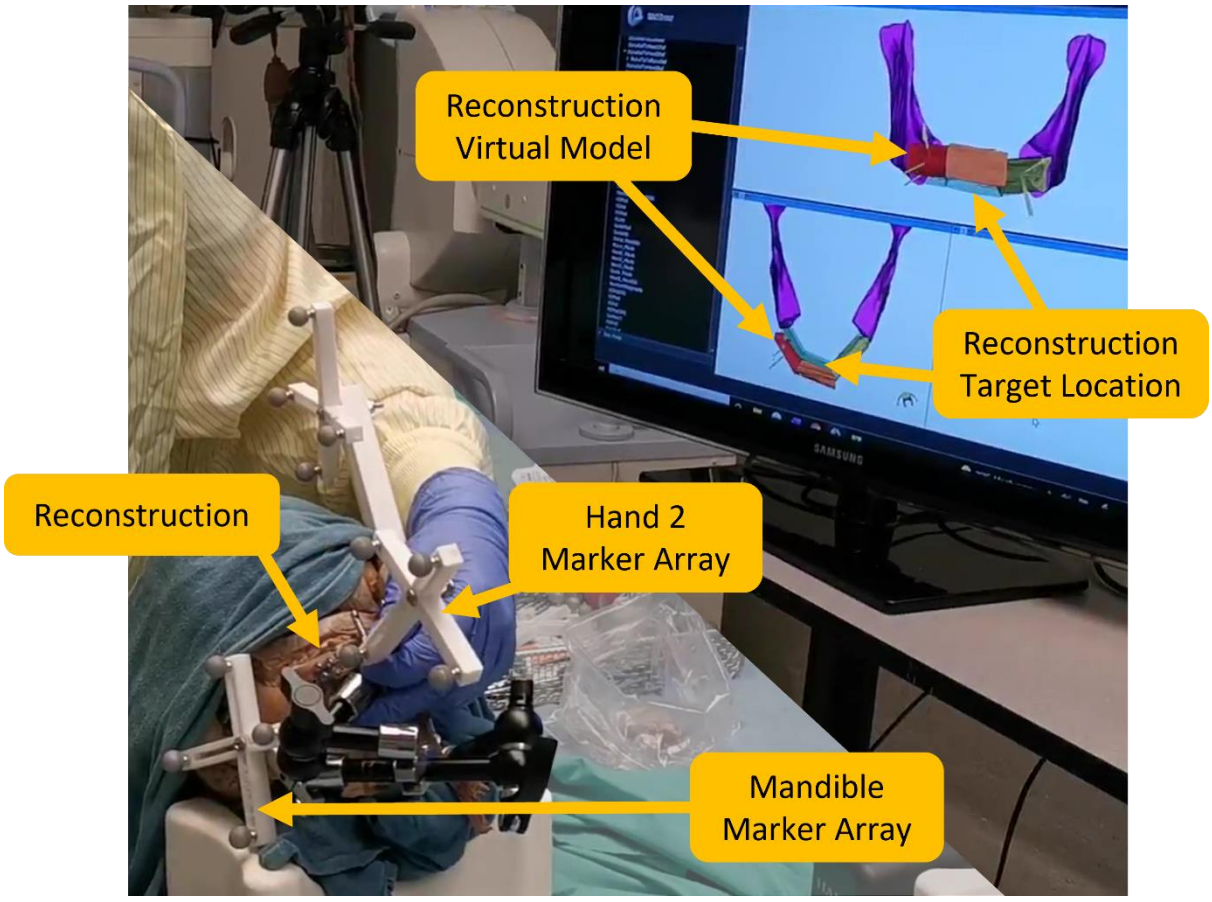

Figure 31 - Reconstruction alignment guidance virtual display.

Once the surgeon feels that the reconstruction is sufficiently aligned, they will secure the reconstruction to the mandible using mini plates. At this point, the image-guided section of the surgery is completed and all additional hardware can be removed.

2.3 Full System Integration and Workflow Testing

I developed these modules concurrently with the design and manufacturing of the hardware undertaken by Georgia Grzybowski, details of which are outlined in (Grzybowski, 2021). We tested individual aspects of the system during development; however, once the first iteration of the system was completed, we fully integrated and tested it before we conducted any accuracy studies.

Georgia Grzybowski, the collaborating ENT surgeon and I completed this initial testing on artificial bone models. These tests generally involved running through the full workflow outlined in section 2.1.3 and iteratively updating the software system (and hardware that is not discussed here) based on our own user experience. To test the system in the most crowded working conditions and using all hardware components, we simulated large tumours to allow three-piece reconstructions to be performed.

Based on feedback provided by the surgeon and our own user experience, we added the following features: (1) additional descriptions in the modules to walk the user through the step; (2) showing a visual warning on the display when marker arrays are not visible by the camera; and (3) adding a step to allow the surgeon to alter the mandible contour before generating the VSP. A list of usability observations and the additional features that were added to address them is outlined in Appendix B:.

2.3.1 Segment Alignment Workflow Testing

Whilst testing the system as outlined above, the question arose of whether it was necessary to use the guidance system to align the fibula segments. It was hypothesised that if the accuracy of the fibula osteotomies was high enough, the surgeon should be able to manually place the pieces together without needing to use optical tracking and guidance. This would reduce the

complexity of the system somewhat as helping hand marker arrays would no longer be necessary and may also reduce the total surgical time.

Alternatively, rather than using the guidance to arrange the segments in the fibula workspace and then aligning them together in the resection gap (as described in section 2.2.3.8), the fibula segments could individually align in the mandible gap directly. This would remove one step from the workflow, potentially reducing the surgical time. However, that would require each segment to be connected to its helping hand and associated marker array whilst in the mandible working area which is a limited space. It would also require the blood supply to the segments to be cut before arranging the segments, therefore potentially increasing ischemia time.

As each of the three proposed workflow techniques presented has its own strengths and weaknesses, the accuracy of each was assessed in a more formal study methodology as outlined below.

2.3.1.1 Methods

Three possible workflows were developed for guiding the alignment of the fibula segments with respect to each other into the resection gap in the mandible, each depicted in Figure 32 below.

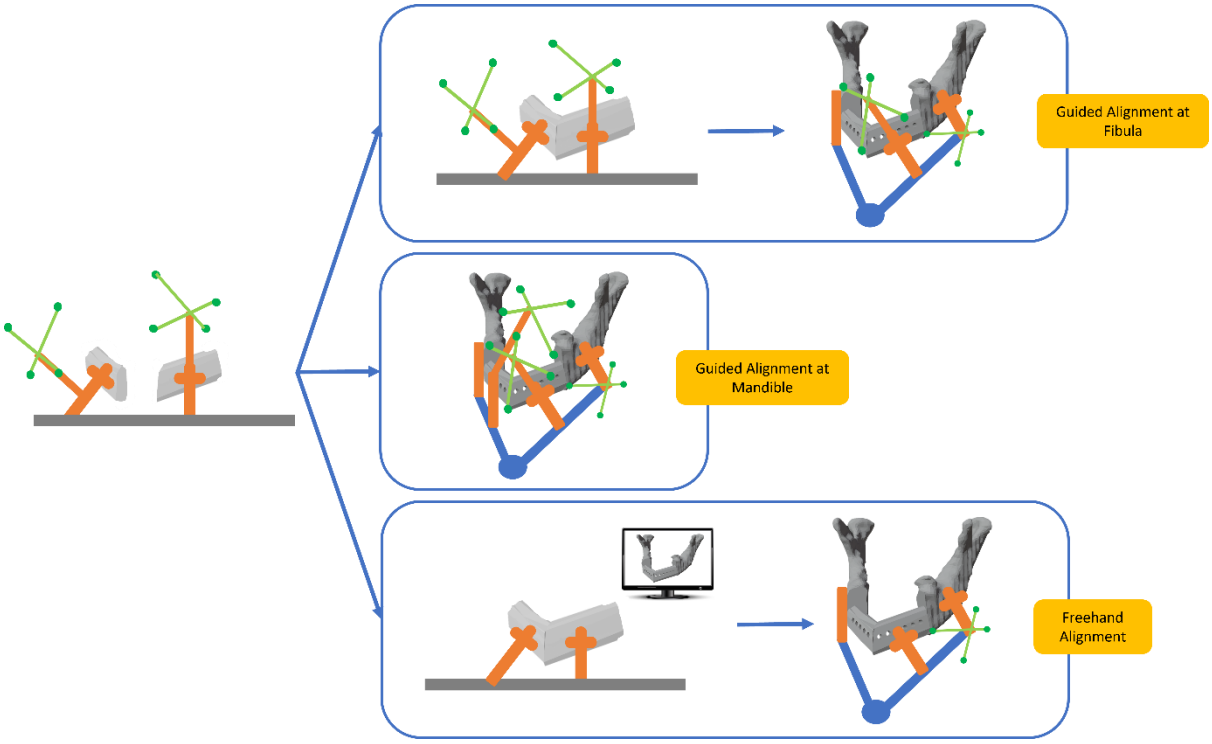

Figure 32 - Potential segment alignment workflows.

Guided Alignment at Fibula (as described in section 2.2.3.8)**:** Fibula segments are arranged with respect to each other using the optical tracking system whilst in the fibula working space. They are then secured together, and all Helping Hands are removed except Helping Hand Two. The full reconstruction is moved up to the mandible workspace whilst rigidly connected to Helping Hand Two and aligned into place in the resection gap using the optical tracking system. The full reconstruction is then secured in the mandible gap and Hand Two is removed.

Guided Alignment at Mandible: All fibula segments are brought into the mandible working space whist connected to their associated Helping Hands. They are then each aligned in the resection gap directly using the optical tracking system. Once the segment is in place, the marker array connected to its Helping Hand can be removed to free up space in the mandible working space. Once all segments are aligned, they are secured to each other and to the mandible.

Freehand Alignment: Fibula segments are arranged with respect to each other only referring to an on-screen depiction of the desired reconstruction (all marker arrays are removed from the Helping Hands). They are then secured together, and all Helping Hands are removed except Helping Hand Two. The full reconstruction is moved up to the mandible workspace whilst rigidly connected to Helping Hand Two and aligned into place in the resection gap again only referring to an on-screen depiction of the desired reconstruction. The full reconstruction is then secured in the mandible gap and Hand Two is removed.

Study Design

Nine similar reconstructions were completed in total, three using each of the segment alignment workflows described above. One set of reconstructions was performed by the collaborating surgeon, one by our thesis supervisor, and one by Georgia Grzybowski and myself. As all participants are within the project group, ethics approval was not required to perform this study.

To eliminate additional errors brought about by guiding the cuts to make the fibula segments, they were 3D-printed to exactly match the VSP for six of the reconstructions. This would help ensure that only the accuracy of the fibula segment guidance method was assessed. As outlined in section 2.1.3, the mandible was fixated using the external fixator device, the osteotomies were made, and their locations digitised. The VSP was generated, and the models of the desired fibula segments 3D-printed using and Ultimaker 2 3D printer. The segments took approximately six hours to print so the reconstruction was completed the following day. A workflow diagram of this methodology is outlined below.

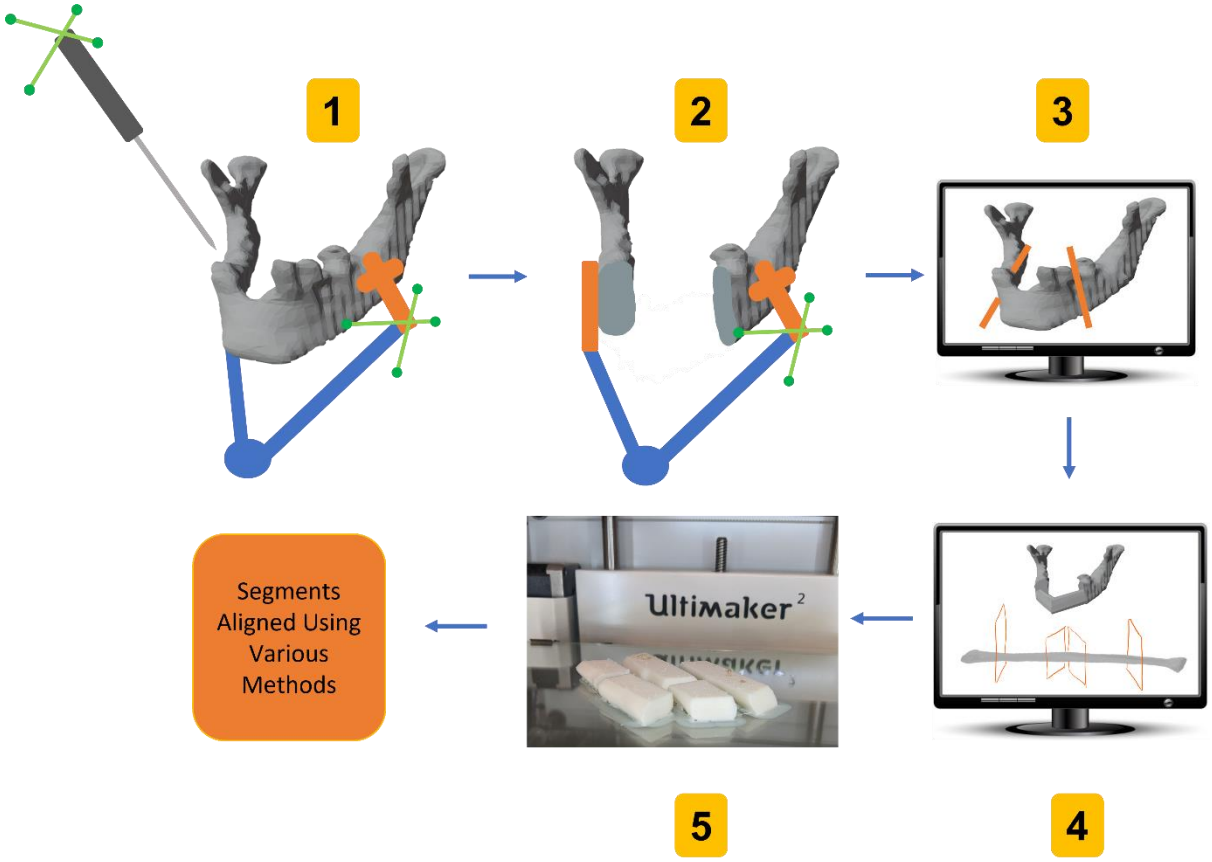

Figure 33 - Workflow diagram of study using 3D-printed fibula segments including the following steps: (1) mandible registration, (2) perform mandible resection, (3) digitise mandible cut planes, (4) generate a VSP, (5) 3D-print planned fibula segments, then perform the guidance method.

The final set of three reconstructions followed the workflow outlined in section 2.1.3 so were performed using fibula segments that were created using the guided cutting method.

Results Analysis

To assess the accuracy of the reconstructions, a CT scan was taken of the reconstructed mandible using a MicroCT (HR-pQCT: XtremeCT, Scanco Medical AG) with an isometric voxel size and slice thickness of 246 micrometers. We then segmented the CT images manually using thresholding and trimming tools in 3D Slicer. From this we generated two 3D models, one of the full reconstructions and one of just the fibula segments. An example of this is shown below.

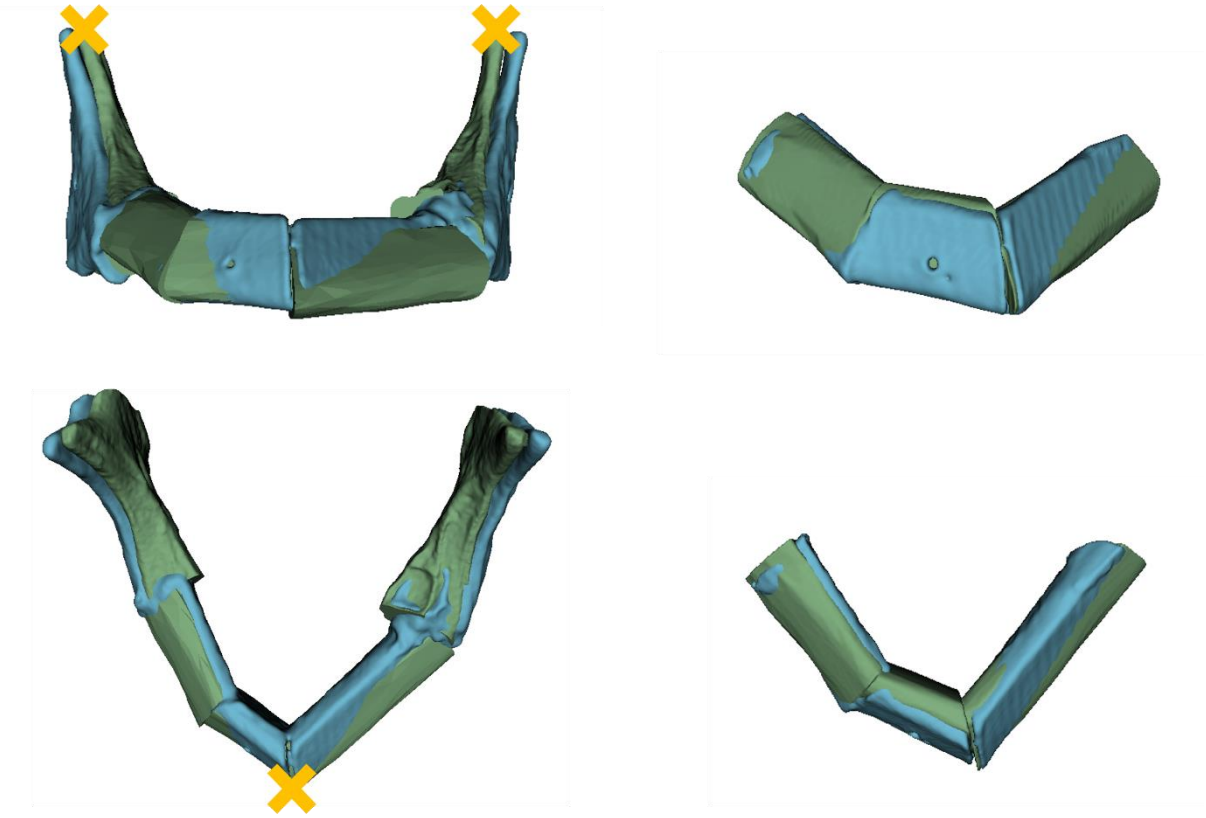

Figure 34 - Example of 3D models created of the full mandible reconstruction and of the aligned fibula segments. The yellow crosses represent the fiducials placed to calculate accuracy metrics.

These models were then used to assess the accuracy of the individual reconstructions. To do this we manually placed three sets of fiducials, one on each coronoid and one on the most projected point of the reconstruction (see yellow crosses in Figure 34). Each set was made up of three fiducials which were independently placed to reduce the error associated with manually identifying a location of placing a fiducial there. This average point for each set was then used to calculate the following accuracy metrics:

Width Deviation: The distance between the average coronoid points was calculated for VSP model and for the post reconstruction CT model. The difference between these two distances is the width deviation.

Projection Deviation: The distance between the centre of the width line and the most projected point on the reconstruction was calculated for the VSP model and the post reconstruction CT model. The difference between these two distances is the projection deviation.

Iterative Closest Point (ICP) Error: The VSP model and the post reconstruction CT model were aligned using paired point registration followed by a model-to-model registration in 3D Slicer. This model-to-model registration uses the same ICP algorithm as described in section 2.2.3.2. However, the fiducials used are the point clouds of each model. The final root mean square distance error achieved indicates the offset between the two models when overlaid. This can be used to show how similar two models are and therefore how well the fibula segments are aligned.

Dice Score: Once the models are overlaid using the above method, we calculated the Dice score in 3D Slicer. This is the ratio of the overlapping volumes to the average of the two volumes. This again can show how similar two models are and therefore how well the fibula segments were aligned.

2.3.1.2 Results

The results described above are shown in the graphs below and summarised in Table 2. The width and projection metrics were consistently high across all trials using the Guided Alignment at Fibula and Guided Alignment at Mandible approaches. This is not seen when using the Freehand method. Subsequently, in all metrics shown in the graphs, the Freehand Alignment produced the best results. However, when the ICP error and Dice score were calculated just using the fibula segment models, the guided alignment methods became more accurate.

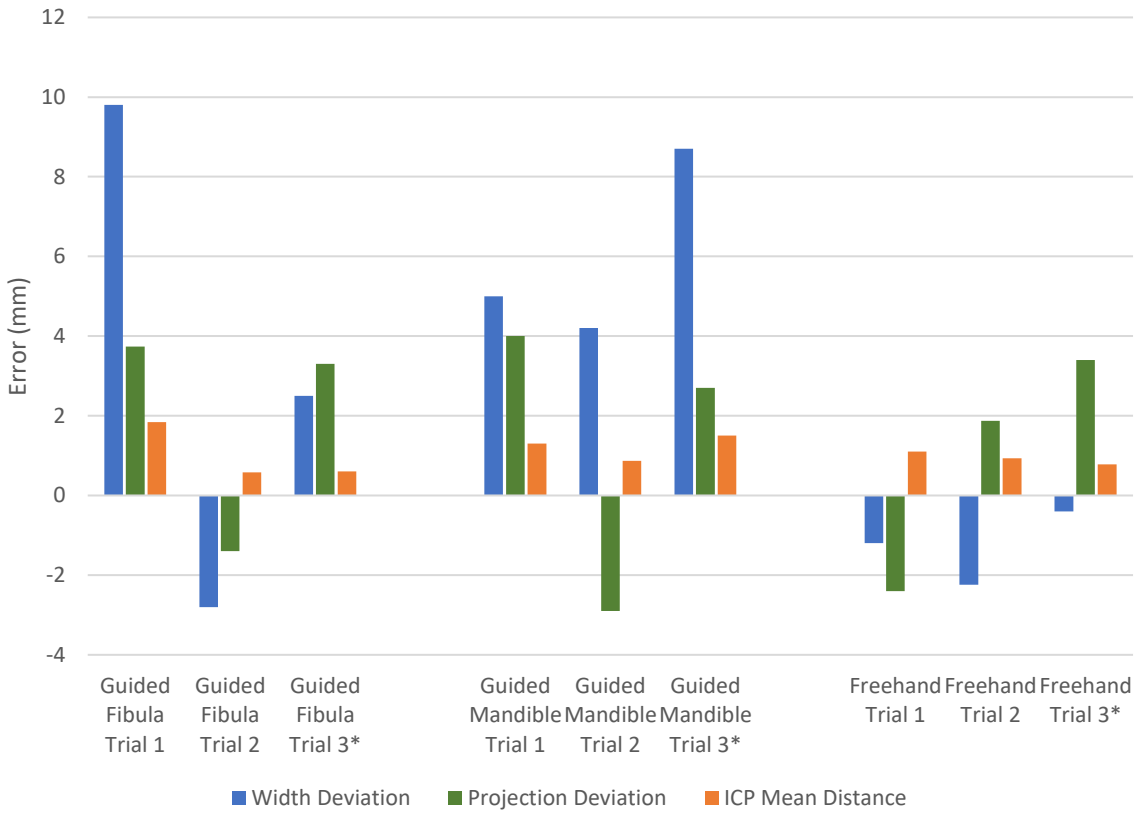

Figure 35 - Width, projection and ICP error results for all three workflow study reconstruction sets

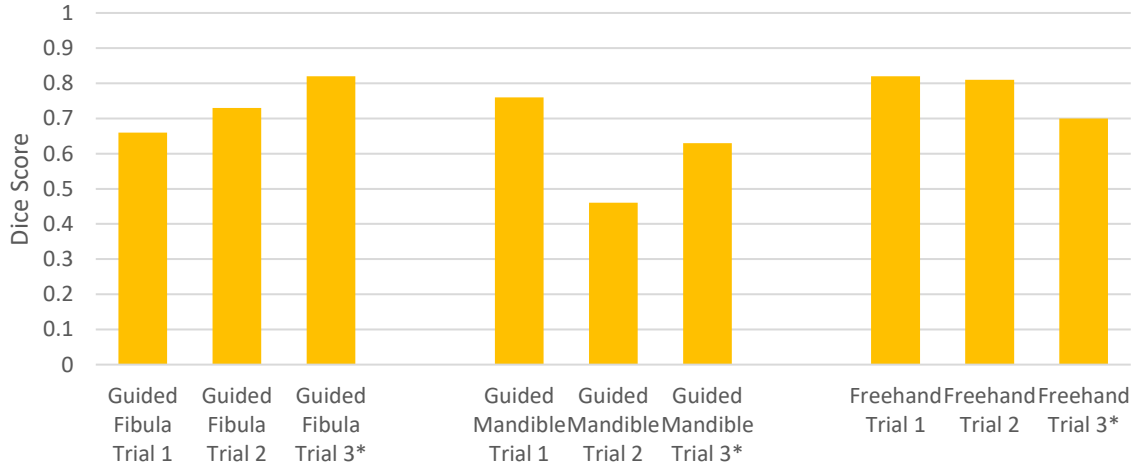

Figure 36 - Dice score results for all three workflow study reconstruction sets

Error Metric	Guided Alignment at Fibula	Guided Alignment at Mandible	Freehand Alignment
Width Deviation (mm)	3.17	6.0	-1.28
Projection Deviation (mm)	1.88	1.26	0.96
ICP Mean Distance (mm)	1.01	1.22	0.94
Dice Score	0.74	0.62	0.78
ICP Mean Distance* (mm)	0.85	0.95	0.72
Dice Score*	0.87	0.85	0.81

Table 2 - Average accuracy results for each segment alignment method (calculated using the fibula segments only model)*

2.3.1.3 Discussion

The errors achieved during this study where slightly worse than expected in most cases. We hypothesised this to be partially due to the mechanism used in the mandible external fixator causing the mandible segments to shift with respect to each other which was indicated from the large width deviation errors. This is further discussed in Georgia Grzybowski's thesis (Grzybowski, 2021).

Segment Alignment Comparison

In terms of alignment accuracy, the most relevant error metrics are the ICP error and the Dice score as they indicate how similar the pre and post reconstruction models are. When comparing between the three segment alignment methods it was expected that the accuracy of the two guided methods would be better than the freehand method. However, in terms of average ICP error Freehand Alignment performs best, followed by Guided Alignment at Mandible and then Guided Alignment at Fibula. Additionally, in terms of average Dice Score, Freehand Alignment still performs best; however, Guided Alignment at Fibula performed better than Guided

Alignment at Mandible. This was somewhat surprising; however, the mandible width deviations were higher for both the guided method and may be contributing to this ranking. It is not clear why this shift is higher for the two guided alignment methods. After noticing this large deviation, during subsequent testing the shift was monitored though the workflow and it was found that a large shift happens when the mandible is initially cut. This was shown to happen for all three alignment methods. This is discussed further in Georgia Grzybowski's thesis (Grzybowski, 2021).

To try and to eliminate additional error associated with the mandible segments moving with respect to each other, the ICP error and Dice score was recalculated for the first reconstruction of each of the workflow methods using the models of only the reconstructed 3D-printed segments. As shown in Table 2, the Freehand Alignment still performed best in terms of ICP error (0.72 mm), followed by Guided Alignment at Fibula (0.85 mm) and then Guided Alignment at Mandible (0.95 mm). However, the Dice score results indicate the Guided Alignment at Fibula performed best (0.87) followed by the Guided Alignment at Mandible (0.85) and finally the Freehand Method (0.81). This result is more aligned with what was expected, which supports the suggestion that movement between the mandibular fragments may have caused the original error.

User Feedback

Due to these contradictory results, it was difficult to determine which alignment method to move forward with based solely on accuracy. Participants' feedback and our own user experience on the ease of completing the reconstructions using each arrangement method was also used. All participants found the freehand method easy to complete and felt they could align the segments quickly using this method. Unfortunately, the reconstructions were not timed so this is based on user perception. However, when using Freehand Alignment, we noticed we heavily relied being

able to visualize distinct points on the segments such as corners or edges. These points could be visualised on the display and allowed us to match the location of these distinct points with respect to the other segments easily. We used this same technique when performing the trial with the imperfect fibula segments as they resembled the display closely enough. However, the Dice score indicated the accuracy of the alignment for this reconstruction was not as good as when the 3D-printed segments were used. This indicates that the presence of soft tissue on the segments could further reduce this accuracy and cause aligning the segments freehand to prove to be more challenging.

In contrast, performing the reconstruction using the guidance methods did not rely on the user being able to visualise the shape of the segment. Participants found that the virtual visualisation for arranging the segments using the guidance required a steep learning curve but was easier after practice. However, they also found that this method took longer than aligning the segments freehand (as no timing measurements were taken this is based on user perception). Having the axis representation attached to the 3D models though helped make the visualisation more intuitive.

When arranging the segments in the mandible directly, the additional constraint of the mandible cut surfaces and using the mandible to orientate the user in virtual space, made using the visualisation easier. However, the additional hardware in the restricted mandible working area was a big hinderance. Frequently segments that had already been aligned had to be moved out of alignment and realigned with the attached Articulating Arm in a different orientation to allow the next segment to reach the target location. Figure 37 shows this interference and small available space in the mandible working area. Additionally, this working area would be further reduced when performing this procedure on a patient due to the presence of the surrounding anatomy.

Figure 37 - Mandible Workspace When Using the Guided Alignment at Mandible Workflow

Study Outcome

Based on these usability comments from participants, arranging the segments directly in the mandible was eliminated as an option as the usability difficulties were not offset by any increased accuracy. To more accurately assess which of the remaining two workflow methods were optimal, we decided to perform further testing using a more realistic model.

Phase One of a cadaver study (outlined in section 4.1) was designed to compare each Freehand Alignment and Guided Alignment at Fibula by performing reconstructions of five cadaver specimens. A feature was added to the segment alignment module to allow the user to choose the freehand or guided segment alignment approach and would subsequently create the appropriate visualisation for each. It is not expected that this option will be present in subsequent iterations of the system, this was only included to complete the cadaver study.

2.4 Final Module Design and User Interface

After making updates and changes based on feedback from the testing described above, the first iteration of the modules was fully complete and ready to be used to complete further

validation testing. The following images outline the user interface for each module and key features each contains described in section 2.2.3.

2.4.1.1 Calibration and Registration Module

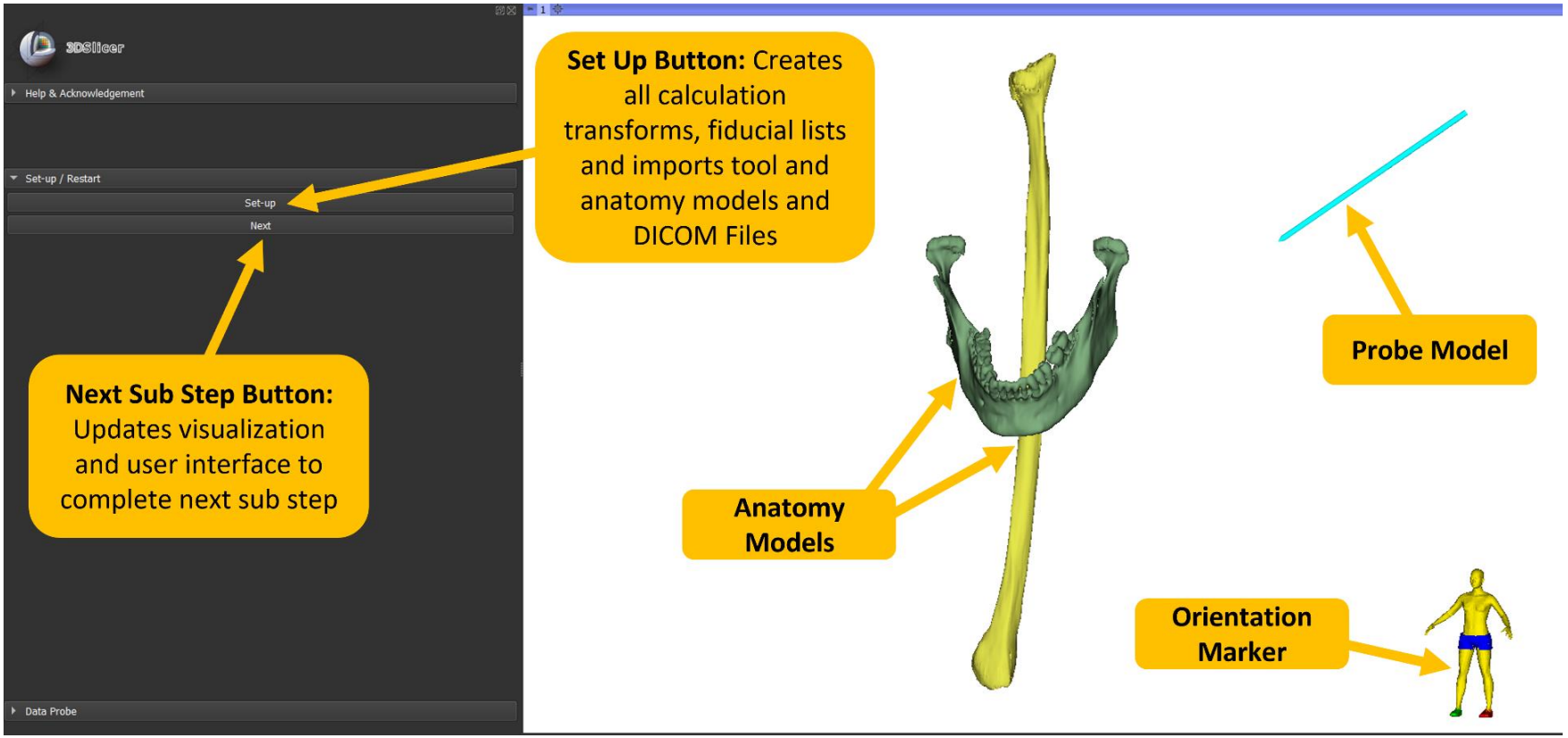

Figure 38 - Set up user interface in 3D Slicer

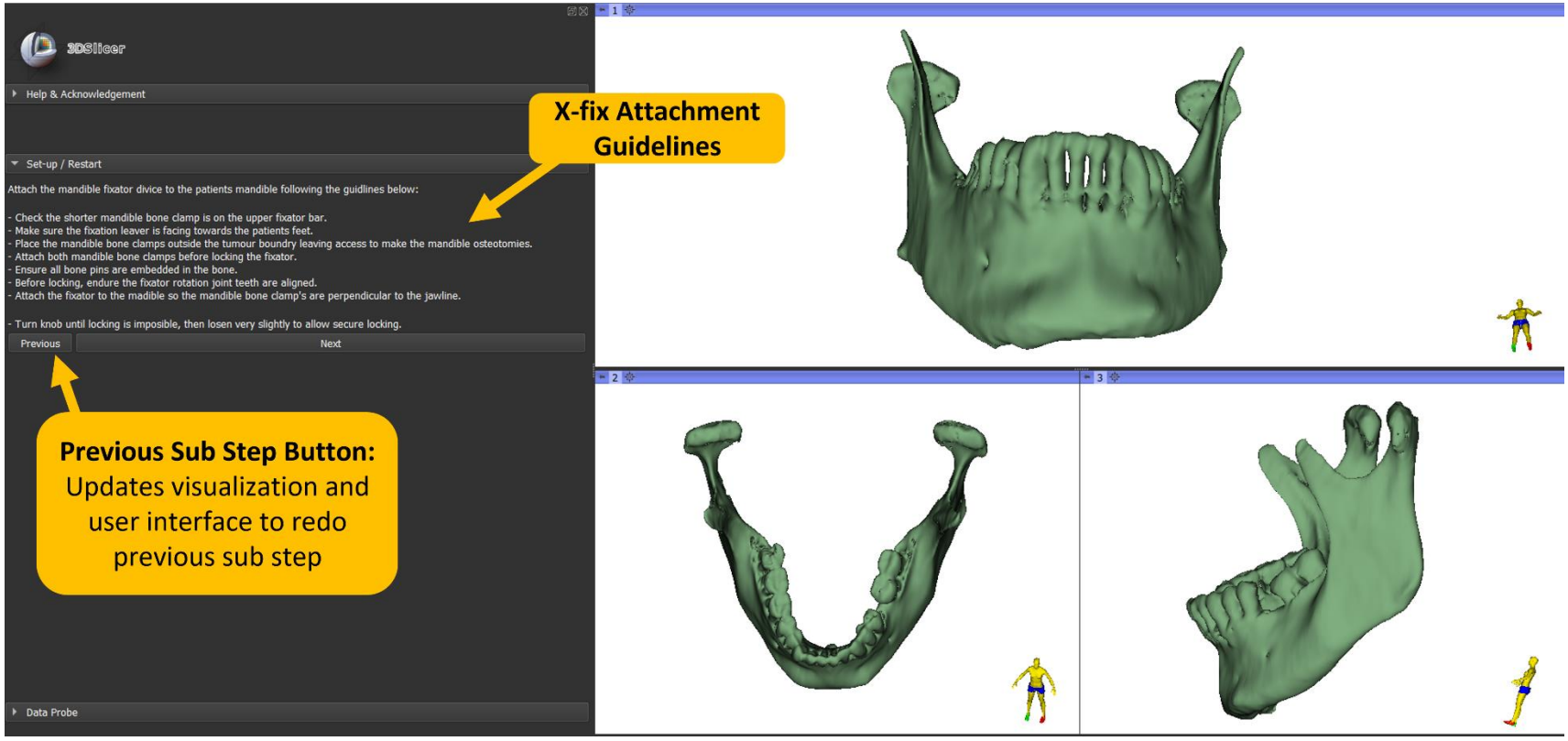

Figure 39 - Attach X-Fix user interface in 3D Slicer

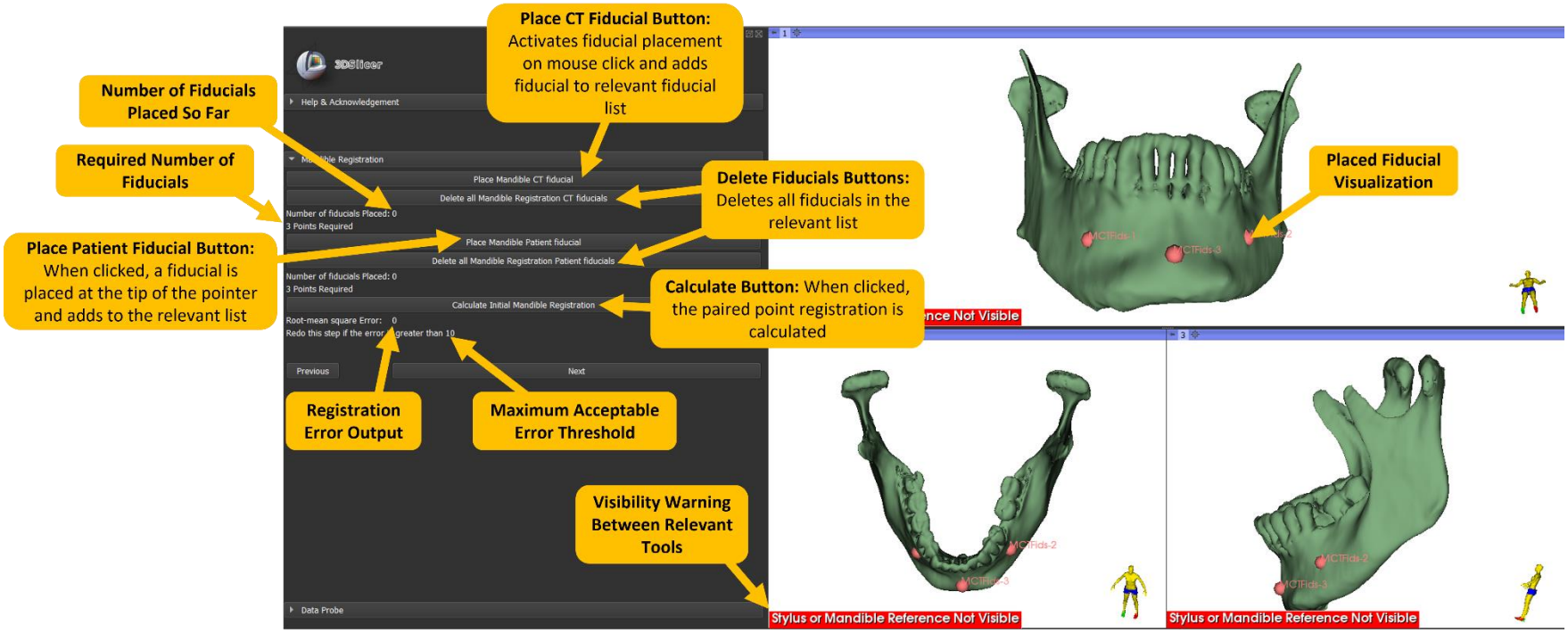

Figure 40 - Initial mandible registration user interface 3D Slicer

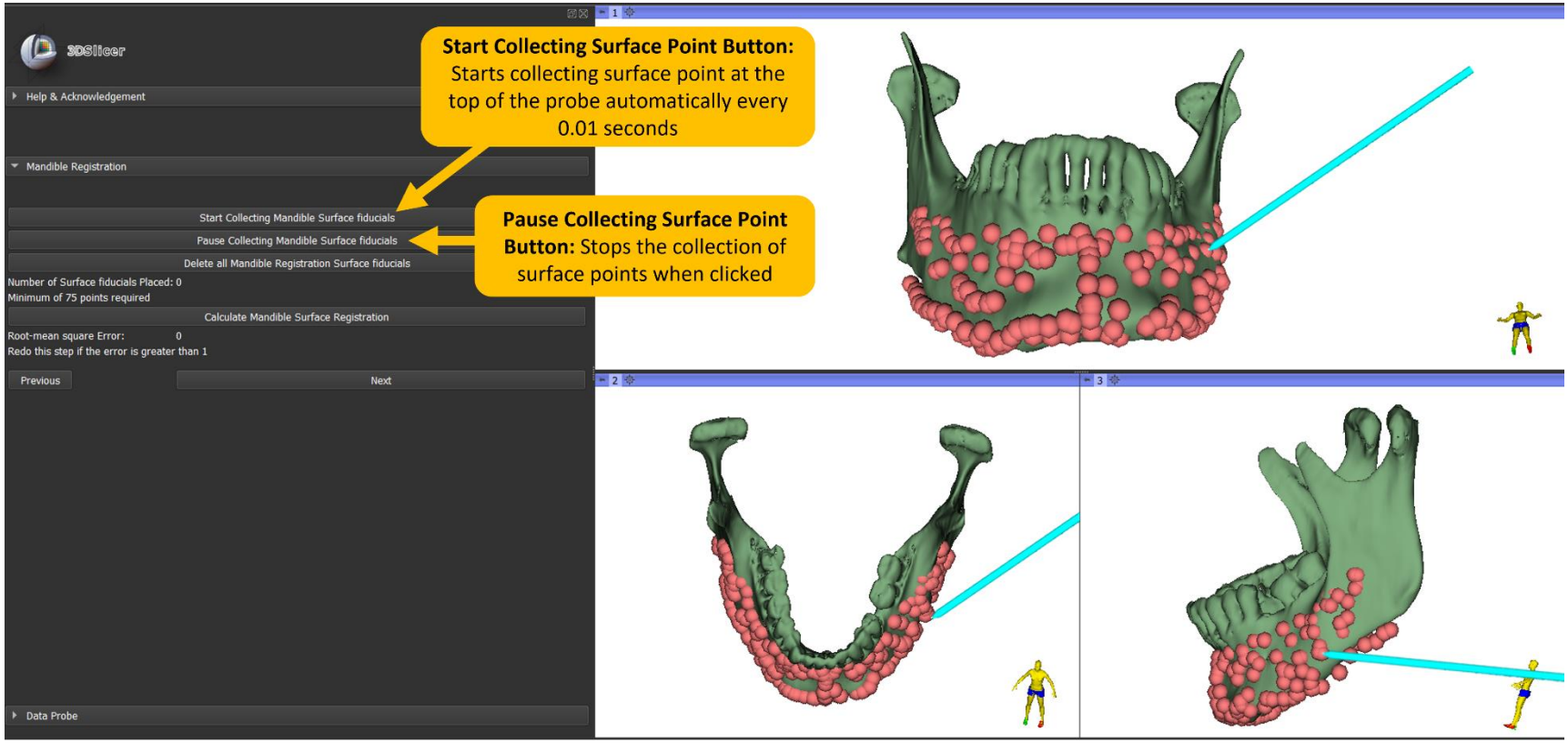

Figure 41 - Surface registration user interface in 3D Slicer

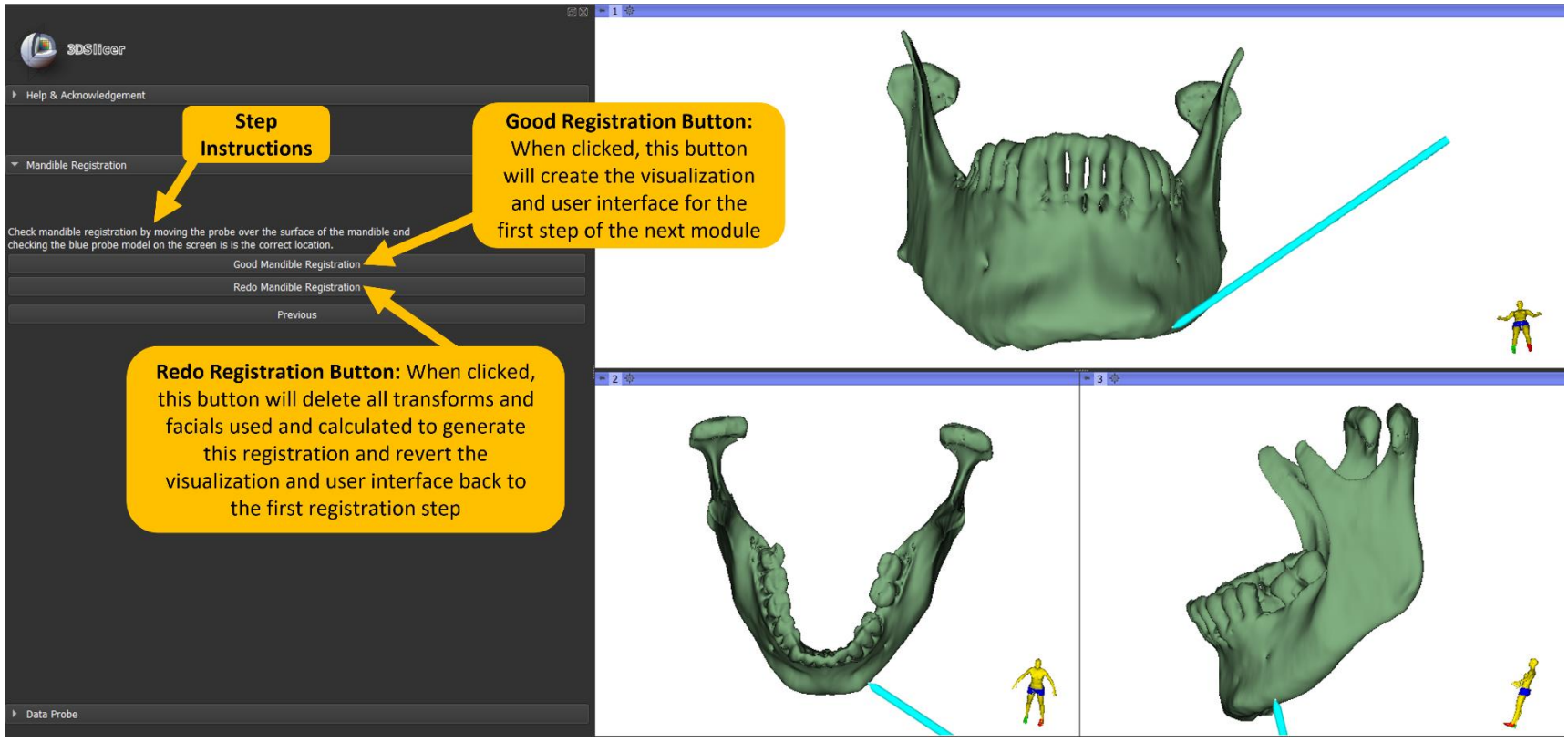

Figure 42 - Registration check user interface in 3D Slicer

2.4.1.2 Mandible Osteotomy Module

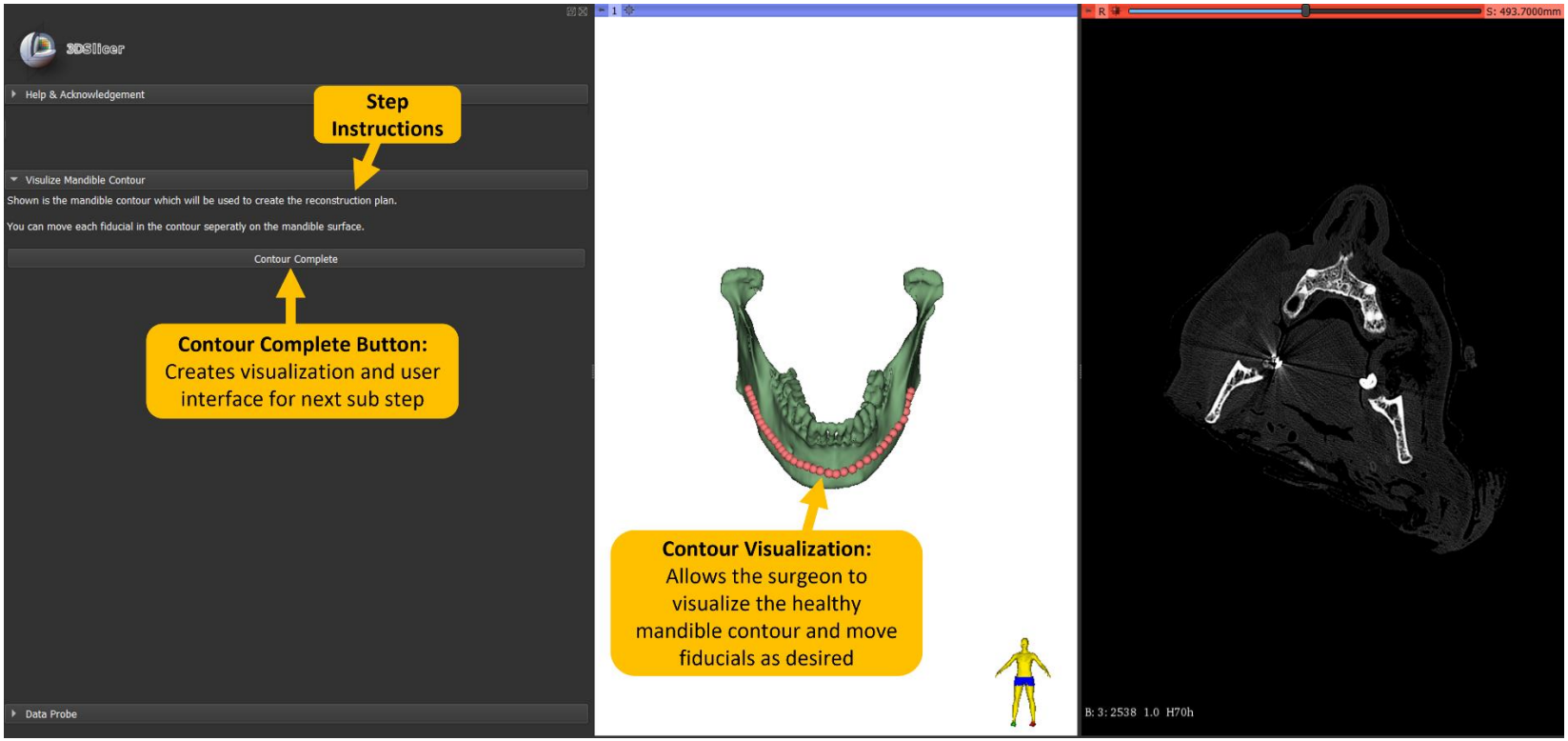

Figure 43 - Contour check user interface in 3D Slicer

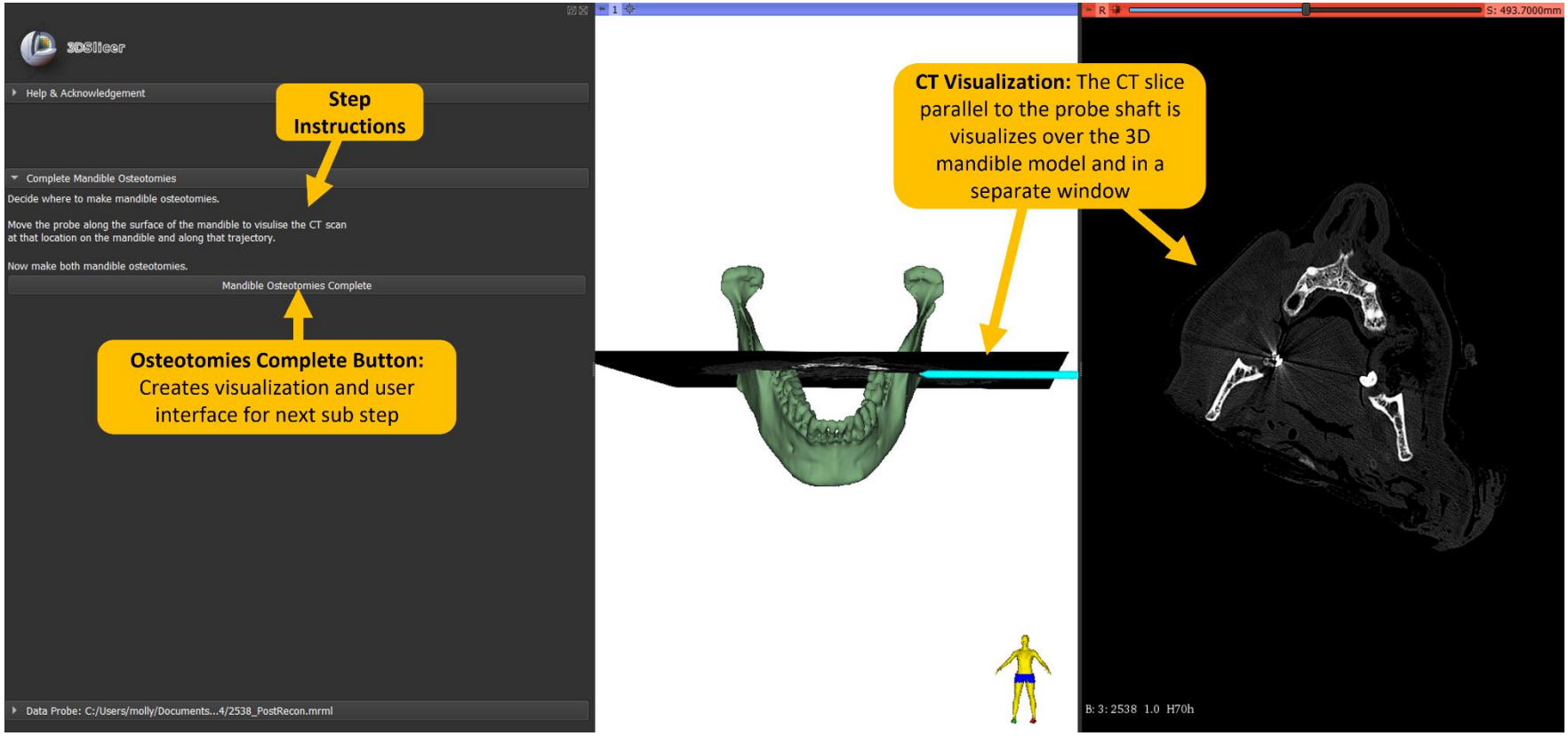

Figure 44 - Visualize mandible CT user interface in 3D Slicer

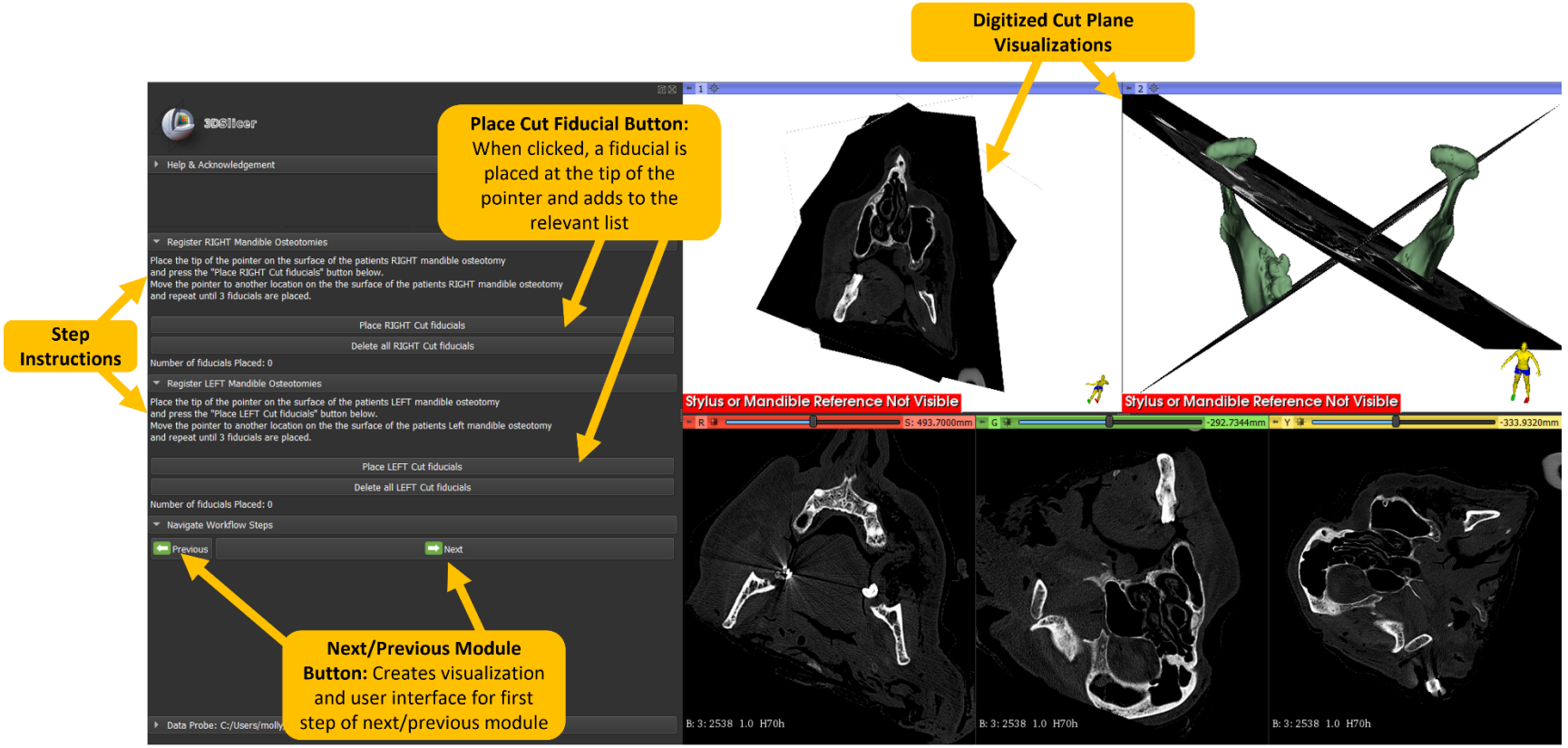

Figure 45 - Digitise mandible cut planes user interface in 3D Slicer

2.4.1.3 Virtual Surgical Plan Module

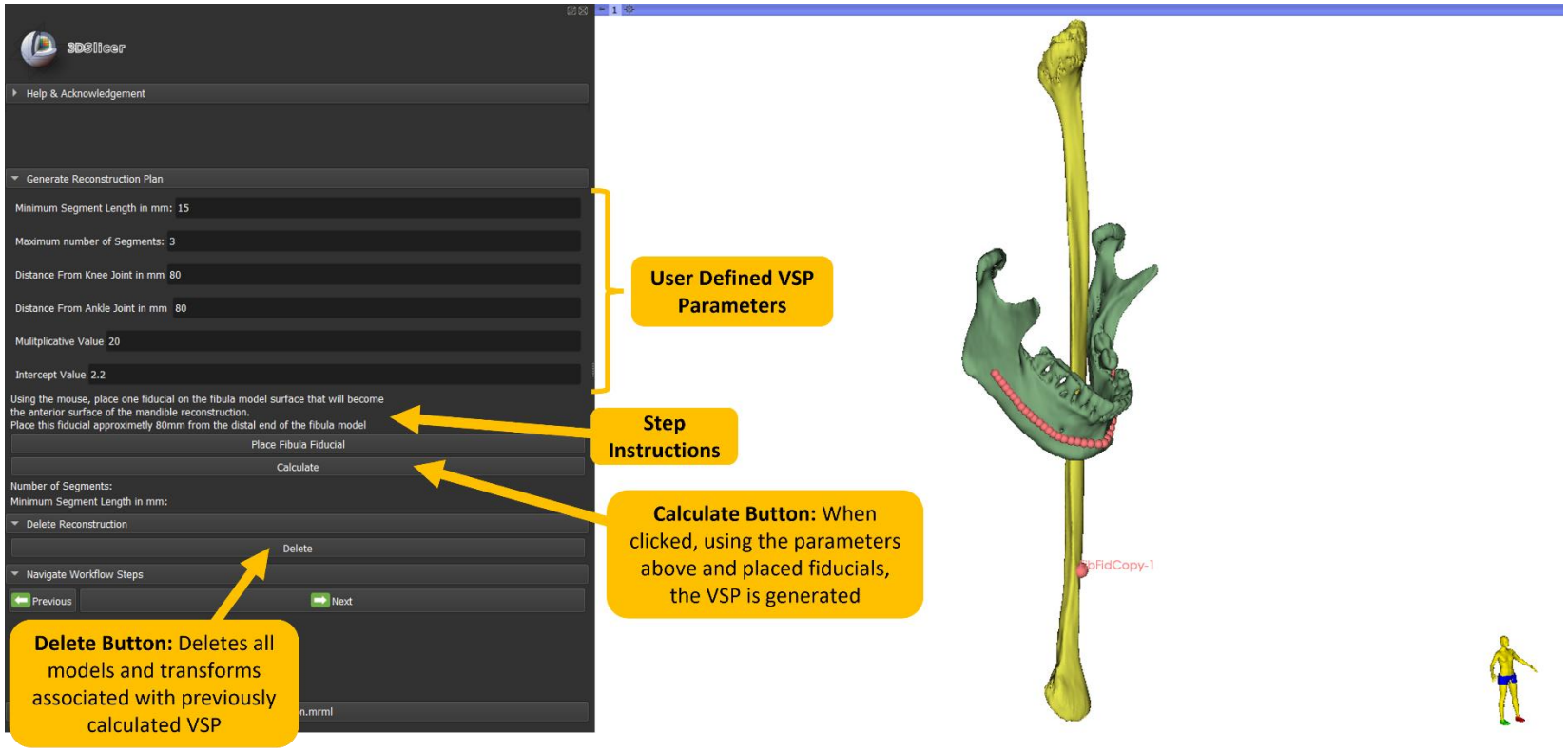

Figure 46 - Generate VSP user interface in 3D Slicer

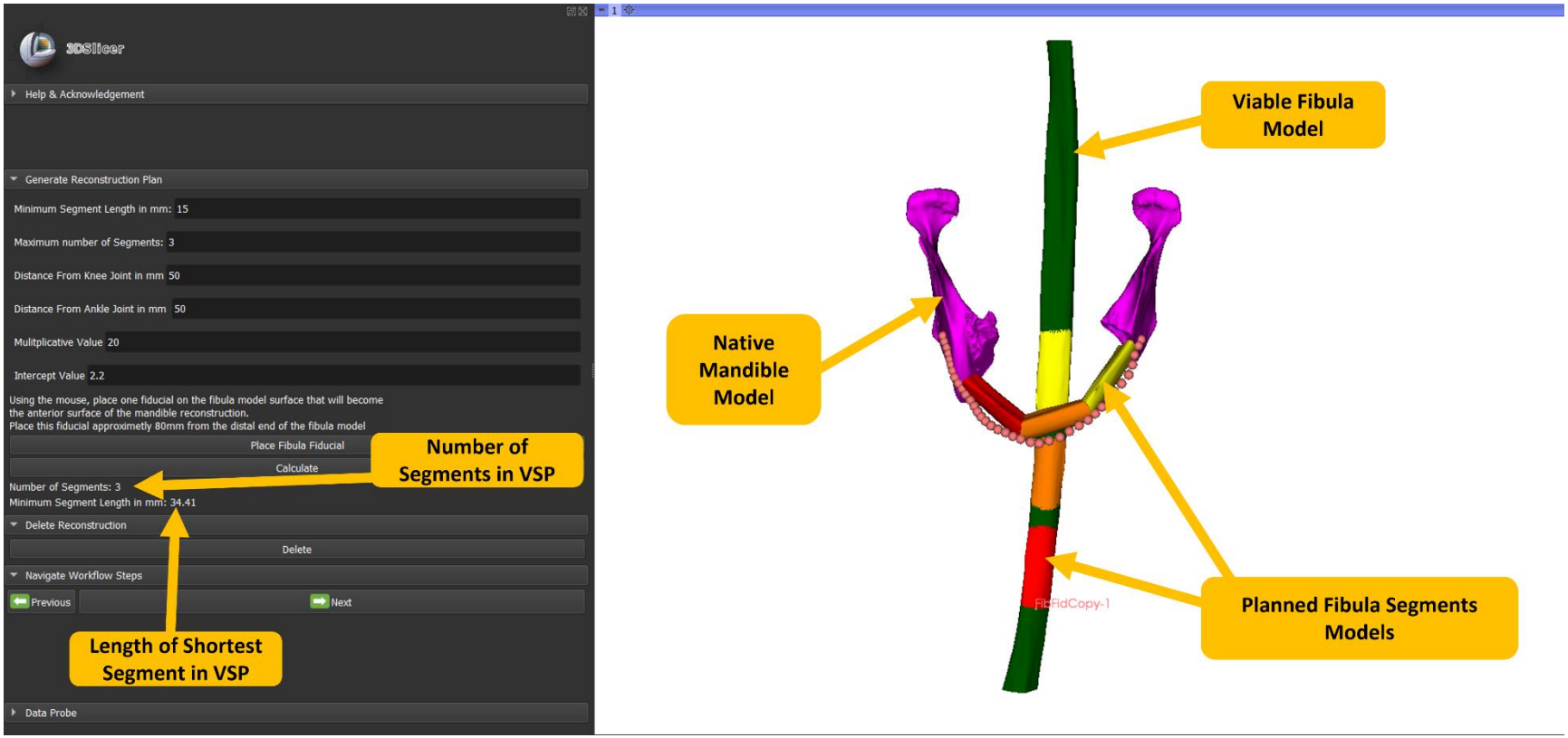

Figure 47 - VSP output user interface in 3D Slicer

2.4.1.4 Fibula Cutting Guidance Module

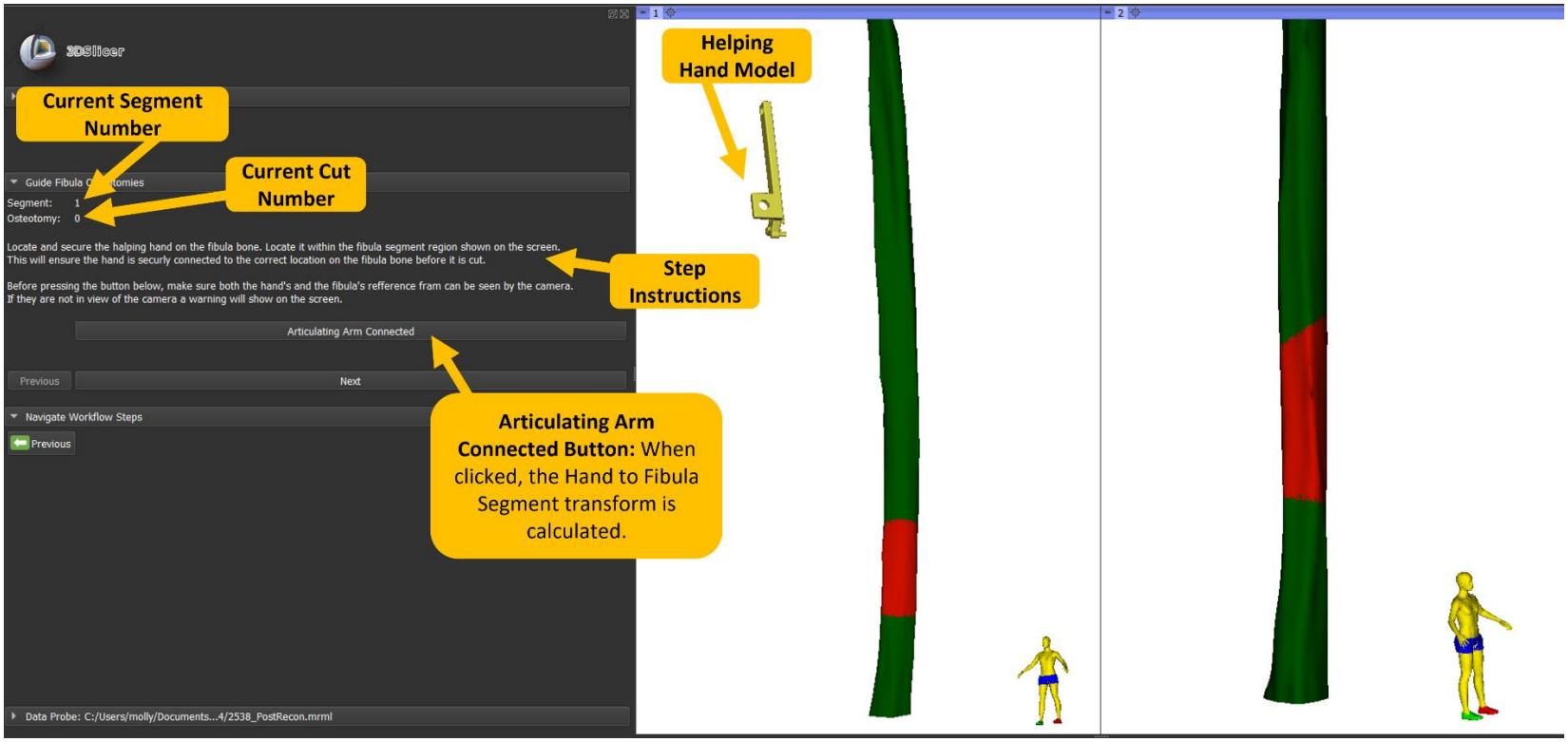

Figure 48 - Place Helping Hand user interface in 3D Slicer

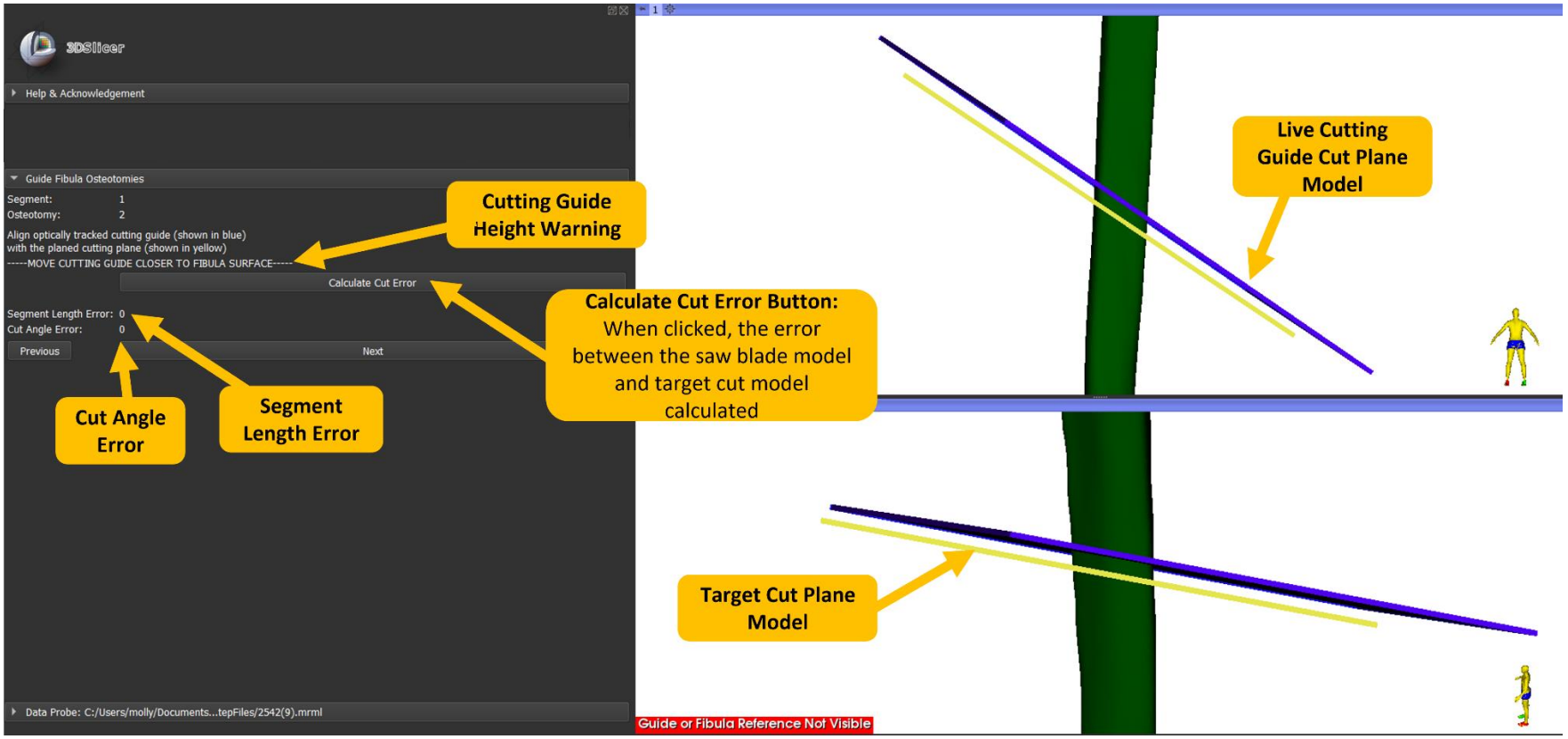

Figure 49 - Fibula cut guidance user interface in 3D Slicer

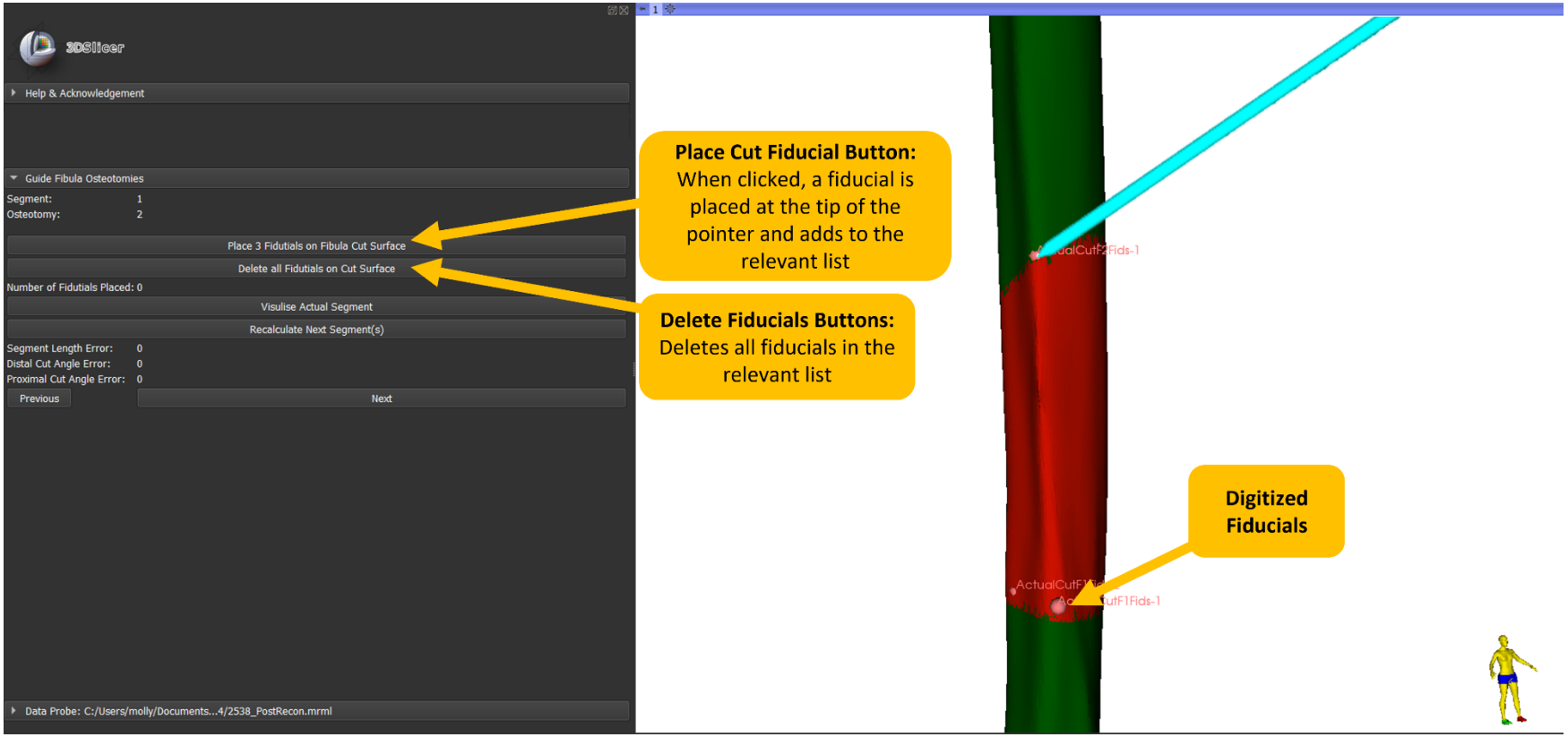

Figure 50 - Digitise fibula cut plans user interface in 3D Slicer

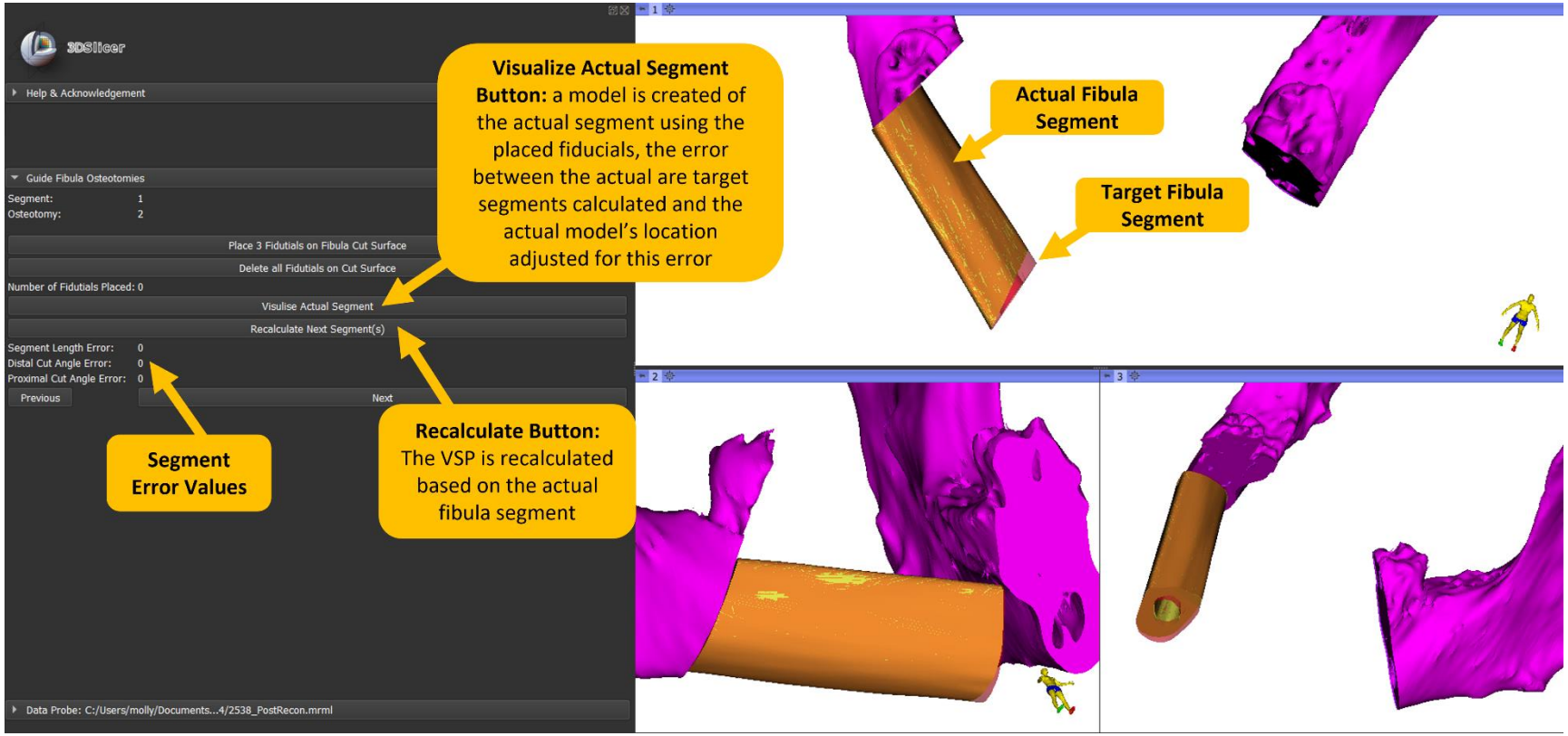

Figure 51 - Visualize actual fibula segment and recalculate VSP user interface in 3D Slicer

2.4.1.5 Segment Alignment Module

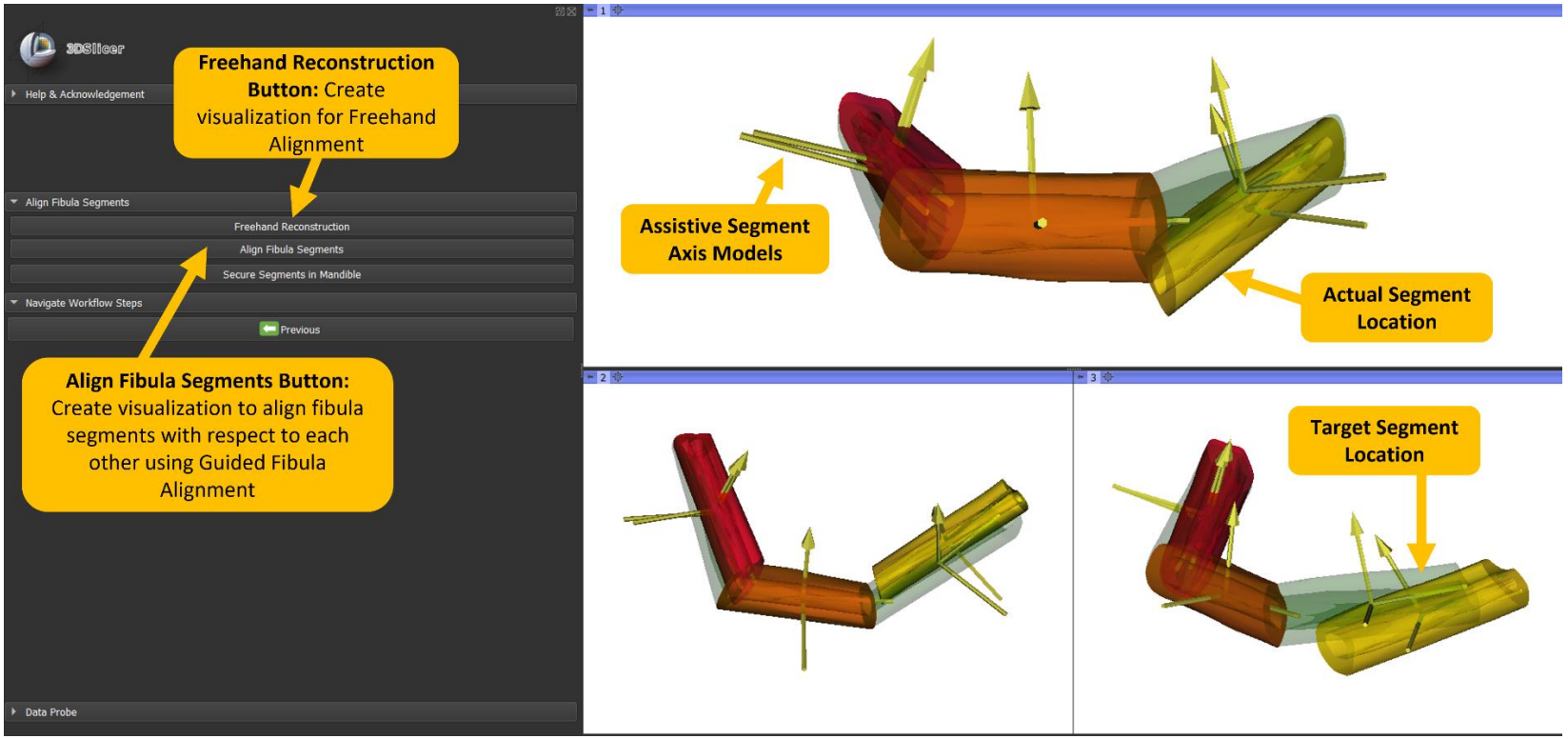

Figure 52 - Fibula segment to segment alignment user interface in 3D Slicer

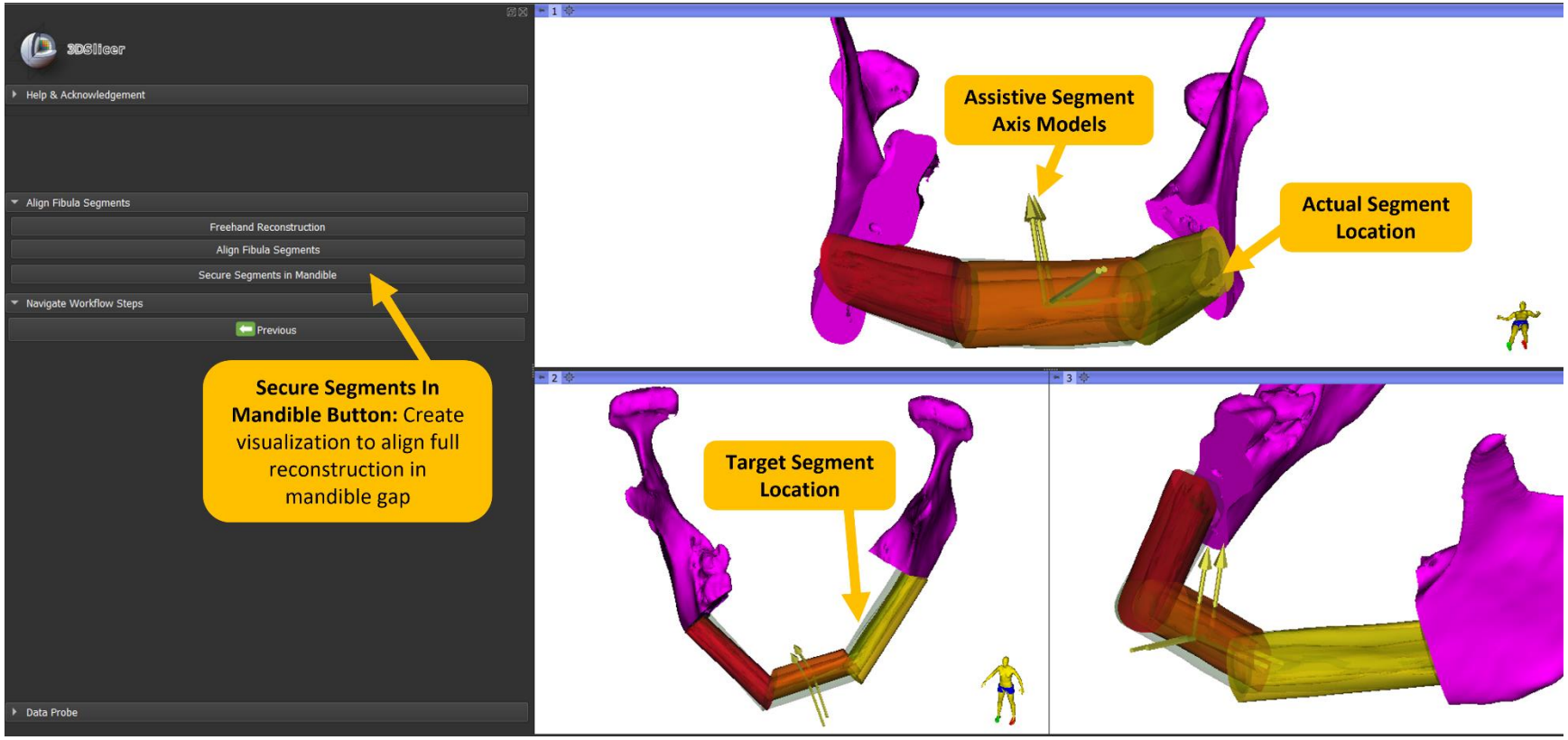

Figure 53 - Segment to mandible alignment user interface in 3D Slicer

3 Fibula Osteotomy Accuracy Study

All of the workflows described in the previous chapter require that the fibular fragments be cut in accordance with a Virtual Surgical Plan. How well these segments correspond to the target segments created in the VSP will affect factors such as the ability of the reconstruction to recreate the healthy mandible contour and the bony union achieved between neighbouring segments and the native mandible. Therefore, it is vital that the method adopted to guide these osteotomies is evaluated. In this chapter, I discuss and assess the performance of several guidance methods. In particular we compared directly tracking the surgical saw against tracking a cutting guide. Both were compared to using the 3D-printed cutting guides for reference.

3.1 Purpose of Study

Only two studies have been published assessing the use of optical tracking to guide surgeons in making these fibula osteotomies. One of these studies implements augmented reality into their system which will not be used in this system (Pietruski, 2019). However, the other study uses an optical tracking camera to directly track a surgical saw to guide these fibula osteotomies using a virtual visualisation on a standard computer monitor (Pietruski, 2019a). The osteotomy accuracies achieved in this paper are comparable to those reported when using 3D-printed cutting guides. As the system used in this paper is similar to our proposed system outlined in section 2.2.3.6, this indicates that using the optical tracking system to guide these osteotomies is a viable solution for our system

Whilst this study reports reasonable accuracies, the osteotomies were performed in a lab environment on saw bones whereas the 3D-printed guide accuracies were computed based on surgical cases. Furthermore, the marker array used to track the fibula is attached to the tibia and assumes rigidity between the two and the registration method uses fiducial markers placed

on the skin rather than on the fibula itself. Therefore, the purpose of the study described in this chapter is to directly compare the accuracy of two optical cut guidance methods against the existing 3D-printed cutting guide accuracy whilst utilising the registration method outlined in section 2.2.3.2. The same optical tracking camera and software described in section 2.2 was used to complete this study.

3.2 Methods

The three cut guidance methods used in this study were: an optically tracked surgical saw (OTS), an optically tracked cutting guide (OTG); and 3D-printed cutting guides (3DG). By performing the same set of osteotomies in the same lab setting using each of the cut guidance methods, a fair direct comparison of accuracy, time and usability of each can be assessed.

3.2.1.1 Participants

Five participants took part in this study in total: one ENT surgeon, one first year medical student, two graduate students (myself and Georgia Grzybowski) and an undergraduate biomedical engineering student). All were members of our research team, so no study approval was required to be obtained. Across the group, they had varying levels of surgical and image guidance experience. All participants had familiarity with mandible reconstruction procedures however, only the surgeon, myself and Georgia Grzybowski had experience using an optical tracking system. The other two participants had neither optical tracking nor surgical experience prior to taking part in this study.

3.2.1.2 Set Up

Each participant performed 36 fibula cuts in total. The same set of 12 osteotomies (derived from 3 different VSPs) were completed three times on three artificial bone models, once with each of

the three cut guidance methods. These artificial bone models were cut into three equal length segments and secured to a wooden board using screws (Figure 54).

Figure 54 - Saw bone model set up

The bone models were divided in this way to allow them to be CT scanned as the CT scanner used (described in section 2.3.1) only had an available volume length of 13 cm. We scanned the bone models and manually segmented each section using thresholding and trimming tools in 3D slicer. These segmentations allowed us to create 3D models of each section of fibula. Only one artificial saw bone was scanned prior to the study as the same brand and model of artificial saw bone was used throughout and the deviation in manufacturing was assumed to be insignificant.

A marker array was rigidly secured to the wooden board to simulate the fibula marker array being connected directly to the fibula. This wooden board was then clamped to the surgical table to prevent relative movement between the saw and the bone whilst the cuts were being made. Each fibula section was registered individually by first performing a paired-point registration method, followed by a surface registration step (for further details see section 2.2.3.1 and Georgia Grzybowski's thesis (Grzybowski, 2021)).

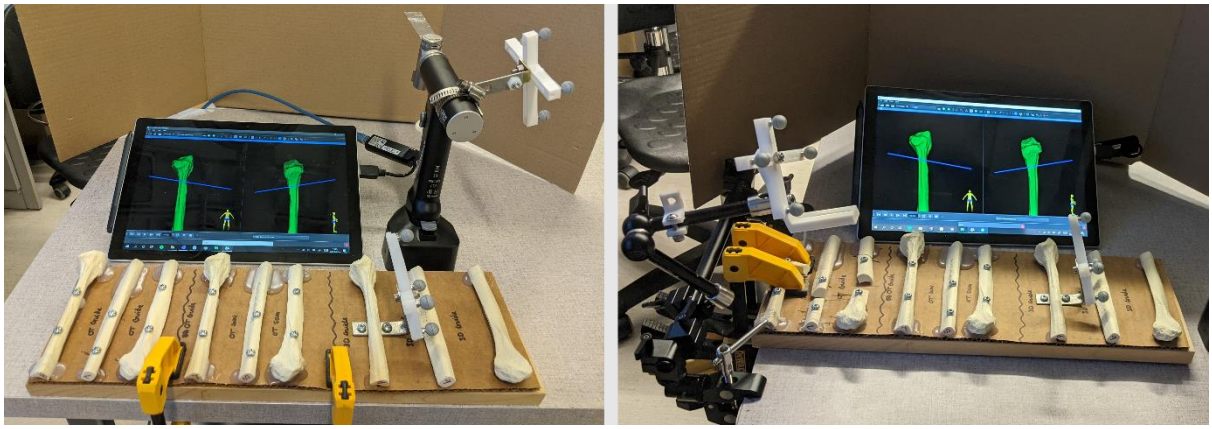

Figure 55 - OTS (left) and OTG (right) cut guidance method set up

3.2.1.3 Cutting Guidance Methods

Optically Tracked Saw (Figure 55): A marker array was rigidly clamped to the barrel of the surgical saw which is freely moved in space to align with the target cut plane. The saw was calibrated using the method described in section 2.2.3.1. This is a battery powered surgical saw with a 1 mm thick oscillating blade shown in Figure 55.

Optically Tracked Guide (Figure 55): The optically tracked cutting guide was 3D-printed and designed, by Georgia Grzybowski, to bolt to an articulating arm which connected to a rail and was rigidly clamped to the table shown in Figure 55. This arm allows the guide to be moved in six degrees of freedom and then locked in position once the user was satisfied with the alignment as indicated on the screen. A marker array was bolted to the guide to allow it to be tracked by the optical tracking camera and was calibrated by performing a paired-point registration.

3D-Printed Guides: The 3D-printed cutting guides were created by a researcher working in Dr Eitan Prisman's Lab to recreate the same segments as the two optically tracked cutting methods (Figure 56).

Figure 56 - 3D-printed cutting guides used in this study

The guides were attached to the artificial bone models using screws; however, no guidance was given as to where they should be placed along their long axis.

The cutting guidance methods and fibula osteotomies were performed in the same order for all participants, OTS first followed by OTG followed by 3DG. To guide the user to align the optically tracked tool with the target cut plane, the same visualisation was used as described in Section 2.2.3.6 and shown in Figure 55 above. As the saw or cutting guide is moved in real space, the saw blade model moves on the display and the user visually aligned this with the target cut model. The error calculation function within the osteotomy guidance module was not used during this study as it had not been developed yet.

3.2.1.4 Image Processing

Once all participants had completed the osteotomies with each cut guidance method, all fibula segments were CT scanned using the same micro-CT scanner and scanning parameters outlined in section 2.3.1. Each fibula segment was then manually segmented using thresholding and trimming tools in 3D Slicer and subsequently converted to a 3D model. Each model mas named using the following name convention: Method (1-3) . Participant (1-5) . Segment (1-6).

3.2.1.5 Results Calculations

These models were then used to calculate the length of each segment and the angle of each cut plane in 3D Slicer. This was done by manually placing three fiducials on the cut surface of the segment model. A plane was then fitted to these three fiducials and the normal of this plane was calculated. This was defined as the cut surface normal. The normal of each cell in the mesh making up the segment 3D model was then compared to the cut surface normal to identify all the cells which make up this cut surface. The average centre of all these tagged cells, weighted by each cell's area, was then calculated to find the centre of each cut surface. This was repeated for both cut surfaces that make up a segment. The vector between the centre of each cut surface (the segment axis) was defined as the length of the segment, and the angle between each cut surface normal and the segment axis was taken as the cut plane angle. This same process was also undertaken to determine the target segment length and cut plane angle. The difference between the target and the actual values is reported in the Results section below.

Throughout the study, all osteotomies were also timed. The time was recorded from when the participant lifted the saw from the table (or loosened the articulating arm connected to the cutting guide), till the saw was returned to the table after the cut was complete. The time to attach the 3D-printed cutting guide was also recorded.

3.2.1.6 Statistical Analysis

The results were statistically analysed using the software SPSS. After performing Kolmogorov-Sminov and Shapiro-Wilk tests, the data was found to not be normally distributed. This led to using statistical tests for independent variables with nonparametric distribution. Kruskal Wallis tests were conducted testing a null hypothesis comparing each cut guidance method, each participants performance, and each fibula segments difficulty.

3.3 Results

The registration error associated with the registration of the precut fibula sections were as follows: the average root mean square error of 0.65 mm was achieved following paired-point registration, and then reduced to 0.30 mm following surface registration.

The graphs below outline the length error, angle error and time per cut results grouped to show distribution between participants, segments and cut methods. The X on the box and whisker plot indicates the mean and the internal horizontal line indicated the median. The top and bottom of the box represent the upper and lower quartile respectively and the whiskers indicate the minimum and maximum values restricted to 1.5 times the interquartile range. Outliers are data points that lie out with these bounds and are shown as a dot out with whisker area.

After performing the statistical analysis of the results shown above, no statistical significance was found other than between the time per cut for each cut guidance method with a significance value of less than 0.001 found between 3DG and OTS and between 3DG and OTG, and 0.031 (after Bonferroni correction) between OTG and OTS. This can also be seen in the graphs where the average cut accuracy of each of the methods is similar; however, the time taken per cut is higher using OTS and higher still using the OTG. The variation between segments and participants in terms of accuracy and time is also minimal.

3.3.1.1 Sorted by Cut Guidance Method

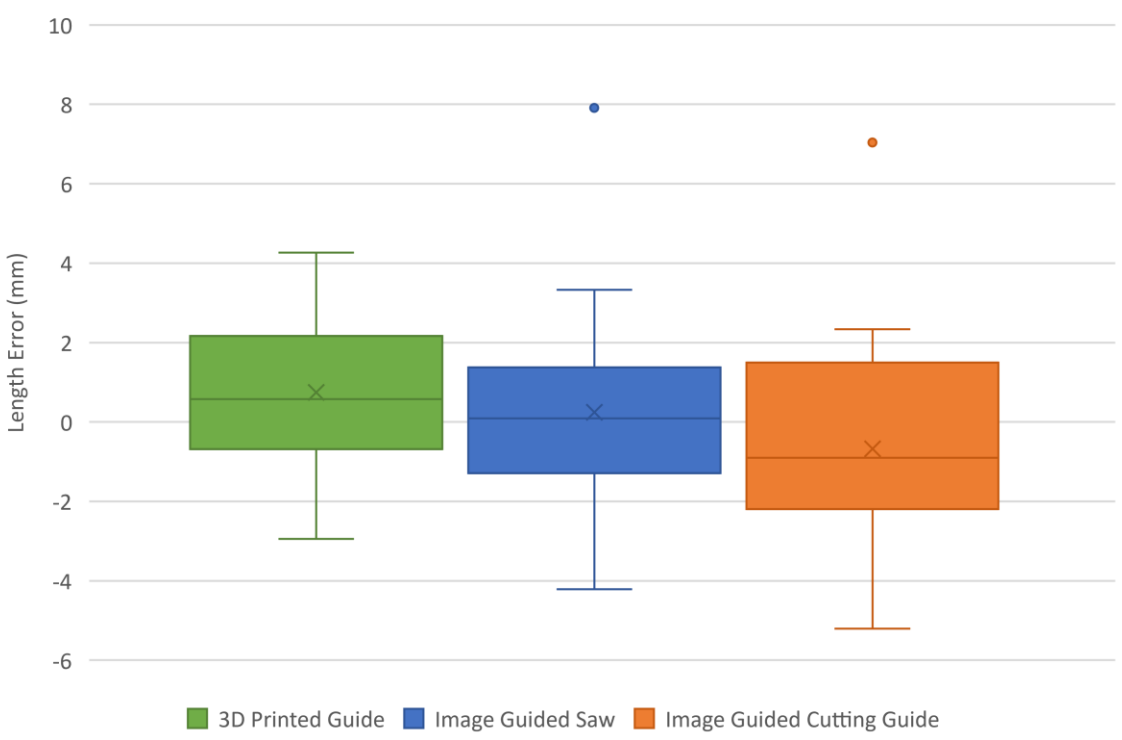

Figure 57 – Segment length error sorted by cut guidance method

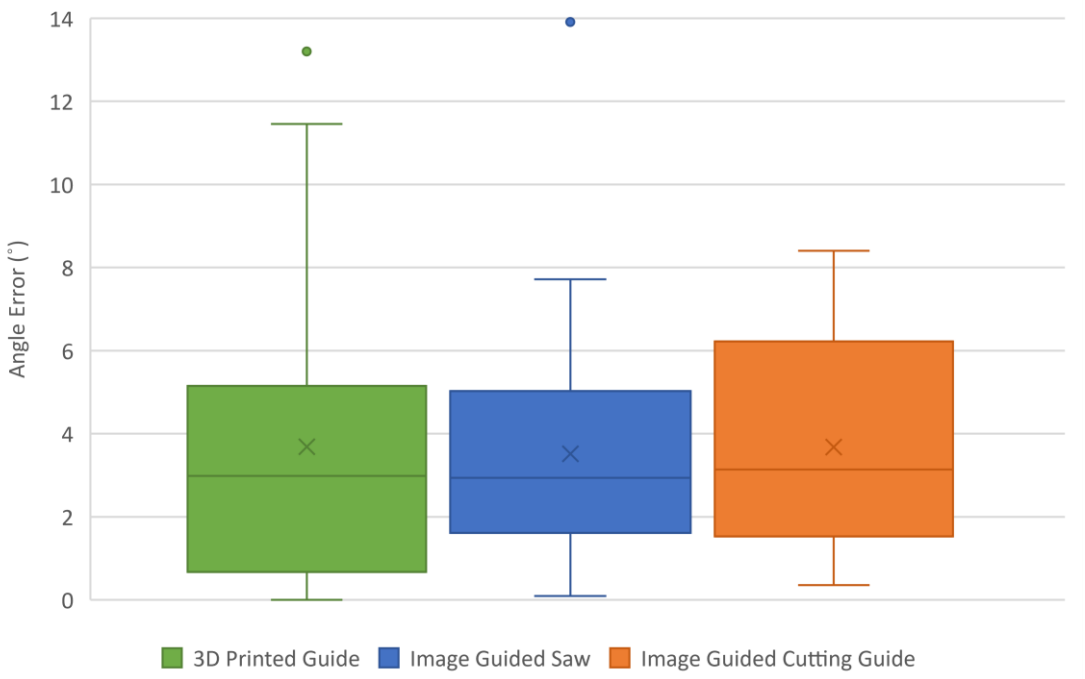

Figure 58 - Cut angle error sorted by cut guidance method

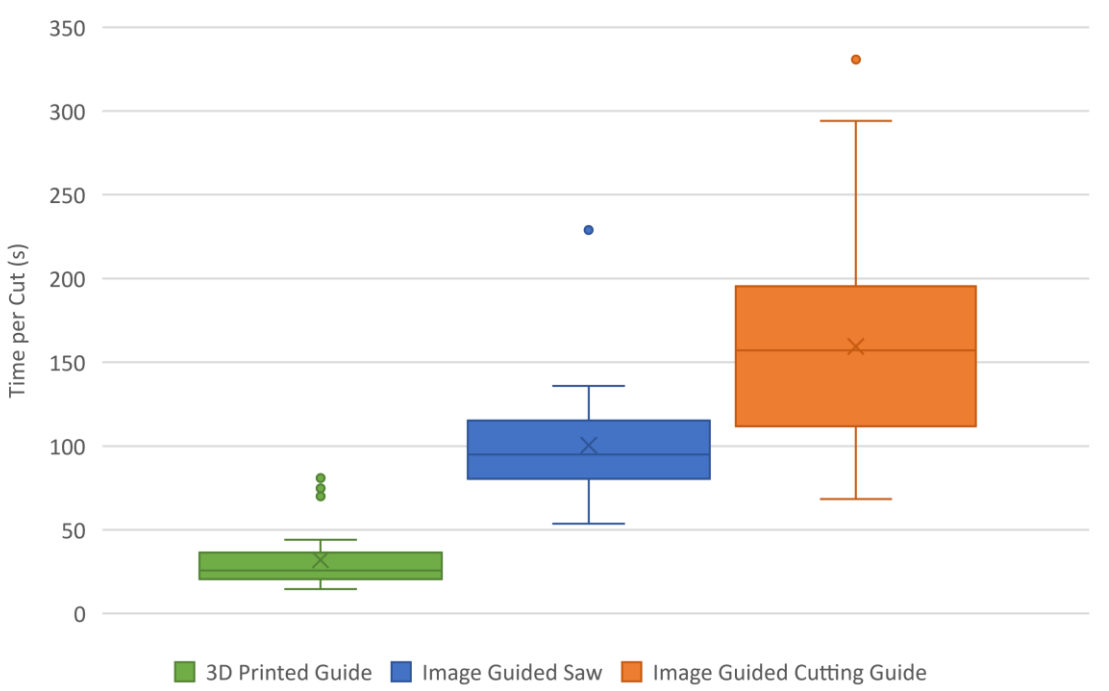

Figure 59 - Time per cut sorted by cut guidance method

3.3.1.2 Sorted by Participant

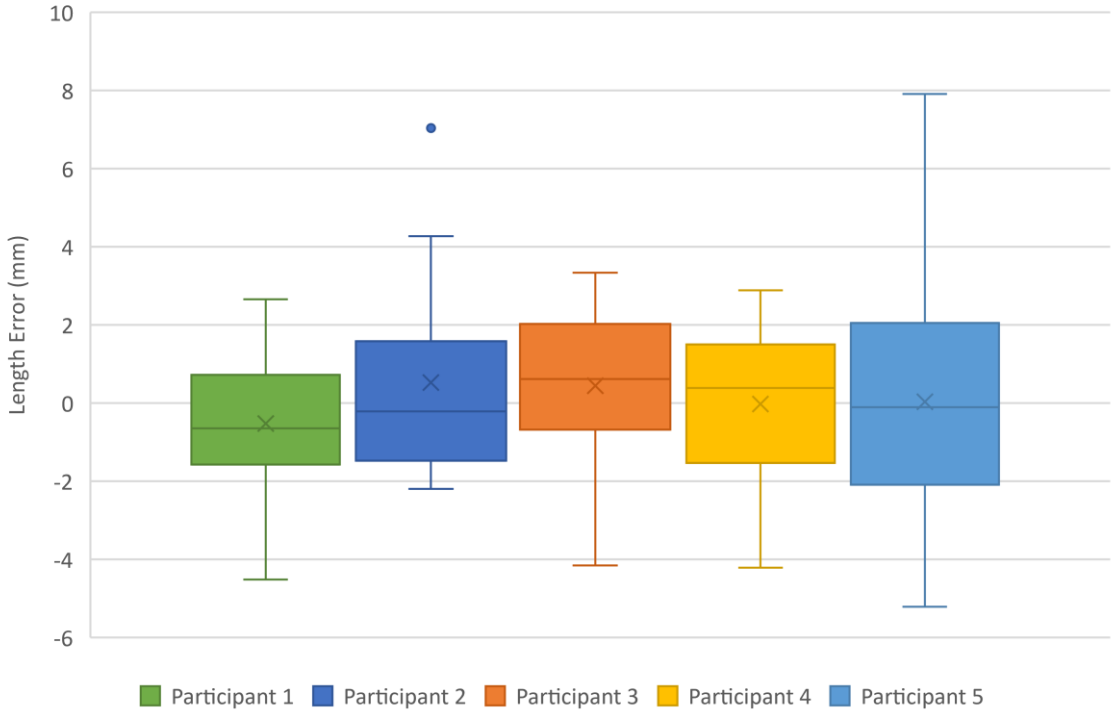

Figure 60 - Segment length error sorted by participant

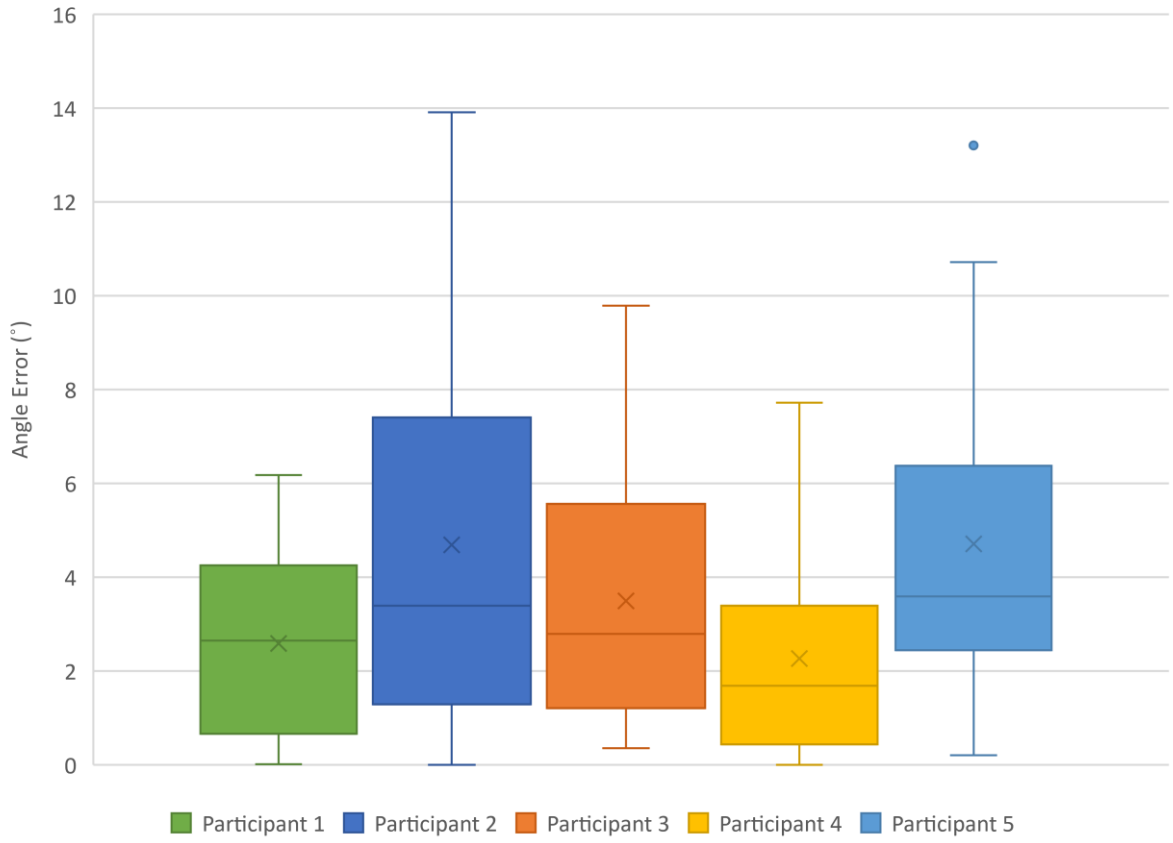

Figure 61 - Cut angle error sorted by participant

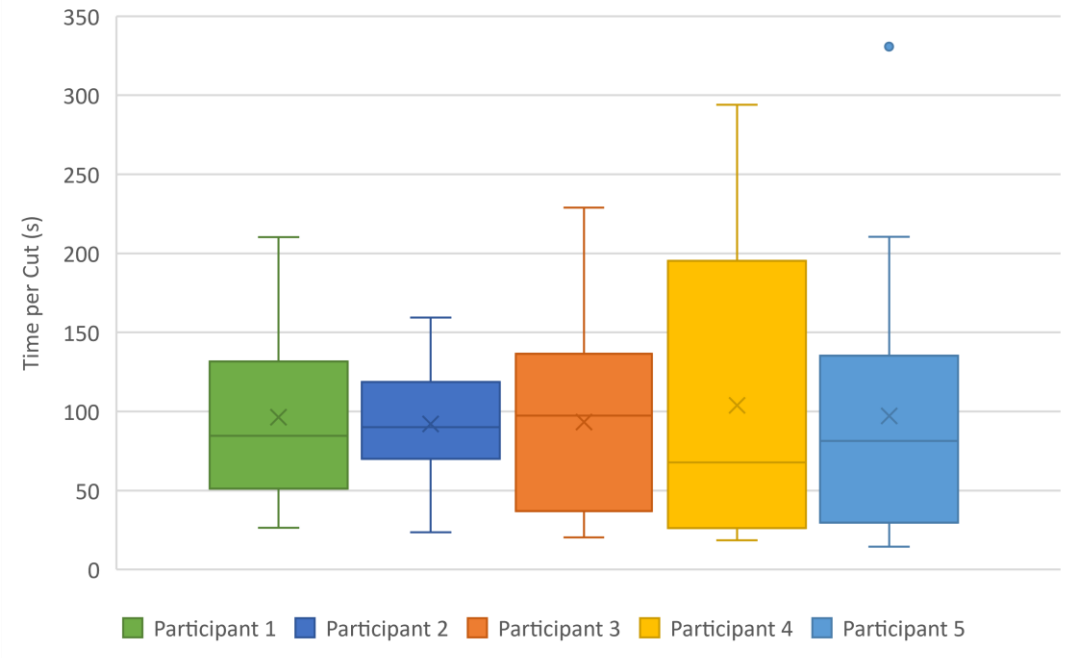

Figure 62 - Time per cut sorted by participant

3.3.1.3 Sorted by Segment

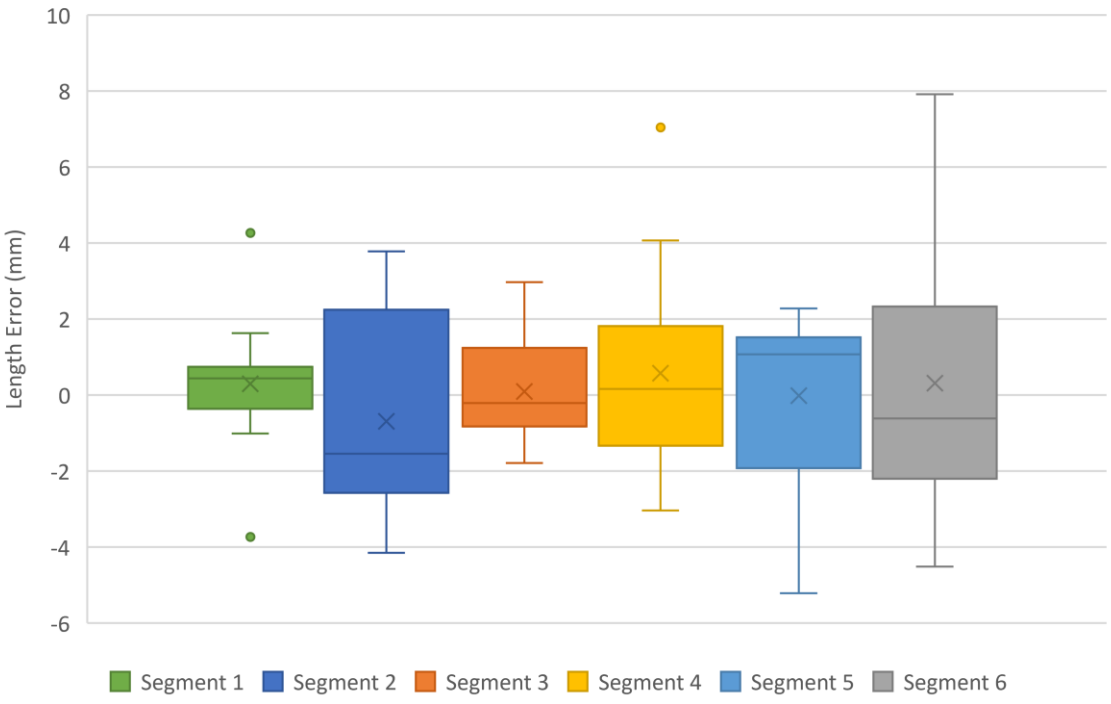

Figure 63 - Segment length error sorted by segment

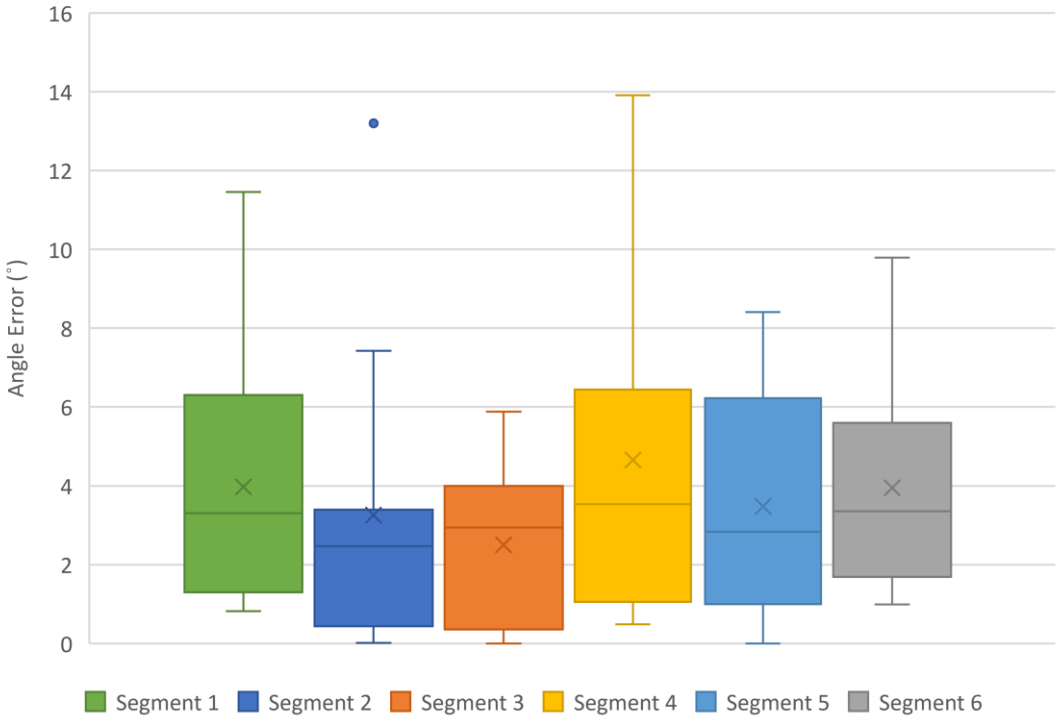

Figure 64 - Cut angle error sorted by segment

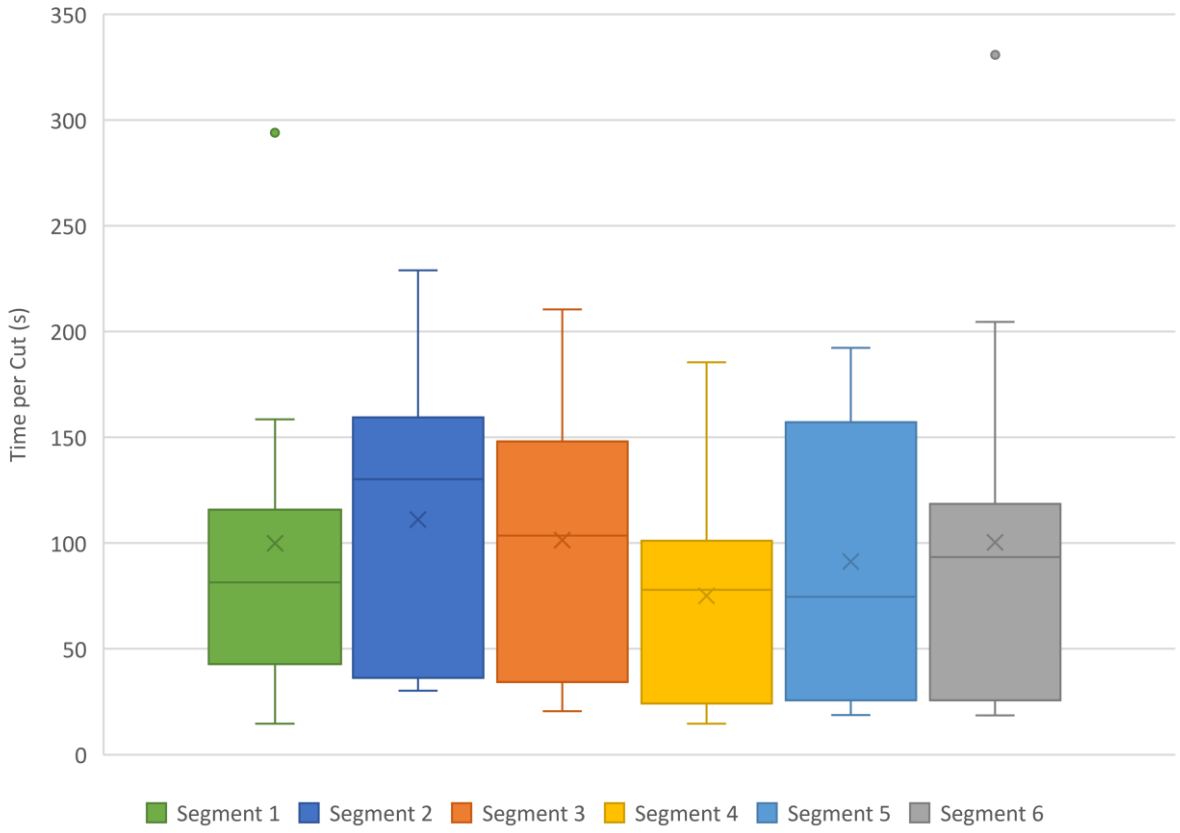

Figure 65 - Time per cut sorted by segment

The table below outlines the average length error, angle error and time per cut for each of the three guidance methods assessed.

Error Metric	3D-Printed Cutting Guide	Optically Tracked Saw	Optically Tracked Cutting Guide
Length Deviation (mm)	0.74 ± 1.85 (1.58 ± 1.19)*	0.24 ± 2.38 (1.64 ± 1.70)*	-0.68 ± 2.66 (2.27 ± 1.58)*
Angle Deviation (˚)	3.68 ± 3.73	3.51 ± 2.93	3.68 ± 2.59
Time per Cut (s)	32 ± 18	100 ± 34	164 ± 63

*Table 3 - Average length error, angle error, time per cut for each guidance methods (*absolute values)*

3.4 Discussion

As specified in section 3.3, there was no significant difference found between the three cut guidance methods in terms of accuracy for either length or angle. This suggests that either optical tracking method is a suitable substitute for the 3D-printed cutting guides and will produce similar, if not improved, accuracy when recreating a VSP. These accuracies are also similar to what was achieved during the previous studies investigating using optical tracking to guide fibula osteotomies published in literature (Pietruski, 2019a). The accuracies achieved during this study are also comparable to those in literature using the 3D-printed cutting guides which achieved a length deviation of 1.91 ± 1.59 mm and an angle deviation of 5.23 ± 5.21˚ (E. Wang, 2020).

3.4.1.1 Time per Cut Comparison

However, a statistically significant difference between all methods in terms of time. As shown in Table 3, the average time to make one osteotomy increased by approximately 215 % (70 seconds) when using the OTS compared to the 3DG. This then increased by a further 63 % (60 seconds) when using the OTG. However, the time included to attach the fibula cutting guide is not included in these values. This was, on average, an additional 2.5 mins per cutting guide which in this study supported four osteotomies; however, in practice one guide could support up to ten osteotomies creating five fibula segments. Additionally, although this time increase is statistically significant, it is not perceived to be surgically significant as it would result in approximately on average only an additional 2 mins when using the OTG per osteotomy. However, we expect that this number would significantly decrease as the user gains experience with the system.

3.4.1.2 Segment Comparison

As the same six segments were created using each cut guidance method, the accuracy and time (within each guidance method) between segments could also be compared. No statistically significant difference was found between the accuracy or time of any segments for all three cut guidance methods, indicating that the optical tracking methods should perform approximately the same regardless of the specifics of the VSP generated.

As the osteotomies were performed in the same order for each participant and for each guidance method, the accuracy and time change from the first to the last segment can give an indication of improvement due to experience with the system. However, as no statistical difference was found between segments, this would imply that there is no improvement associated with additional experience with the system. However, this is contradictory to user feedback obtained from the participants. All participants felt that when using both optical tracking cut guidance methods, it was quicker and more intuitive to achieve alignment with the target cut plane the more the system was used. This may be due to the small sample number. As only 12 osteotomies were performed per guidance method, the benefit gained from additional experience with the system may not have been significant enough yet to reflect in the accuracy results.

3.4.1.3 Participant Comparison

There were also no significant differences found in accuracy or time taken between participants for any of the cutting guidance methods, which suggests that a participant's surgical experience or experience using optical tracking systems has a negligible effect on their performance when using these systems.

3.4.1.4 Cut Guidance Method User Feedback

The lack of significant difference between accuracy for each cut guidance method supports the proposal to use optical tracking to guide the fibula osteotomies. However, this statistical equivalence does not lend support to using either OTS or OTG over the other. As mentioned above, although the OTG would add additional time to the surgery, this is not deemed surgically significant. Therefore, the usability of each method became the most important aspect.

Participants noted that the OTS method required users to continually look at the display to ensure the tracked saw remained in place throughout the cut. This would pose a safety concern during surgery as it is vital for the surgeon to look where they are cutting to ensure the safety of the patient and themselves. In contrast, the OTG method allows the user to look at the surgical field while making the cut as the guide is locked in place once aligned. While there are several options that could be implemented to move the visualisation of the planned cut plane into the surgical field for use with the OTS approach, such as using an Augmented Reality (AR) headset or a transparent screen mounted on the saw barrel, this would increase the complexity and cost of the system by adding additional components and technology. Using AR would also introduce additional registration errors which may affect the accuracy of recreating the plan cuts. Using the OTG method solves this field of view issue in a simple way.

Based on this, the optically tracked cutting guide was integrated into this surgical system and used for all further testing.

4 Integrated System Validation Testing

After selecting the fibula osteotomy guidance method described in the previous chapter, we moved to full system validation testing. Although many of the system's individual components, as well as some of the integrated system had been assessed for accuracy previously, these assessments had only been completed on artificial bone models. While useful, using this type of model neglects any error or user difficulties associated with the presence of soft tissue around the bone, as well as the space constraints experience when the full patient body is present. The system had also only been tested by users within the project group. Therefore, we proposed two studies: (1) a cadaver trial, split into two phases, aimed at assessing the performance of the system in a more surgically-realistic setting, and (2) a user study aimed at seeking additional input about the usability of the system prior to undertaking the next round of design to refine the system for use in surgery. This chapter outlines Phase One of the cadaver study and discusses the results and user feedback obtained. The user study and Phase Two of the cadaver trial were not completed during this thesis. However, we sought and were granted full approval by UBC Research Ethics Board for both studies. A brief description of the proposed methods for the user study and Phase Two of the cadaver trial is included in section 5.3.

4.1 Cadaver Trial Phase One – Evaluating Practicality in Surgically-Realistic Setting

As mentioned above, the system and its components were tested on artificial bone models. However, many of the steps in the workflow may be affected by the presence of soft tissue as well as the space constraints imposed by the rest of the patient body. Therefore, before undertaking any further validation testing, it was important to trial the system on a more realistic specimen. Phase One of the cadaver trial was developed as a proof-of-concept study to allow

the system to be further developed based on feedback from its use on a cadaver whilst evaluating which of the two segment alignment methods outline in section 2.3 should be taken forward.

4.1.1 Method

4.1.1.1 Study Outline

In order to evaluate feasibility under more realistic conditions, we asked a collaborating surgeon to perform five end-to-end procedures using our system on cadaveric specimens. Two of the procedures were done using the Freehand Alignment workflow, and three using the Guided Alignment at Fibula workflow. We evaluated the accuracy of the reconstruction and the time needed and sought freeform feedback about any issues that surfaced during the procedures.

4.1.1.2 Specimen Choice and Participants

For this phase of the cadaver trial, five pro-sectioned human cadaver specimens were used. The head, sectioned just below the chin, and the lower left leg, sectioned just above the knee from the same full cadaver were used for each simulated procedure. When obtaining the cadavers, it was specified that only specimens with intact, unaltered mandible and fibula were viable for this study. The cadaver specimens were provided and sectioned by UBC Body Donation Program. Full ethical approval was obtained from UBC Research Ethics Board for this study (application number H20-04052).

The first of the five specimen sets was used in a trial run conducted by myself and Georgia Grzybowski to ensure that all aspects of the system could be successfully used on a cadaver model. The remaining four sets were each assigned one of the two segment alignment methods (Freehand Alignment and Guided Alignment at Fibula). A similar mandible resection and three-

piece reconstruction was carried out on each of the specimen sets by either a team of two ENT surgical fellows or one attending ENT surgeon. During the procedure Georgia Grzybowski assisted with the surgical procedure whilst I operated the software and collected the timing data.

4.1.1.3 Initial Image Processing

Before the study began, each specimen set was CT scanned by UBC Radiology using their clinical full size scanner CT Scanner. The standard scanning protocol for a clinical head and lower leg CT were used with 1 mm slice thickness to ensure a realistic CT was obtained. Manual segmentations were performed on all CTs using thresholding and snipping tools in 3D Slicer. Due to the high porosity of the cadaver bones, small holes were present after this initial segmentation. These were manually filled using the paint tool in 3D slicer in areas where they would affect the usability of the model; however, the majority were at the proximal and distal ends of the fibula and on the mandible condylar process. These areas are not exposed during the surgery and are therefore not used for registration. Therefore, the holes in these areas were left and example of this is shown in Figure 66 below.

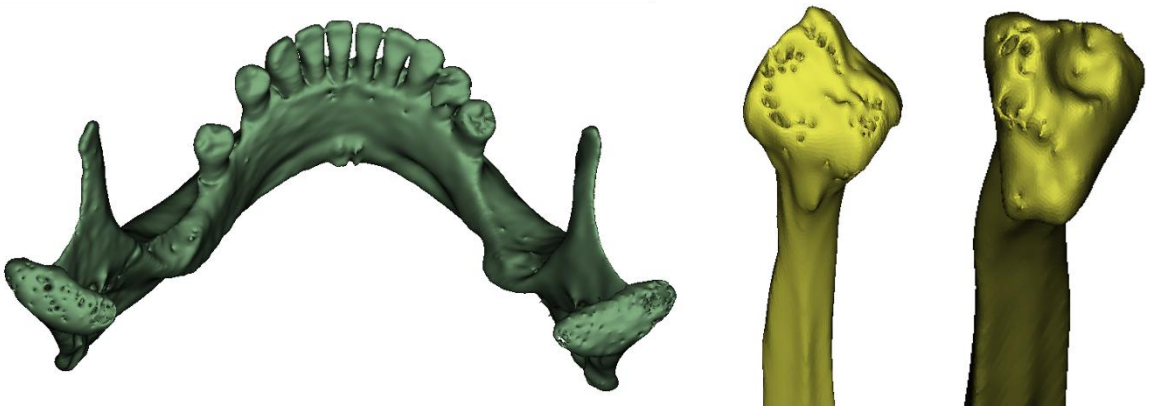

Figure 66 - Holes in the mandible and fibula segmentations

These segmentations were used to produce a 3D model of both mandible and fibula which are used to register the patient's anatomy, create the visualisations used during the image-guided steps in the surgical workflow as well as to generate the VSP.

4.1.1.4 Specimen Preparation

All specimen sets were dissected prior to the study beginning. This was performed by the participating ENT surgical fellows to ensure a realistic amount of soft tissue was left on the bone, and the typical dissection technique used in surgery was followed. The mandible was exposed using an apron incision below the chin. The skin was retracted up over the face to expose the mandible. The remaining soft tissue connected to the mandible and the periosteum around the resection area was removed. Figure 67 shows one head specimen after dissection.

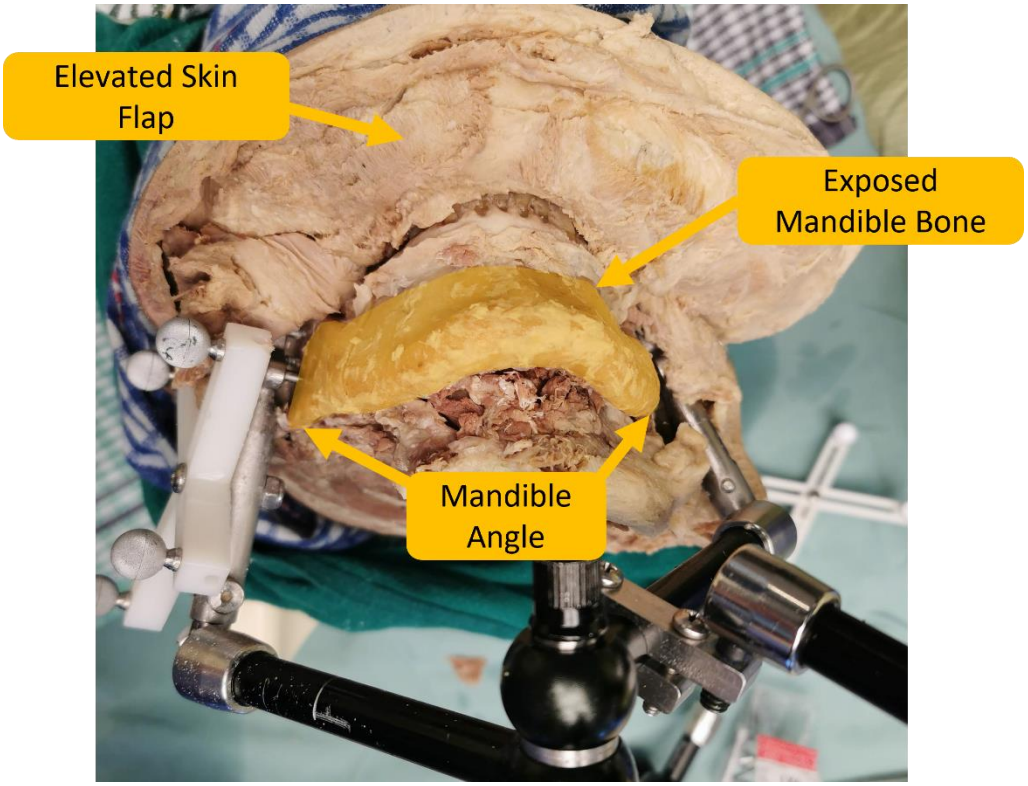

Figure 67 - Mandible exposed for cadaver trial phase one

As all reconstructions were to use three fibula segments, and due to the size constraints caused by the use of mini plates discussed in section 2.2.3, a large mandible resection had to be performed requiring complete exposure of the mandible from angle to angle.

To expose the fibula, an elliptical incision down the length of the lower leg was performed. Surrounding muscles were detached from the anterior and posterior surface of the fibula. The muscle connected to the medial side of the fibula was divided so the pedicle could be identified. The pedicle must remain connected to the fibula to allow the reconstruction to be vascularised once transplanted into the mandible. As such, this muscle is not dissected off the medial side of the bone after being divided, leaving a layer of soft tissue surrounding the pedicle connected to the fibula. Soft tissue and periosteum on the other two surfaces were partially removed as per a typical fibula flap harvest. As the proximal and distal ends of the fibula cannot be used to ensure joint stability, these were not exposed during the dissection. Figure 68 below shows one lower leg specimen after dissection.

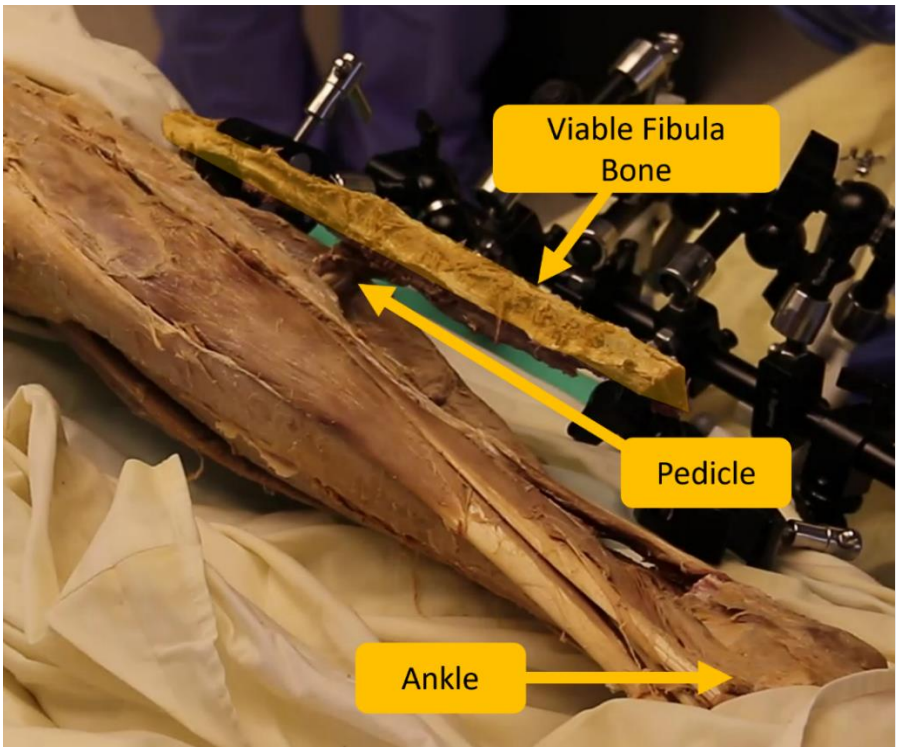

Figure 68 - Fibula exposed for cadaver trial phase one

4.1.1.5 Surgical Workflow

The new surgical workflow was followed as outlined in section 2.1 and 0. The ENT fellows performed the first two procedures, and the ENT surgeon performed the remaining two, each undertaking one visual alignment workflow and one guided alignment workflow. The steps in each workflow are outlined in Table 4 below.

1. Attach mandible fixation device on either side of the tumour boundary leaving enough space for a mini plate to be connected to the native mandible.
2. Perform paired-point registration followed by surface registration on the exposed mandible.
3. Using the visualisation of the mandible CT scan and surgical observation, decide where the mandible osteotomies should be made and perform them using the surgical saw. Additional soft tissue may need to be dissected to allow the resected portion of the mandible to be removed.
4. Using the probe, register the location of each mandible osteotomy.
5. Perform two osteotomies on the fibula preserving at least 8cm of bone proximally and distally. Additional dissection of surrounding soft tissue may be required to then allow the viable section of fibula to be extracted from the leg whilst still connected to the pedicle.
6. Attach the fibula reference frame as proximally as possible on the extracted fibula.
7. Perform paired-point registration followed by surface registration on the exposed fibula.
8. Generate the virtual surgical plan.

<table>
<tr><td colspan="2">9. Align and secure the helping hands on the lateral fibula surface within the respective segment boundaries shown on the display and according to the rules of thumb.
10. Align the cutting guides with the plan using the guidance visualisation and make the fibula osteotomy. Repeat for the second osteotomy to create the fibula segment.
11. Using the probe, register the actual location of each cut plane making up that segment.
12. Recalculate the VSP based on the actual fibula osteotomies.
13. Repeat steps 10 to 12 to create, digitise and update the remaining two segments.</td></tr>
<tr><td>14. Using the reference model displayed, visually align the segments with respect to each other.</td><td>14. Using the guidance visualisation, align the segments with respect to each other.</td></tr>
<tr><td colspan="2">15. Secure the segments together using mini plates.</td></tr>
<tr><td>16. Move the segment into the mandible area and visually locate within the mandible resection.</td><td>16. Move the segment into the mandible area and using the guidance visualisation, locate the reconstruction within the mandible resection.</td></tr>
<tr><td colspan="2">17. Secure the reconstruction to the native mandible.
18. Remove the mandible fixation device.</td></tr>
</table>

Table 4 - Cadaver trial phase one surgical steps

Unfortunately, the VSP updating function of the system (i.e., following the fibula cuts) was only used for the first two procedures as an issue with the functionality of the module arose during the experiments and, due to time constraints, it was not possible to fix this before proceeding with the study. Therefore, the final two procedures did not utilise the plan updating function. This may have affected the accuracy results of the final two procedures.

The start and end times of each of the steps outlined in Table 4 were recorded. The total surgical time and ischemia time were also recorded and included time between steps. The average time for each step was then calculated and compared to the 3D-printed guides surgical workflow step time.

4.1.1.6 Postoperative Image Processing

Postoperative CT scans were taken of the head sections using the same CT scanner and scanning protocols outline above. We then created individual segmentations of the mini plates, each fibula segment, and the native mandible segments manually using thresholding and trimming tools in 3D Slicer. Due to the differing density of the bones across their cross sections, when generating 3D models from these segmentation, internal geometry (e.g., voids) was sometimes created. Before using these models to assess the reconstruction accuracy, this internal geometry was removed. We did this in MeshLab by first selecting low quality vertices within the mesh (all internal vertices). These vertices were deleted and any holes on the surface were filled using the inbuild automatic surface reconstruction function. The models were then imported back into 3D Slicer and merged to create one solid 3D model of the full reconstruction.

4.1.1.7 Results Calculations

The width, projection and registration results were based on fiducials placed in the 3D Slicer software on the full reconstruction model. One fiducial was placed on each coronoid process tip, each mandible angle and the most anteriorly projected point of the reconstruction. This was repeated 3 times and an average of the three points at each location was recorded from which the coronoid width, angle width, and mandible projection values were calculated (Figure 69).

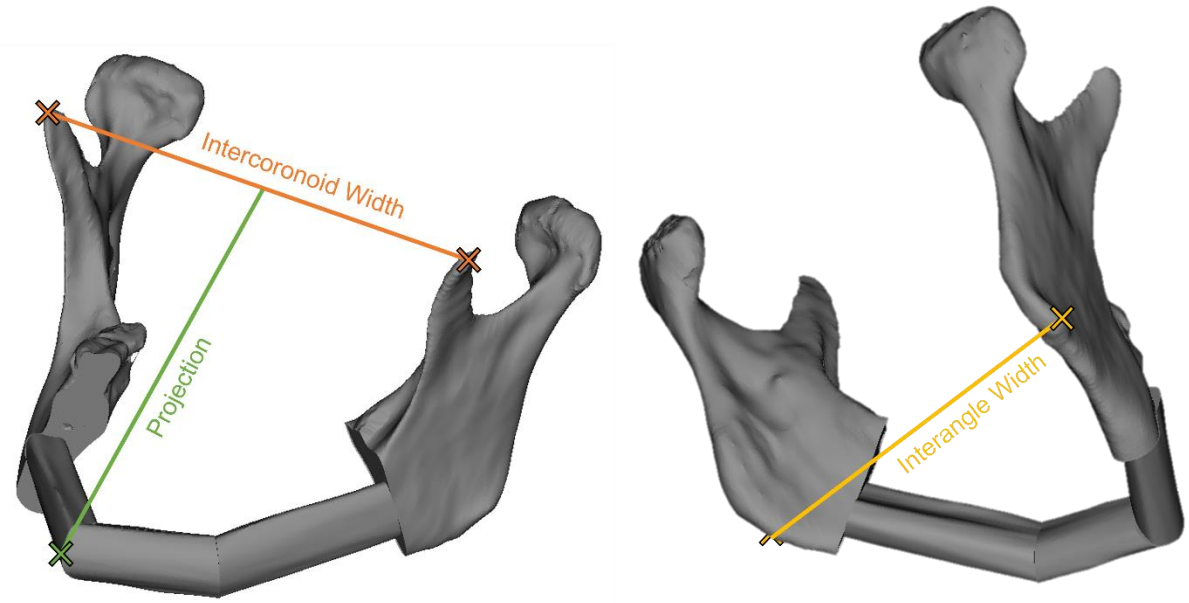

Figure 69 - Placed fiducial locations and calculated width and projection diagram

These fiducials were also placed on the VSP 3D model, and the same calculations run to allow a comparison between the actual and target reconstruction to be obtained.

Paired-point registration using the coronoid and angle fiducials was carried out between the two models to align them in the 3D Slicer Workspace. Model-to-model registration was used to determine ICP error; however, the models were not aligned using this as it reduced the accuracy of the alignment of the models. This then allowed the Hausdorff distance and Dice score to be calculated between the two models. Both metrics were calculated for the full reconstructed mandible and the fibula segments alone to determine how well the reconstruct

was aligned in the mandible gap. A second registration was also performed using additional fiducials placed only on the fibula segments. The Hausdorff distance and Dice score were then recalculated only using the fibula segment models to determine how well each fibula segment was aligned with respect to the others.

The fibula osteotomy guidance accuracy was also evaluated. This was performed using the same method describe in section 3.2.1.5 for the fibula guidance evaluation study. However, as well as the actual segments being compared to the target segments, they were also compared to the digitised segments created when updating the VSP during surgery. This allowed the accuracy of the digitising step to be determined. The same method was also employed to determine the accuracy of digitising the mandible cut planes.

Finally, the distance between the internal surface of the mini plates and the underlying bone surface was evaluated. This was done by manually periodically placing ten fiducials along the internal surface of the plates. The closest distance was then calculated between each of these fiducials and the reconstruction model to find the maximum and average plate to bone distance.

Although too small a number of reconstructions to be used for statistical analysis, this study allowed the system to be tested on a realistic model whilst forming a hypothesis based on its performance.

4.1.2 Results

We calculated the following results using the 3D models discussed above and a module we created for this trial in 3D Slicer that compiled all the steps required to calculate the different metrics into one user interface. A table containing all numerical results is included in Appendix C:.

The graph below outlines the width and projection results for all five (including the trial run) procedures performed. The average intercoronoid width deviation was -0.1 ± 1.31 mm and average internal width deviation was -0.86 ± 0.63 mm. Both these measures indicate how well the mandible segments are held with respect to each other. Both guidance metrics perform similar for this metric. The projection is more indicative of how well the segments are placed in the mandible gap. The average projection deviation achieved was 0.17 ± 1.81 mm. The ICP also indicated the accuracy of the alignment of the segments as it compares the similarity of the pre and post operative models. The average ICP error achieved was 0.64 ± 0.17 mm and is relatively consistent between the Freehand and Guided method.

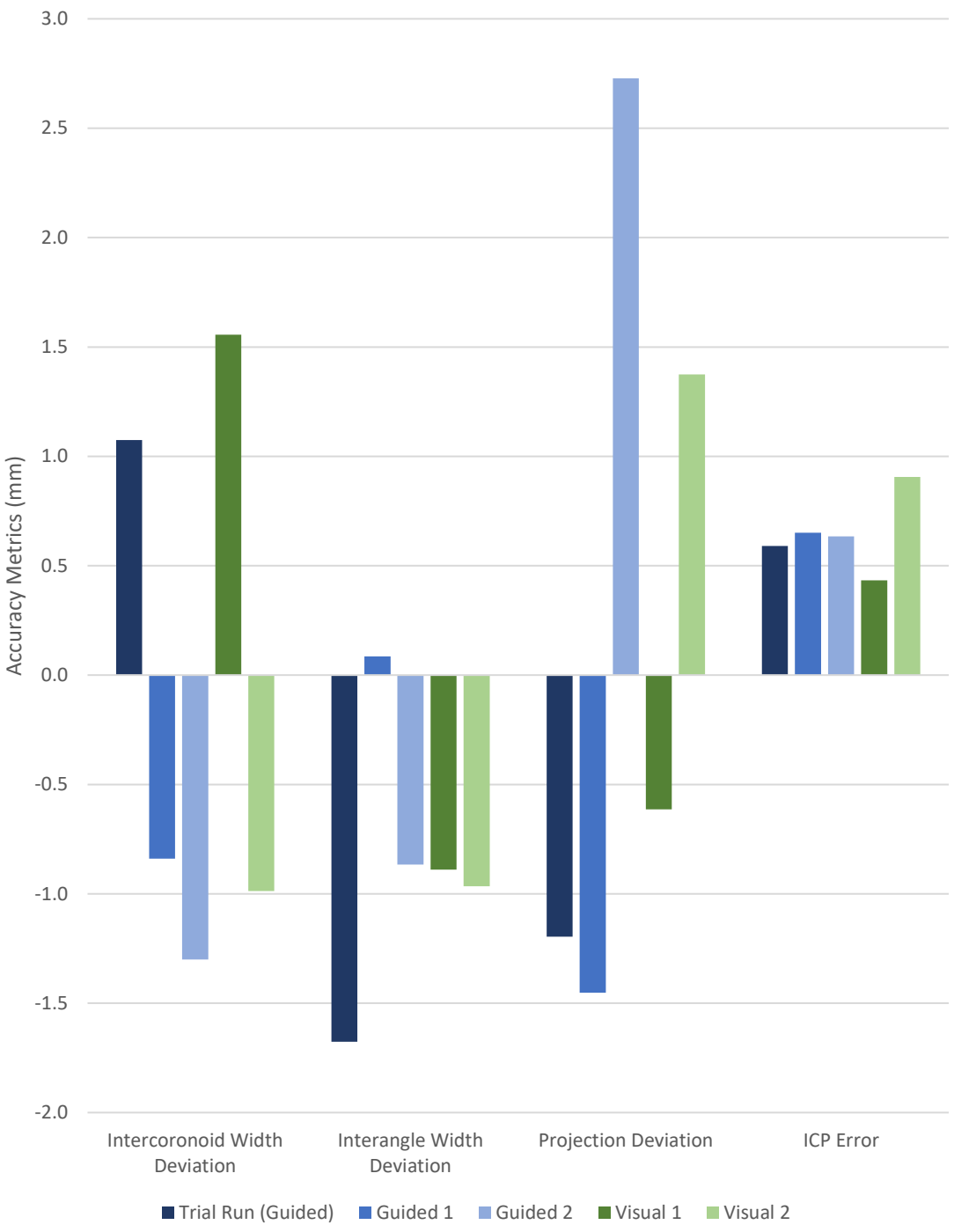

Figure 70 - Width and projection results for each procedure

All Hausdorff distance and Dice score results are shown in the graphs below. Large Hausdorff 95 distances were found when using the full reconstruction for three of the five trials. The Hausdorff 50 distance for the same trials show a much less apparent error. Visual trail 2

produced a consistently higher error even when using just the fibula segment models. The dice score for all trials are similar with the guided alignment workflow achieving a higher average of 0.82 ± 0.09 compared to 0.78 ± 0.13 for the Freehand method.

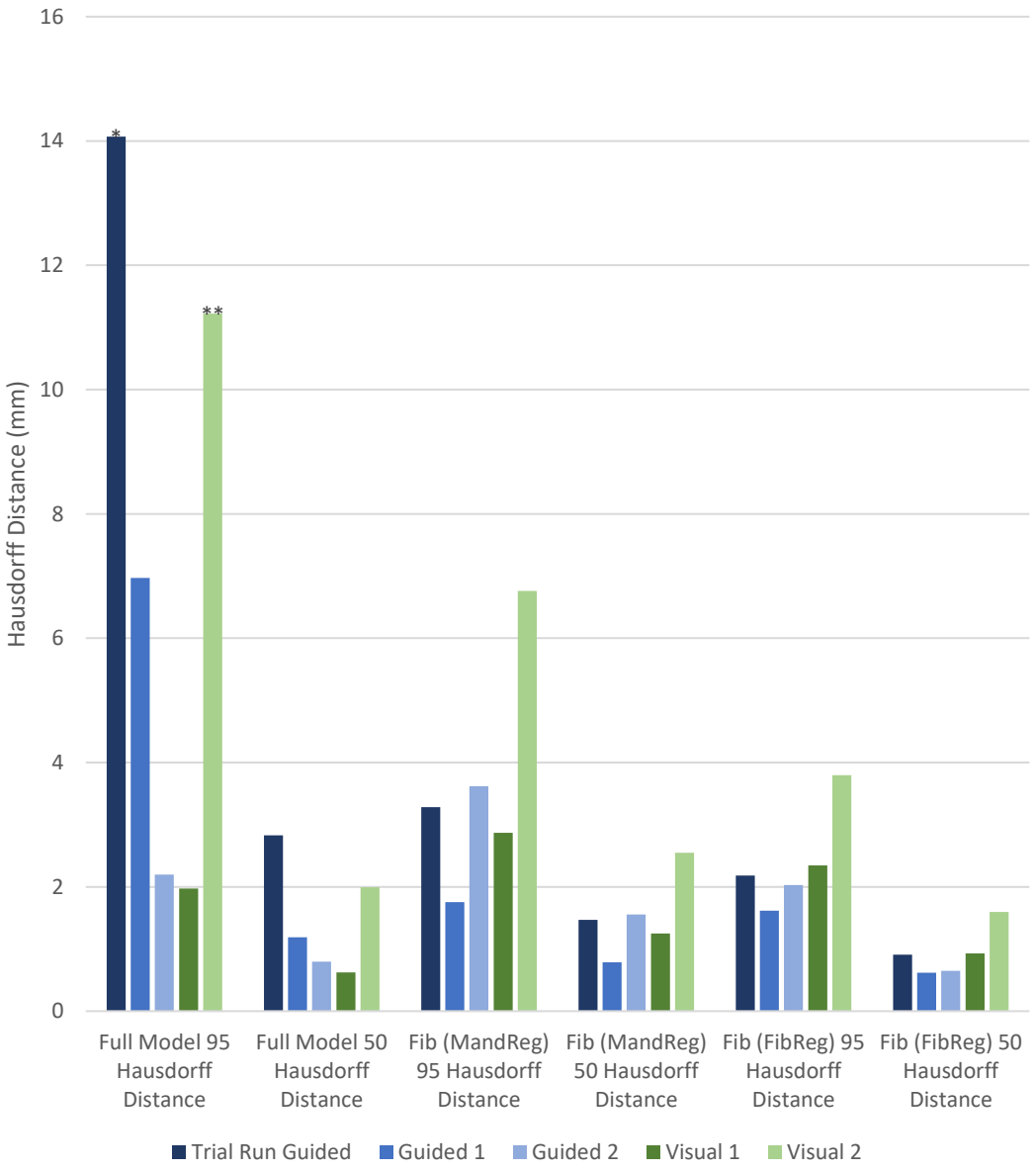

Figure 71 - Hausdorff distance results for each procedure
*(*A large section of mandible was chipped off during the procedure leading to large Hausdorff distance)*
*(**Mandible cuts planned were not digitised accurately)*

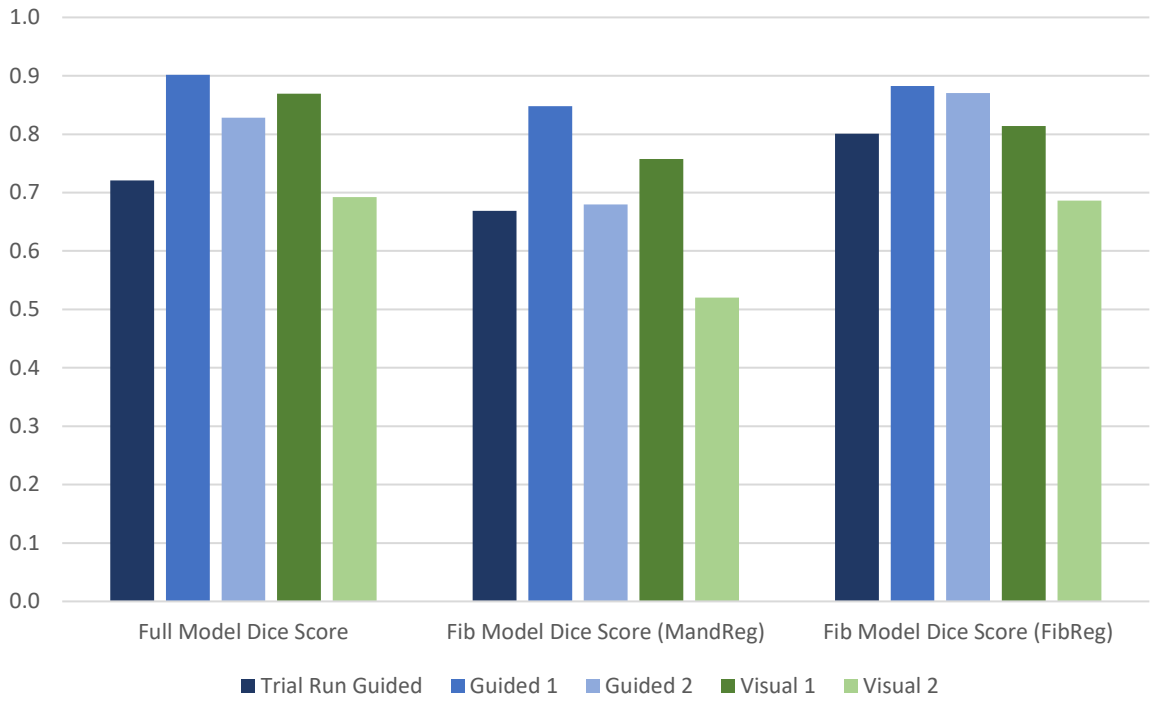

Figure 72 - Dice score results for each procedure

The length and angle deviations compared to the target and the digitised models calculated for all reconstructions are shown in the following graphs. Segments outlined in orange were manually trimmed when placing them in the mandible and therefore the deviation from the target for these segments is not wholly associated with the accuracy of guiding the cuts using the image guided system. The average length and angle error calculated across all trials was 0.33 ± 0.75 mm and 2.25 ± 0.83˚ respectively. Adding the ability to update the VSP should negate the affect of these errors; however, that depends on the accuracy of digitising the actual cut planes. This error is comparable in size to the cutting guidance error with an average length deviation of -0.36 ± 1.90 mm and angel deviation of 3.85 ± 2.27˚.

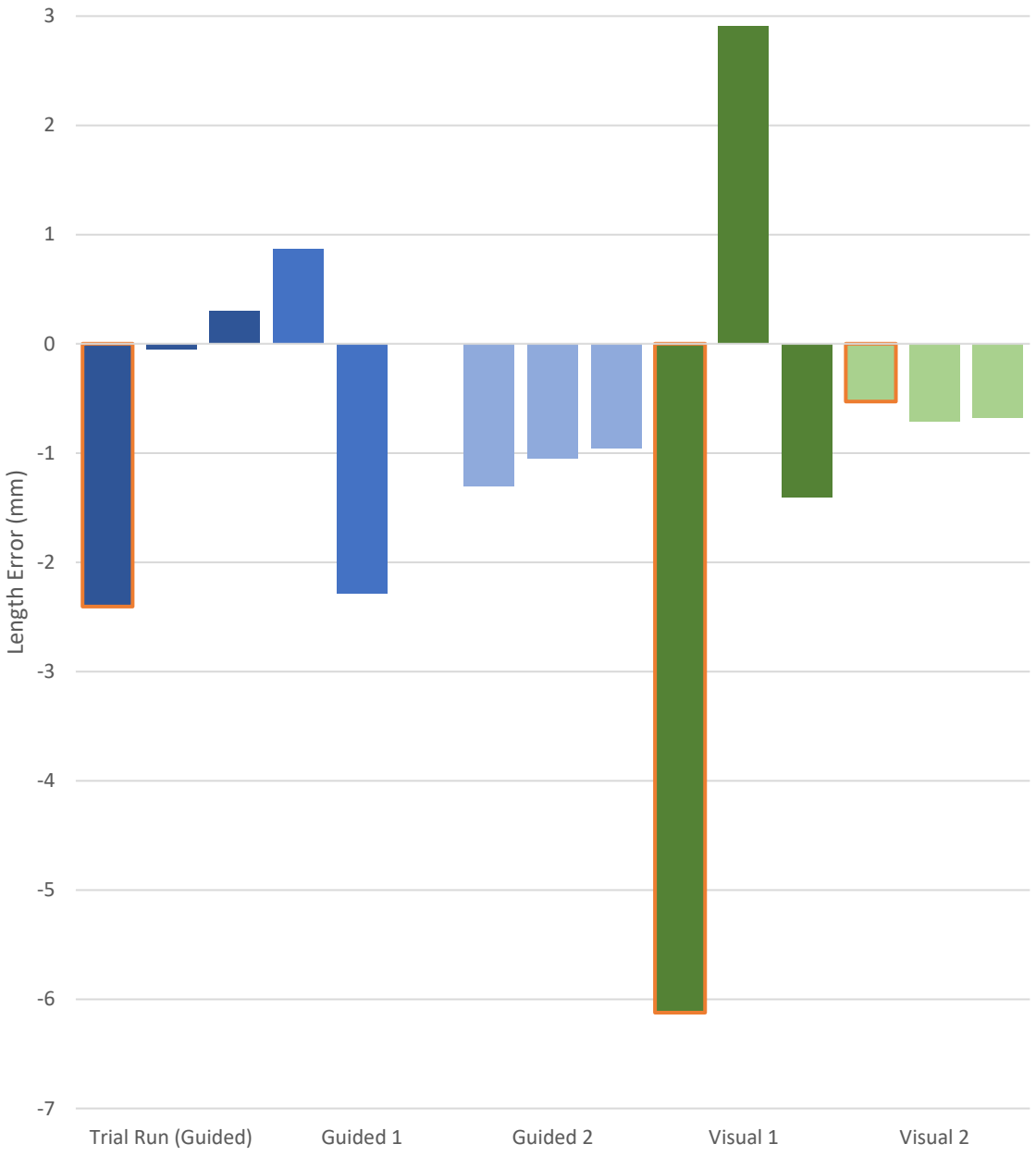

Figure 73 - Fibula segment length deviations from target segments

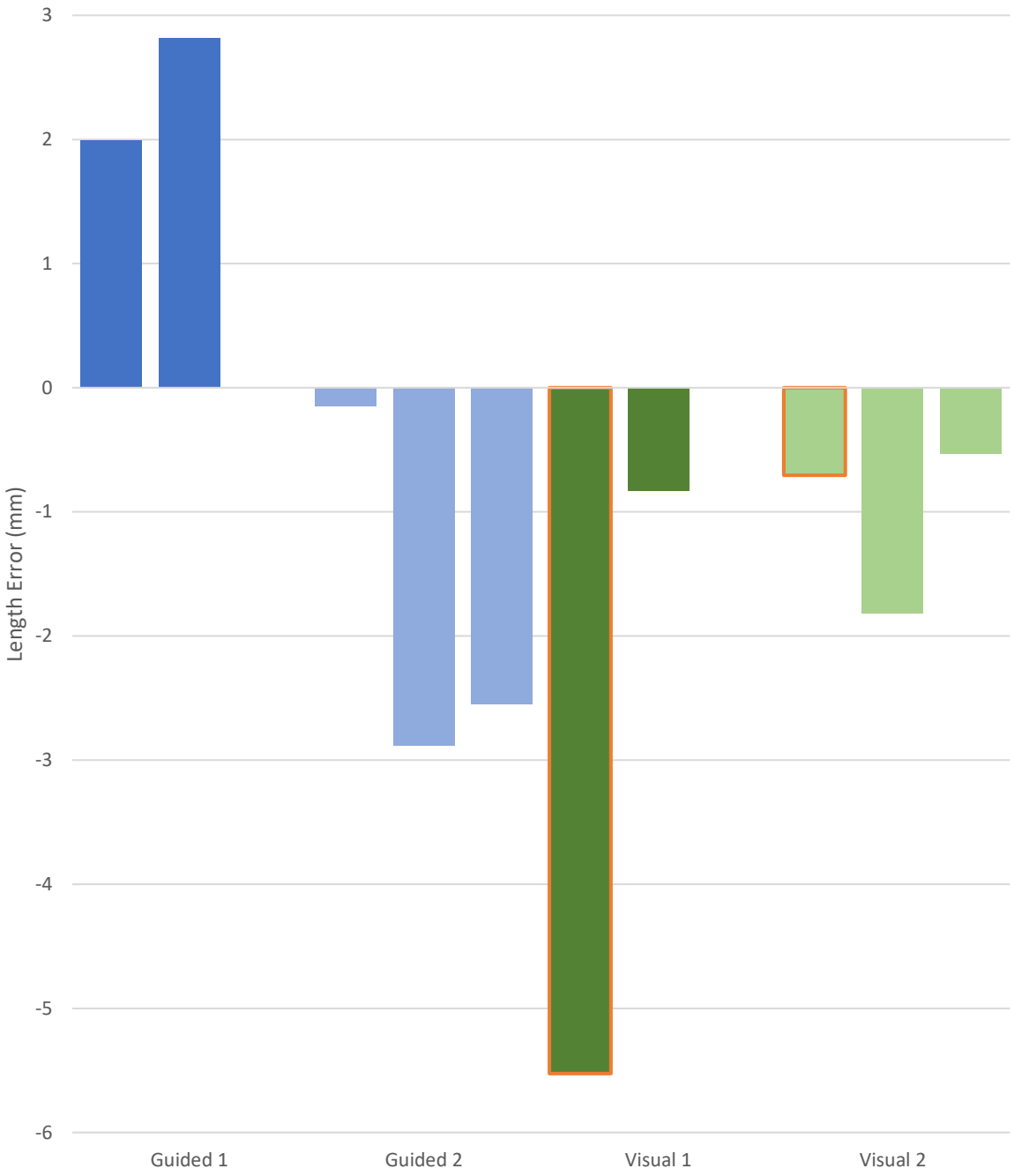

Figure 74 - Fibula segment length deviations from digitised segments

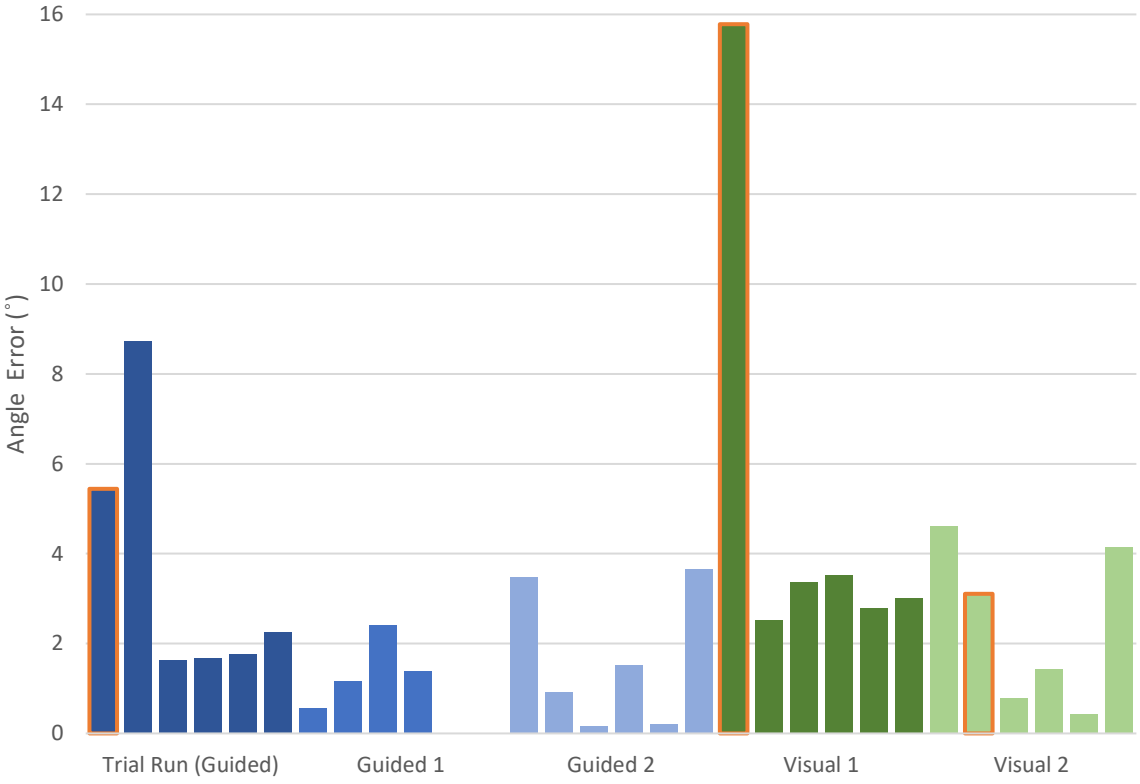

Figure 75 - Fibula segment angle deviations from target segments

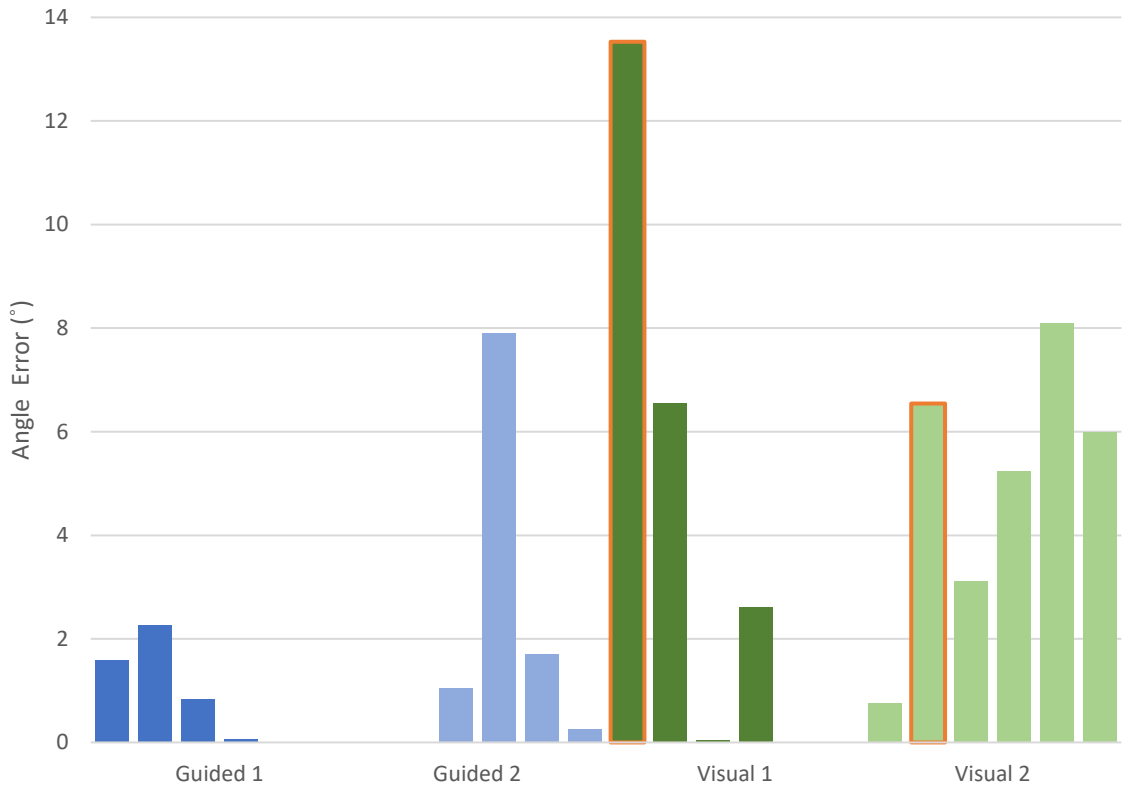

Figure 76 - Fibula segment angle deviations from digitised segments

The displacement and angle deviation between the digitised location of the mandible cut planes and their actual location is shown below. Visual trial two incurred higher errors than all other trials. However, the rest of the trials perform similar to the error achieved when digitising the fibula cut planes using the same process.

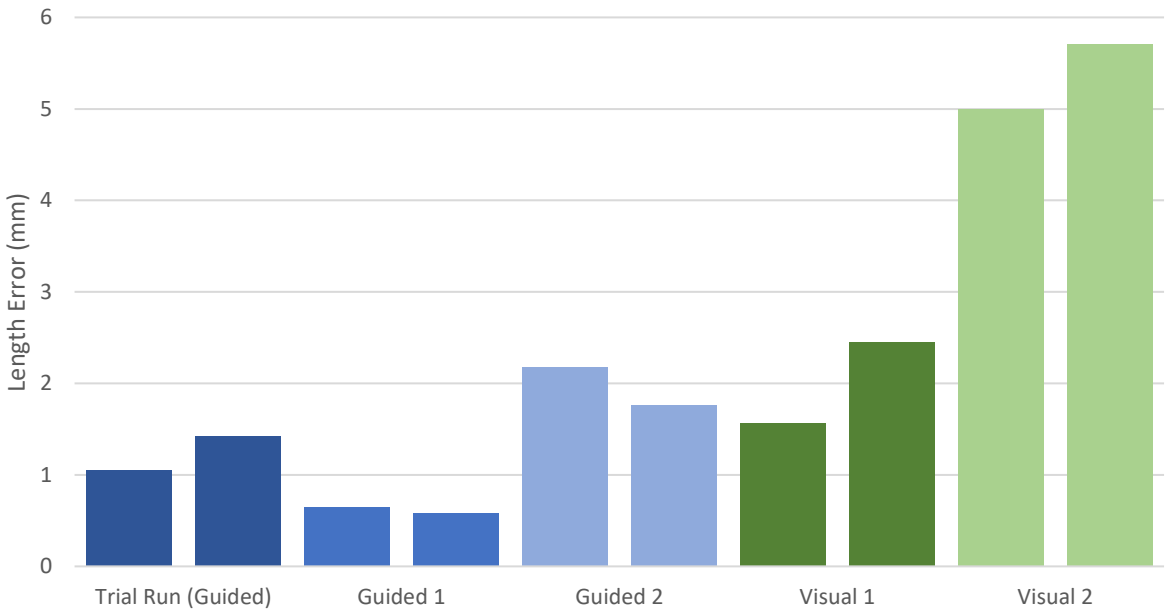

Figure 77 - Mandible osteotomy displacement deviation from digitised cut plane

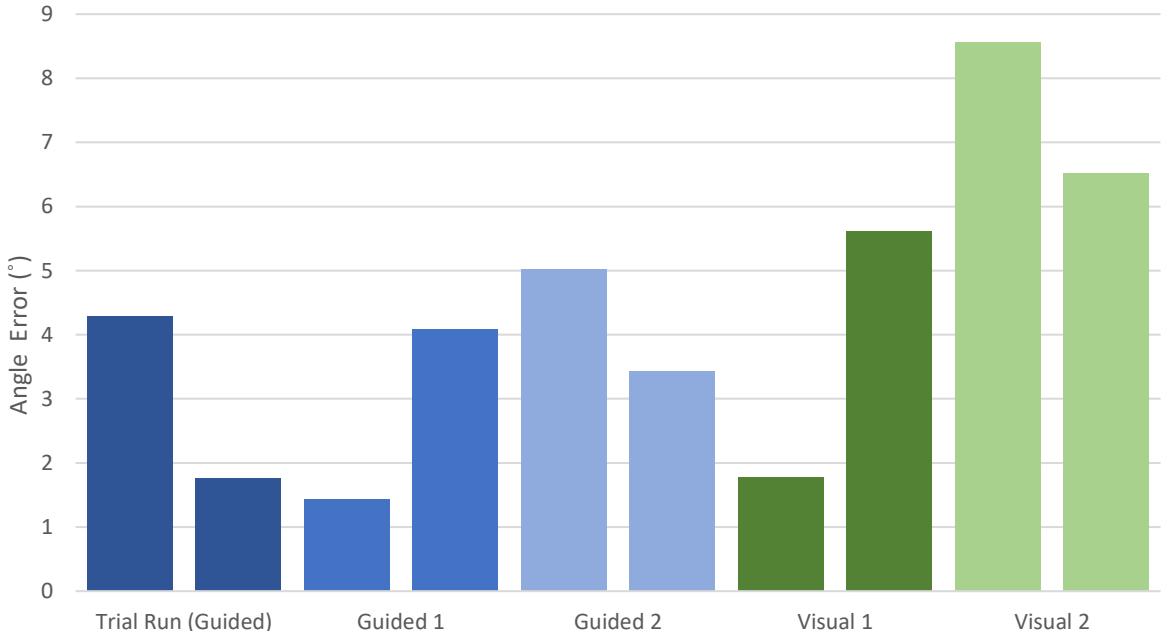

Figure 78 - Mandible osteotomy angle deviation from digitised cut plane

One additional metric measured during this study was the distance between the reconstructed mandible and the inner plate surface. The graph below (Figure 79) shows the maximum and average distance for each cadaver study completed. Only one instance was the maximum plate distance over 1 mm with an average of 0.41 ± 0.23 achieved across all studies.

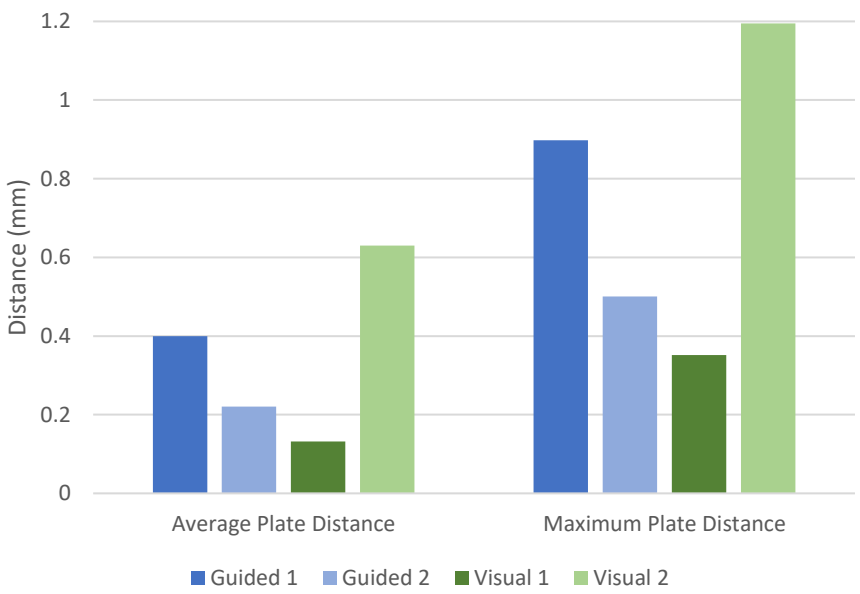

Figure 79 - Maximum distance between reconstructed mandible and mini plate

The average values of all the metrics outlined above are detailed in the table below.

Accuracy Metric	**Freehand Alignment Average**	**Guided Alignment at Fibula Average**	**Overall Average**
Intercoronoid Width Deviation (mm)	0.28 ± 1.80	-0.35 ± 1.26	-0.1 ± 1.31
Interangle Width Deviation (mm)	-0.93 ± 0.05	-0.82 ± 0.88	-0.86 ± 0.63
Projection Deviation (mm)	0.38 ± 1.41	0.03 ± 2.34	0.17 ± 1.81
Projection Point Distance (mm)	5.92 ± 2.75	4.20 ± 0.71	4.89 ± 1.74
ICP Error (mm)	0.67 ± 0.33	0.62 ± 0.03	0.64 ± 0.17
Full Model Dice Score	0.78 ± 0.13	0.82 ± 0.09	0.80 ± 0.09
Fibula Segments Dice Score (Mandible Registration)	0.64 ± 0.17	0.73 ± 0.1	0.69 ± 0.12
Fibula Segments Dice Score (Fibula Registration)	0.75 ± 0.09	0.85 ± 0.04	0.81 ± 0.08

Accuracy Metric	Freehand Alignment Average	Guided Alignment at Fibula Average	Overall Average
Full Model Hausdorff Distance 95/50 (mm)	6.60 ± 6.54 / 1.31 ± 0.97	7.75 5.97 / 1.61 1.08	7.29 ± 5.38 / 1.49 ± 0.92
Fibula Segments Hausdorff Distance 95/50 (Mandible Registration) (mm)	4.82 ± 2.75 / 1.90 ± 0.92	2.88 ± 0.99 / 1.27 ± 0.42	3.66 ± 1.87 / 1.52 ± 0.65
Fibula Segments Hausdorff Distance 95/50 (Fibula Registration) (mm)	3.07 ± 1.03 / 1.26 ± 0.47	1.94 ± 0.29 / 0.72 ± 0.16	2.39 ± 0.83 / 0.94 ± 0.39
Average/Maximum Plate to Bone Distance (mm)	0.38 ± 0.35 / 0.77 ± 0.60	0.42 ± 0.21 / 1.03 ± 0.61	0.41 ± 0.23 / 0.93 0.54
Mandible Cut Digitisation Linear Error (mm)	3.68 ± 1.99	1.27 ± 0.63	2.24 ± 1.76
Mandible Cut Digitisation Angle Error (˚)	5.63 ± 2.84	3.34 ± 1.44	4.25 ± 2.29
Fibula Segment Length Error / Absolute (mm)	0.03 ± 1.02 / 1.43 1.03	-0.56 ± 0.63 / 1.15 ± 1.06	-0.33 ± 0.75 / 1.26 ± 0.92
Fibula Segment Angle Error (˚)	2.51 ± 0.75	2.08 ± 0.98	2.25 ± 0.83
Fibula Cut Digitisation Length Error / Absolute (mm)	-1.00 ± 0.25 / 1.00 ± 0.25	0.27 ± 3.02 / 1.15 ± 0.38	-0.36 ± 1.90 / 1.57 ± 0.70
Fibula Cut Digitisation Angle Error (˚)	5.74 ± 0.08	2.08 ± 1.09	3.85 ± 2.27

Table 5 - Average overall accuracy metrics and separated averages for each alignment tested

The graph below (Figure 80) shows the total procedure time and ischemia time recorded for each reconstruction.

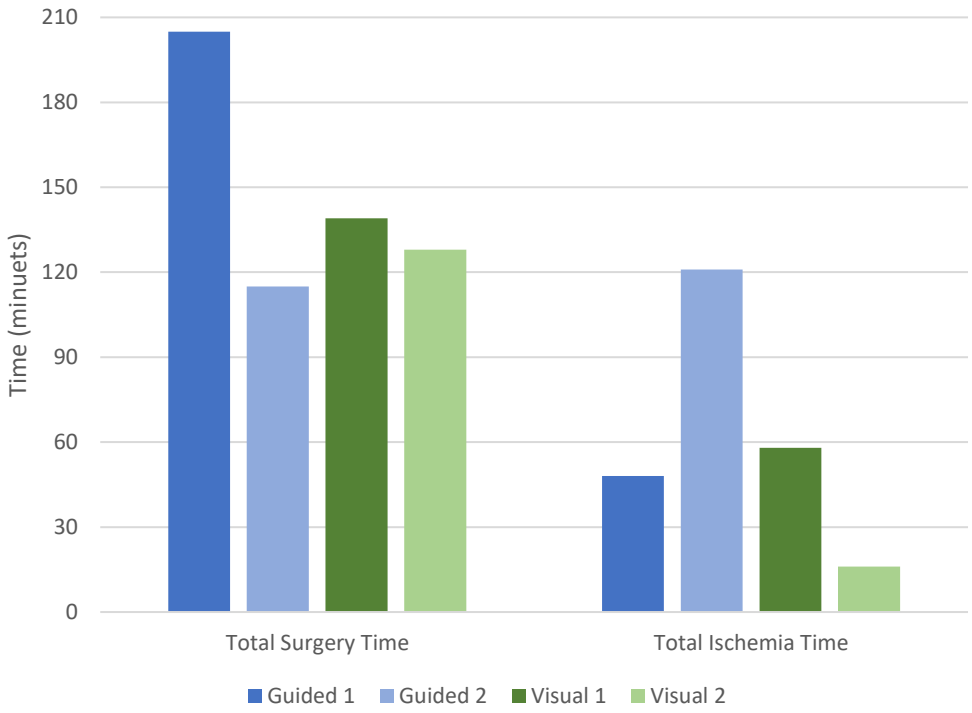

Figure 80 - Total time and ischemia time for each procedure

Using the average time for each surgical step in the workflow (label IGS), the following chart (Figure 81) was generated outlining the time required for each main step compared to the same step in the 3D-printed guides workflow (label 3DG). A more detailed chart showing all sub steps is included in Appendix D:. This chart also shows the shortest time for each surgical step in the workflow (label IGS*). The graph shows and increase between the 3D-printed guide method of 30 minutes when compared to the shortest step time and 1 hour and 45 minuets when compared to the average step time; however, the presurgical time of 22 hours is completely eliminated. The ischemia time for both the average and shortest step time is reduced compared to the 3D-printed guide methods by 10 and 15 minutes respectively. The largest increase in time per step between the average and shortest step sets for the cadaver study timings is during the fibula cutting guidance and the segment alignment guidance steps.

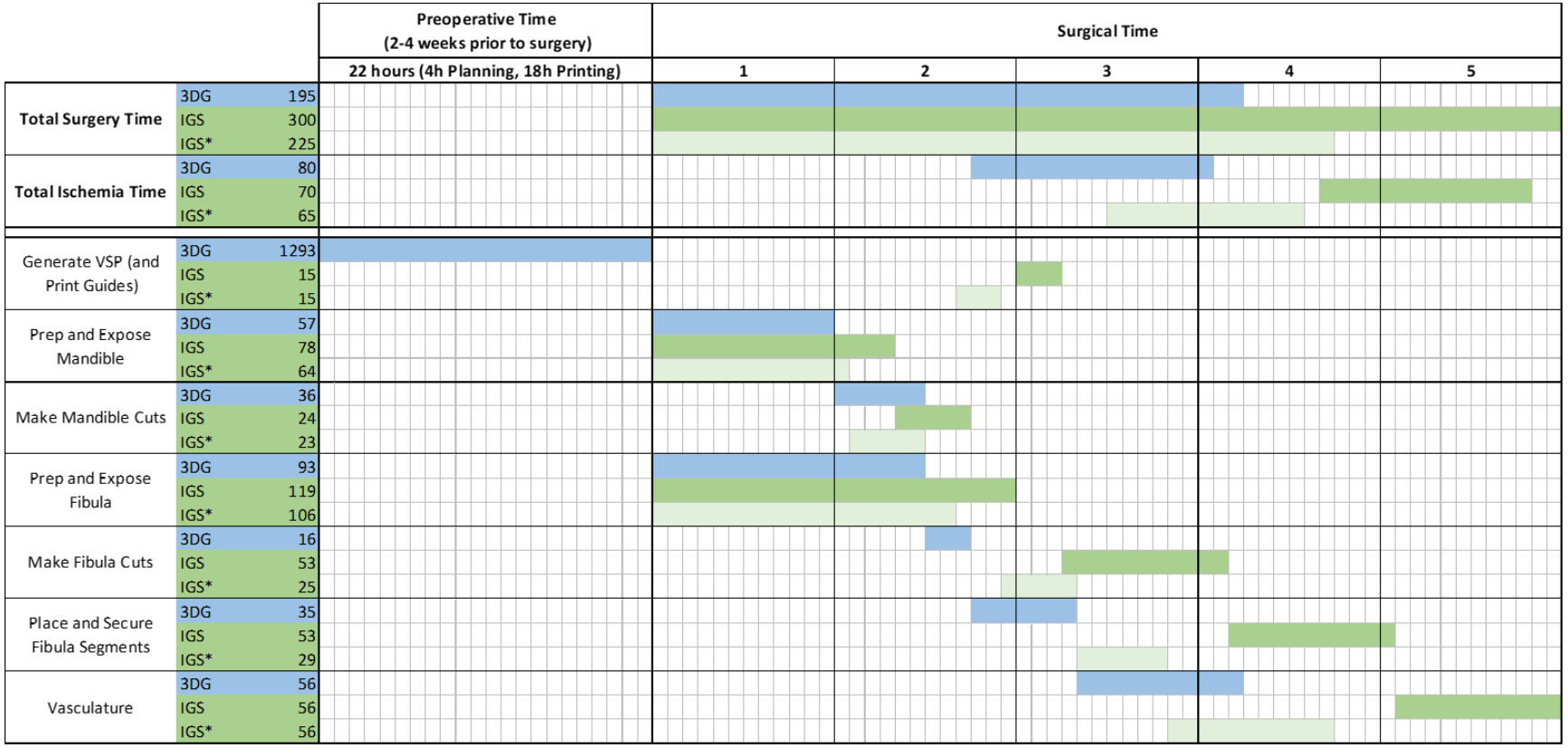

Figure 81 - Time map of main surgical steps in current and proposed workflows

4.1.3 Discussion

The typical accuracy measurements reported for mandibular reconstruction surgery (width, projection) achieved in this study align with what is seen in literature. One recent paper published by a member of the ISTAR group compared these metrics from a number of different centres using the 3D-printed guide techniques (E. Wang, 2020). The comparison table below outlines the average accuracies shown in that paper (minimum and maximum instance of each metric is also shown in brackets) against the accuracies found during this cadaver study.

Source	ICP Error (mm)	Segment Length Deviation (mm)	Segment Angle Deviation (˚)	Width Deviation (mm)	Projection Deviation (mm)
Literature Average (E. Wang, 2020)	1.27 (0.59 to 1.63)	1.70 (1.3 to 2.4)	4.01 (2.29 to 5.23)	3.02 (2.32 to 3.86)	3.47 (2.39 to 4.31)
Phase One Cadaver Study Averages	0.64	1.26	2.84	1.15	1.47

Table 6 - Comparison of results achieved in literature using the 3D-printed cutting guides and the results achieved in phase one of the cadaver trial

In all instances above, the metrics calculated for the cadaver study achieved lower deviation from the VSP than the 3D-printed cutting guides. Although the projection accuracies shown above are comparable to the literature, it was noted that based on the way the projection distance is measured, the height of the projection point in the mandible will also affect this metric. To try and determine the actual change in projection point, the distance between the projected points was measured directly (Table 5). This is higher than expected which may be due to inaccuracies in digitising the mandible cut planes discussed earlier forcing the segments to be projected out or in due to the difference in resection size.

4.1.3.1 Segment Alignment Method

One of the main aims of this phase of the cadaver study was to determine which segment alignment method to take forward in the new surgical workflow. Based solely on the accuracy results shown above, there is only a slight advantage of one method over the other. The Dice score and Hausdorff distance are the main indicators of segment alignment accuracy as discussed in section 2.3.1, with these metrics calculated using the mandible registration outlining how well the full reconstruction construct is aligned in the resection gap, whereas using the fibula registration indicating how well the segments are aligned with respect to each other.

In both instances, as indicated in Figure 71 and Figure 72, the guided method produced a marginally higher average Dice score and lower Hausdorff distance compared to the visual method suggesting that the guided method produced a more accurate alignment with respect to the VSP. Although too few samples were tested in this study to statistically determine, this difference would not likely affect the surgical outcomes of the procedures. Additionally, both procedures that used the visual alignment method required a fibula segment be trimmed before the reconstruction could fit in the resection gap. Figure 82 below shows the trimmed fibula piece. This was not required when using the guided alignment method.

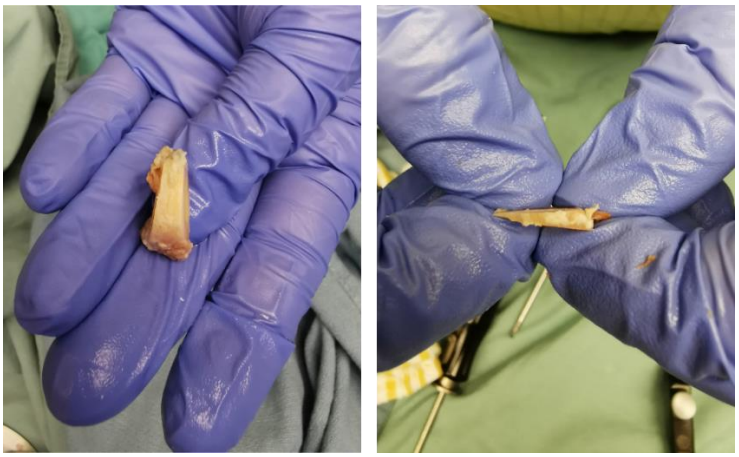

Figure 82 - Trimmed fibula segments when using visual alignment method (Left – Visual 1, Right – Visual 2)

These findings, combined with the positive user feedback attained for the guided method (outlined in section 4.1.4) justified moving forward with the image-guided segment alignment method in all future studies and fully integrating this into the workflow.

4.1.3.2 Surgical Saw Issues

Although the accuracies achieved in the cadaver study were comparable to literature, there are two main situations related to the surgical saw blade used that occurred during the study that may have reduced the accuracy of guiding fibula osteotomies. The first is the fact that the saw blade used was not new and had been used for many studies previously. This meant that the blade was not very sharp and often required a lot of force to be applied to allow it to successfully cut through the cadaver bone. This in turn created a lot of vibration throughout the system, often leading to the cutting guide loosening and shifting whilst the osteotomies were being performed. This itself may have induced some additional error in the position and angle that each fibula osteotomy was made.

To combat these excessive vibrations, an alternative saw was used. However, this saw had a much thinner blade, 0.4 mm compared to 1 mm. As the cutting guide was designed for the thicker saw blade, when the thinner blade was inserted into the cutting guide slot it was not rigidly constrained to follow the prescribe cutting plane as it could move horizontally and rotate within this slot. This means that even if the cutting guide was perfectly aligned with the target, an error would be induced in where the actual cut plane was performed based on where within the cutting guide slot the saw blade was positioned. The other error induced by using a thinner blade is when calculating the VSP itself. The plan is generated to account for the bone removed by the thickness of the saw blade and therefore if a thinner blade is used, less bone is removed by the thickness of the blade. To allow this to be altered in the future, a user input should be added to the VSP module.

4.1.3.3 Reflective Marker Visibility

Another area where the system may have introduced some additional error is during the guided alignment of the fibula segments. During both cadaver procedures using the guided alignment method, the location of the fibula segment with respect to its neighbour in real space was significantly different to the visualisation of these two segments generated on the display. The way this display is generated is based on the transform calculated between the hand reference frame and the fibula segment (the calculation of this is explained in section 2.2.3.5). This calculation will include a small error as it utilises the fibula registration transform. However, the observed deviation was perceived to be much higher than what the fibula registration could cause.

The cause of this additional error is hypothesised to be due to how well the tracking camera can see the marker arrays. After testing this theory, it was discovered that the camera's perceived location of a marker array changed depending on whether it can see all four or only three of the reflective markers making up the array. In the diagram shown in Figure 83 the gray silhouette is the actual location of the Helping Hand and marker array; however, one of the four reflective markers is not visible and therefore, the camera perceives the location of the marker array offset from this (H1'). If the hand to segment transform ($T_{S1H1'}$) was calculated when only three reflective markers were visible (as depicted here), the transform would be calculated between the offset marker array coordinate frame (H1') and the segment (S1).

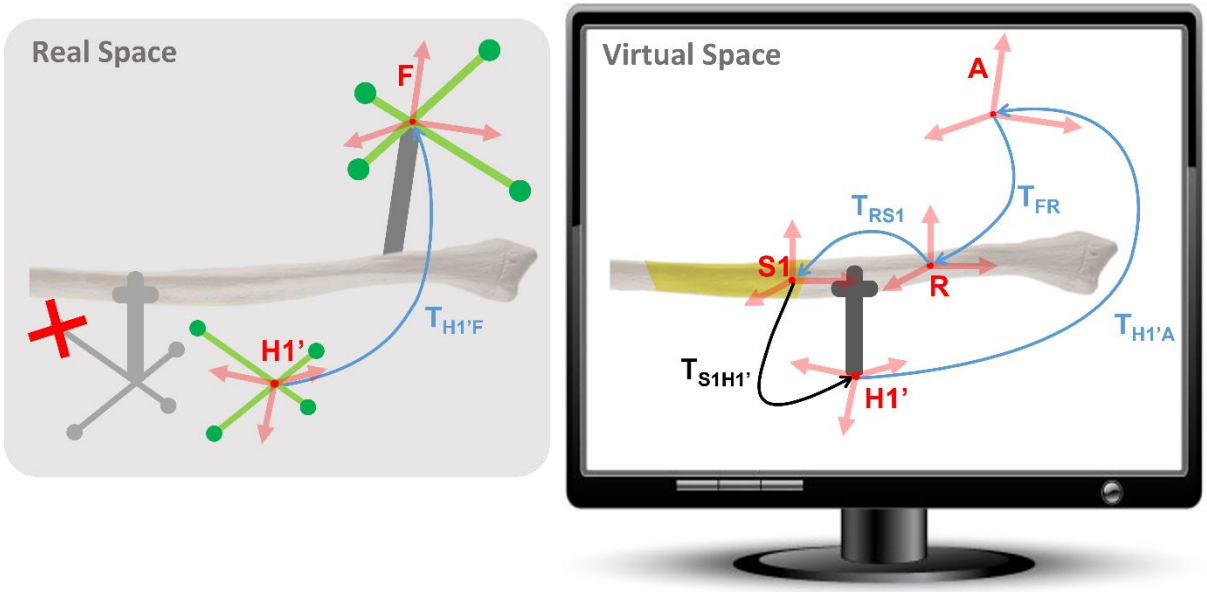

Figure 83 - Fibula segment tracking when reflective markers not visible transform calculation diagram

The offset in this diagram is exaggerated as it is clear the 3D model of the Helping Hand in virtual space is not an accurate representation of where the hand is in real space. However, this was not always obvious in practice and therefore, went unnoticed until attempting to align the segments with respect to each other as show in Figure 84 below.

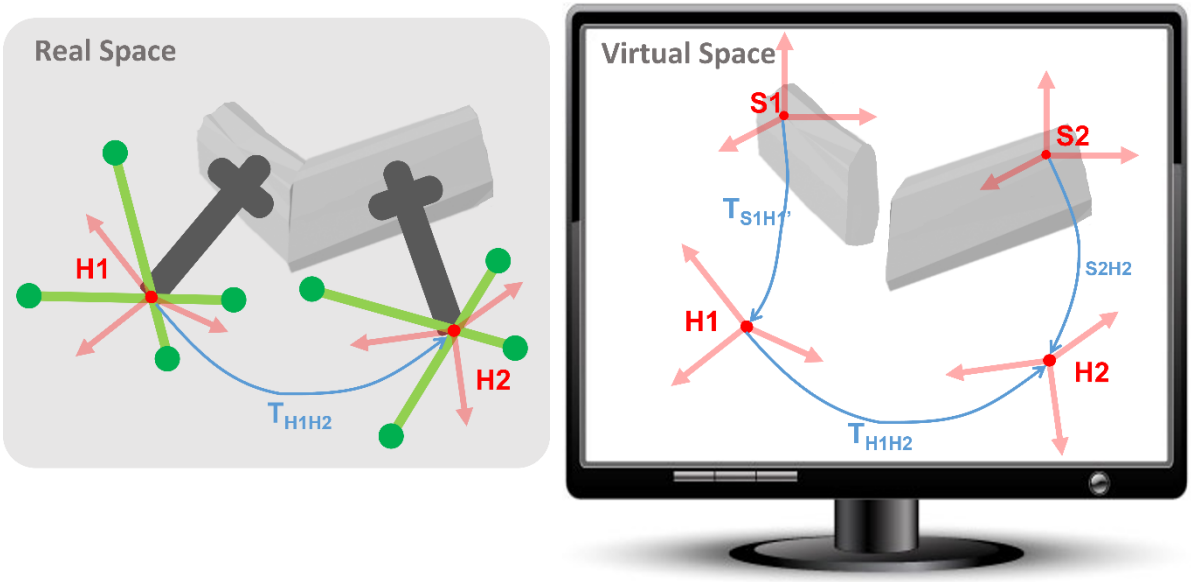

Figure 84 - Fibula segment location when reflective markers not visible transform diagram

At this point all four reflective markers can be seen, but the hand to segment transform ($T_{S1H1'}$) was calculated based on the offset marker array location (H1'). When the visualisation of the segment with respect to its neighbour is created, $T_{S1H1'}$ is used to place the segment model in virtual space. However, now all four reflective markers are visible, the transform between the Helping Hand marker array coordinate frame (H1) and the segment model coordinate frame (S1) is required which is no longer equal to $T_{S1H1'}$. The difference between these two transforms is visualised as an offset between neighbouring segments where there is not one in real space. This meant that when the participants were trying to align the segments using the offset visualisation, the segments were aligned using the guidance and then altered visually to account for this offset. It is anticipated that better alignment could be achieved using the guidance method once this error is fixed. To do this, the ROM files for each marker array should be generated to only track when all four reflective markers are visible. Although potentially increasing the frequency of line-of-sight issues between the camera and the marker arrays, this will stop any error being incurred due to the number of reflective markers visible and should eliminate the visualisation issue observed during Phase One of this cadaver trial.

4.1.3.4 Cut Plane Digitisation

This issue may also contribute to the error associated with using the probe to digitise the mandible and fibula actual cut planes which were much higher than expected. If only three of the reflective markers on the probe or mandible/hand marker arrays could be seen when the fiducials were placed, then the system would perceive the probe point to be at a different location. Consequently, the cut plane calculated from the three fiducials placed would then be offset. However, additional investigation should be done to further assess the accuracy of this digitisation method before any further studies are conducted.

This error between the actual cut plane location and the digitised cut plane location for the mandible osteotomies is equivalent to how well the 3D-printed guide method replicates the VSP mandible resection planes. Although this error was higher than expected for this system, it is still comparable to the 3D-printed guides method which achieved a linear and angular deviation of 1.69 mm and 10.16˚ respectively (Hanken, 2015).

The error associated with the digitised points used to determine the actual fibula cut planes does not have an equivalent error in the 3D-printed guides technique. This is an additional error associated with this image guided system and as such should be minimised as much as possible. As the process of digitising these planes introduces additional error into the system, the option to update the VSP or not was included in the modules. As this error is bigger than expected the decision of whether to update the plan or not would need to be considered more carefully. However, if this added error can be reduce enough, and as the additional time incurred to perform the VSP update is minimal, it may be feasible to remove this decision step and always update the VSP.

4.1.3.5 Flexibility in the System

However, the current method of updating this plan is unreliable for different fibula and mandible models. It is hypothesised that if the model has too much internal geometry, the recalculation of VSP does not perform correctly. This is why this function was only used for two of the four reconstructions. However, when used, this function showcased the flexibility that it brings to the overall system. During the second cadaver trial, the quality of the fibula was significantly lower than anticipated. Therefore, when the second hand was screwed into the fibula it fractured causing much of the fibula to become unviable. Eventually too much of the bone became unviable and the plan had to be substantially altered to only utilise two fibula segments. Being able to alter the VSP so dramatically during the surgery highlights how flexible this system is. In

this case even after the first segment is cut, the rest of the plan can be completely altered to ensure an optimal reconstruction is created.

4.1.3.6 Plate Bone Gap

One complication associated with this type of mandible reconstruction is plate extrusion. This is where the reconstruction plate erodes though the soft tissue over time and becomes exposed. A recent study suggested that if the distance between the plate and the reconstruction bone surface is less than 1 mm, there is a 86% lower likelihood of plate extrusion (Davies, 2021). From Figure 79, the average plate to bone distance achieved during this cadaver trial in all instances are below this 1 mm threshold with the maximum only deviating above this in one instance during Visual 2. On further investigation, when aligning the segments in the mandible, a step was created between the last fibula segment and native mandible shown in Figure 85 below. It is at this point that the plate to bone distance exceeds 1 mm.

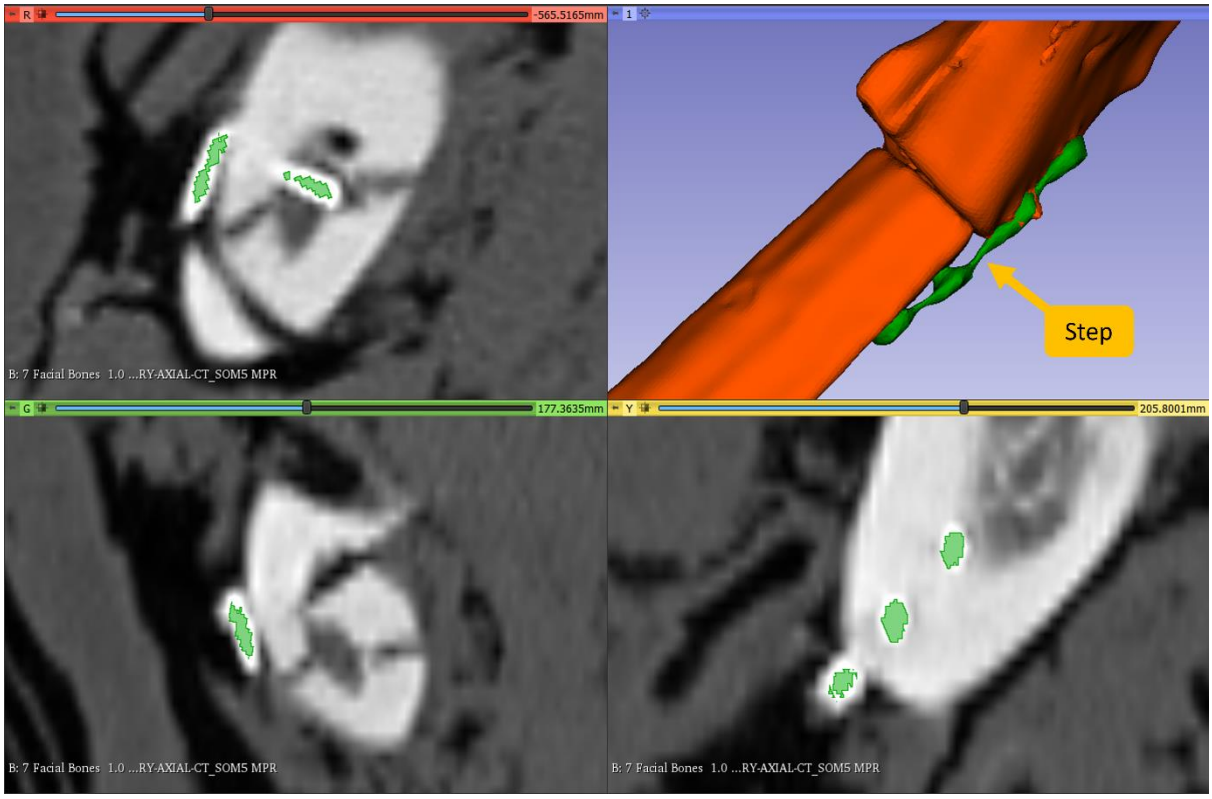

Figure 85 - Visual 2 Plate Segmentation and 3D Model at Maximum Plate to Bone Distance Location

Figure 85 also shows the plate segmentation used when calculating this distance. The green areas overlayed on the CT scans show the area included in the segmentation. However, this area does not extend across the full plate (depicted as the bright white area directly surrounding the green) at this section of the CT. This may be artificially increasing the plate to bone distance here above what it actually is.

4.1.3.7 Procedure Times

Figure 80 shows the total procedure time and ischemia times recorded for each cadaver study. These times are different to what is shown on the time map (Figure 81) as additional steps are included in the time map that were not performed during the cadaver trial. The time to perform these steps was taken from the associated 3D guide method step time as they should be equivalent. Additionally, for both the total procedure time and ischemia times shown in Figure 80, time in between steps is included. This is important to note as significant additional time

spent troubleshooting and discussing may be included in these values that is not representative of what would typically be experienced if this system is implemented into an operating room. The ischemia time for cadaver study Guided 2 is much higher than the other four studies. This is because the pedicle had to be cut before arranging and securing the fibula segments with respect to each other. There was not enough room to arrange the segments due to interference between the leg and the hand reference frame.

Although this system greatly increases the flexibility of the procedure, it is clear from the time map (Figure 81) that it also increases the total surgical time. This was expected as several additional steps must be performed in order to use the optical tracking system such as the registration steps. The time to generate the VSP is now also included in the surgical time. However, the 22 hours required before surgery to generate the VSP and print the cutting guides is completely eliminated. This is also based on an inhouse timescale, if this service was outsourced to a commercial company the lead in time that is eliminated could be up to four weeks (Pietruski, 2019a) and could potentially save thousands of dollars. This would have to be weighed against the additional cost incurred due to the longer surgical time.

It is shown in the time map that the fibula preparation step (including fibula registration) can be done concurrently with all the initial mandible steps which is technically possible. However, to do this, two tracking cameras would be required as well as two displays and the system would need to be altered to allow both visualisations and connection to be active at once. This additional equipment may not be available during every surgery. This could add an additional 5 - 20 minutes to the total surgical time.

4.1.3.8 Ischemia Time

The ischemia time during the surgery is also an important aspect of the surgery. Based on timing taken of the cadaver trial, this could be reduced by approximately 10-15 minutes when

using the optical tracking system. This is because the fibula segments can be aligned with respect to each other and secured together with the mini plates all before ischemia time is started. It has been shown in literature that decreasing the ischemia time less than three to five hours does not affect the likelihood of postoperative complications (S. Y. Chang, 2010)(Gürlek, 1997). However, during discussions with the participating surgeon in this study it was noted that working in ischemia time is stressful. Therefore, using a system that generally decreases the ischemia time even by 19% as shown here may provide greater reassurance to the surgeon and potentially reduce the stress cause by operating during ischemia time.

4.1.4 User Feedback

After completion of all reconstruction procedures, a meeting was held with all participants to discuss the usability and functionality of the system as a whole. All users expressed being impressed with the ability of the system to complete a reconstruction and generate a VSP during the surgery without any preplanning required. However, the system is only in initial design stages, and therefore there are a number of improvements that should be made to address the problems and limitations highlighted by the participants.

4.1.4.1 Mandible Registration

The mandible registration process was liked by the participants, who found that the unique points to use for the paired point step were not too difficult to find. However, it was noted that this may become harder where smaller tumors are simulated as a much smaller surface of the mandible will be exposed. This will reduce the option for landmarks for paired point registration as well as reduce the accessible surface available for surface registration. This would be further hindered by the possibility of the tumor damaging the surface of the bone and eroding the surface that is exposed. As the exposed surface is the area where the registration accuracy needs to be highest, when the surface area is smaller the accuracy in the exposed area should

still be acceptable; however, if the bone is damaged, surface registration may not be possible. To investigate this further, a variety of tumor sizes should be simulated and the registration accuracy evaluated.

4.1.4.2 Mandible Resection

Before performing the mandible resection, the system allows the user to visualise the preoperative CT scan using the probe. This visualisation was positively received by all participants and is anticipated to be very helpful during surgery. However, some participants mentioned that if the visualisation were controlled by an optically tracked saw, they thought this would be more beneficial. When the probe is used, the optimal location is found but then the prob is removed to allow the osteotomies to be made. This means the surgeon has to estimate where the probe was at the time of measurement. However, if the saw itself were controlling the visualisation, the optimal location could be found and the osteotomies performed straight away.

4.1.4.3 Fibula Registration

One aspect of the system that was noted by participants was knowing where to place the fibula reference frame. As at this point in the workflow the fibula has not been registered yet, so there is no way to guide the placement of the reference frame. However, it is important that it is placed far enough away from the final segment (the location of which is also not known yet) to stop interference between the final helping hand and the fibula reference frame. Therefore, during the study participants were verbally advised to place the reference frame as proximally as possible however, a visual representation of this on the 3D fibula model may be beneficial to remind users.

It was also noted that one of the most difficult and time-consuming steps in the image-guided workflow was performing the paired-point fibula registration. As the section of viable fibula is

largely uniform along its length, finding distinct points that can be accurately (within 1 cm) located on both the patient and the 3D model is challenging. One factor contributing to this is the orientation of the fibula 3D model on the display. As all the surfaces look similar it can be difficult to determine where a point on the patient anatomy is in correspondence to the 3D model. Therefore, it would be helpful if the 3D model surfaces or ridges were visually distinguishable from each other - for example, if the medial side were green or the anterior ridge were blue etc. Although not helping identify potential registration points, once a point is found on either the model or the patient, this would speed up the process of replication of that point.

Additionally, using the drawing motion to collect surface points on the fibula was challenging due to the higher volume of soft tissue left on the fibula surface. This drawing motion meant that the probe point frequently got stuck on soft tissue, causing it to skip across the surface. It was also difficult to ensure that the point of the probe was resting on the bone directly with no soft tissue in between. Therefore, rather than collecting fiducials every 0.01 s, the module was altered to allow the user to manually place fiducials only when they were sure the probe was on the bone surface. The user would lift the probe off the surface and move it to the next location and then, when ready, use a foot pedal to collect the fiducial.

4.1.4.4 Helping Hand Placement

Although the Helping Hands are currently partially guided into location, it was noted that it may be beneficial to have a more specific guidance method to locate them on the fibula. Especially once dental implants are incorporated into the surgery, the interference between the Helping Hand screw and the dental implant post may become an issue and so a more specific location on the fibula segment would be beneficial.

4.1.4.5 Fibula Osteotomy Guidance

Using the guidance system to make the fibula cuts was also discussed. It was noted that interpreting the guidance visualisation and manipulating the cutting guide was difficult at first. However, it was a quick learning curve and after only a few attempts it became much more intuitive and faster to align the cutting plane to the desired accuracy. The option of adding continuously updating numerical displacement and accuracy measures to the visualisation was suggested to participants. The consensus was that this would not greatly increase the usability of this aspect of the system once the user is efficient at interpreting the guidance module, which as noted above did not take very long, this would generally be ignored and only checked once the user thought they were in good alignment. Alternatively, certain users may be distracted by reducing the visible numerical error to zero adding extensive time to this surgical step when it may not be required. However, it may still be worth adding as it could help users during training and speed up the learning required to efficiently use the guidance system.

The system does currently calculate the error between the placed cutting guide and the target cut plan. However, only when the calculate error button is pressed. Users found this function helpful to verify they were satisfied with the cutting guide location. However, it was noted that a suggested maximum error should also be displayed to help the user decide whether it is worth trying to reposition the guide. Similarly, when the error is computed between the target and actual segment (based on digitised fibula cut planes), the system should advice whether these errors are sufficiently large to warrant recalculating the VSP.

4.1.4.6 Segment Alignment

Finally, when guiding the segments into alignment, all participants agreed that the guided method was preferable. The additional reassurance gained from having the segments guided was beneficial as this meant the user could guide the segments into place but still clinically

evaluate the reconstruction. If, for example, it was deemed clinically beneficial to slightly change the angle of one segment with respect to the other, the effect of this could be virtually observed in the mandible resection gap. Hence, greatly reducing the risk that the full reconstruction once plated together would then not fit in the mandible resection and allowing the surgeon to confidently make this judgment call. Additionally, the guidance system can help determine where trimming should be made to a fibula segment to fit the reconstruction in the resection gap if necessary.

All additional participant observations relating to the device design are discussed in Georgia Grzybowski's thesis(Grzybowski, 2021).

5 Discussion and Conclusions

The studies outlined in this thesis showed that it is possible to perform a mandible reconstruction on-the-fly using an image-guided system. The following chapter outlines the contribution made in developing this system and the limitations of the system. It also outlines two planned future studies as well as suggested developments to be made to the system.

5.1 Thesis Contributions

In collaboration with Georgia Grzybowski, a fully optical tracked workflow and intraoperative system was developed and tested for mandibular reconstruction surgery. The development of the system components was evenly divided between collaborators. All software aspects of the system were developed as part of this thesis while the hardware components were developed by Georgia Grzybowski and outlined in their thesis.

5.1.1.1 System Overview

The developed surgical workflow integrates image guidance into all aspect of mandibular reconstruction surgery. Software modules within the 3D Slicer platform were created to facilitate this. The first module allows the user to register the patient anatomy to the preoperative CT scans using the pair point registration technique followed by a surface registration technique. The following module then creates a visualisation that allows the surgeon to visualise the preoperative mandible CT scan as the tracked probe is moved across the mandible using the optical tracking system. This assists them in deciding where the mandible resection planes should be made during the surgery. The mandible osteotomies are then performed and digitised and a VSP is generated based on this. The VSP module is based on previous work performed by researchers in Dr Eitan Prisman's lab (Luu, 2018). A subsequent module then allows the Helping Hands to be partially guided onto the fibula. The required transforms are then

calculated to allow the individual segments to be tracked once cut from the rest of the viable fibula.

Following this, a visualisation is generated to allow the surgeon to make the required fibula osteotomies using the optically tracked cutting guide. The accuracy achieved when using the optically tracked cutting guide was comparatively assessed against two alternative guidance approaches: (1) using an optically tracked saw and (2) the conventional 3D-printed cutting guides. This study found no significant difference between any of the three cutting methods assessed in terms of accuracy. However, a statistically significant difference between the time per cut was found between all three methods. Although statistically different, this increase in time per cut was not deemed surgically significant.

Additionally, user feedback obtained during this study highlighted the safety concern associated with using the OTS method as it required the user to continually look at the guidance display whist making the cut to ensure the saw remains aligned with the target. Making cuts in this manner poses a serious safety concern for both the surgeon and the patient. For this reason, the optically tracked cutting guide method was fully integrated into the developed system and used for all further testing. The average accuracy achieved when using this method was -0.68 ± 2.66 mm length deviation and 3.68 ± 2.59˚ with an average time per cut was 164 ± 63 seconds.

Once each fibula segment is cut, the surgical plan can be updated to account for any errors made during the cutting process. Following the completion of all the fibula osteotomies, and whilst the segments are still connected to the leg blood supply, the next module creates a visualisation that guides the user to align the fibula segments with respect to each other. Once secured together with miniplates, the final module creates a visualisation to guide the full reconstruction into aligned with respect to the native mandible where it is then secured with miniplates.

We performed a proof of concept study where the system was used to perform five reconstruction procedures on cadaver specimens to evaluate its accuracy on a realistic model. The system was successful at creating a clinically acceptable mandible reconstruction in all five cases without any preplanning required. The accuracy metrics analysed for these procedures were consistently comparable to those reported in literature for the 3D-printed cutting guide method. The time required to complete the procedure using the developed workflow was approximately 30 minutes longer (shortest time per surgical step); however, ischemia time was reduced by approximately 15 minutes.

5.1.1.2 Literature Comparison

A fully image guided workflow has not been previously developed for this type of surgery to the best of our knowledge. A number of studies have looked at using image guidance to perform the mandible osteotomies based on a presurgical plan (X. F. Shan, 2015)(Pietruski, 2019b)(Pietruski, 2016)(Hasan, 2020)(Bernstein, 2017). However, all of these studies use the image guidance to replicate the presurgical planned mandible osteotomies. Our system allows the surgeon to make these cuts on-the-fly and uses the tracking system to digitise where these planes were made so the VSP can be generated intraoperatively.

Only two studies by the same research group have been conducted previously guiding the surgeon in making fibula osteotomies (Pietruski, 2019)(Pietruski, 2019a). Both studies use a similar visualisation system to the one developed in this thesis; however, they directly track the surgical saw as appose to the tracked cutting guide system implemented in our system.

Additionally, image guidance has been shown to help in guiding the placement of the fibula segments in the mandible resection (X. F. Shan, 2015)(Zhu, 2016)(Huang, 2015). These systems use a tracked probe and touch points on the fibula segments to determine their location in the mandible gap. However, our system directly tracks the fibula segments and creates a

visual representation of the reconstruction to allow the surgeon to align the segments with the VSP.

This thesis has highlighted the feasibility of using a fully optically tracked system to perform mandible reconstruction surgery whilst achieving comparable accuracies to the current 3D-printed guide method. By eliminating the need for patient-specific 3D-printed guides, the VSP no longer needs to be generated before surgery and the lead time associated with the design and manufacture of guides is removed. This workflow was also shown to greatly increase the flexibility of implementing the VSP during surgery, allowing it to be updated through the surgery to account for errors or changes in surgical procedure.

5.2 System Limitations

Although eliminating the lead in time and reducing ischemia time, the total surgical time is generally increased which will add additional cost to the surgical procedure. This is partially addressed through performing some steps concurrently. However, there are some restrictions on this when using this system. As the plan is not known until after the mandible osteotomies are completed, no further step after registering the fibula can be commenced until the mandible osteotomies are digitised and the VSP is generated. This leaves the system susceptible to large delays if the initial mandible steps take longer than anticipated.

Although the optical tracking camera is approved for use in an operating room, the software system designed within the 3D Slicer platform is not. As 3D Slicer is an opensource software, it is only possible to use this in the operating room under research expectations. Therefore, if in the future the system was to be commercialised, the software system would need to be moved to a non-opensource platform or a stand-alone software created. Furthermore, the generation of the VSP currently utilises an older version of the system used clinically. This clinical system,

developed in Artisynth, incorporates additional functionality that would remove a number of the manual steps required in the 3D Slicer VSP module to fix the rotation of the fibula segments in the mandible, as well as increase the robustness of updating the VSP.

Additionally, the system has a minimum allowable segment size significantly larger than the current 3D-printed guides techniques. Due to the length of the mini plates and the size of the Helping Hands, each fibula segment must be greater than 28 mm. This reduces how well the reconstruction can conform to the natural mandible contour. It may be possible to use alternative mini plates that still allow two screws to be fixed into each but vertically rather than horizontally. However, these types of plates are not typically used for this type of surgery so may not provide adequate rigidity to hold the reconstruction during healing.

Finally, if the guidance system fails during surgery, the VSP could be generated by manually approximating the location of the mandible cuts in virtual space. However, the fibula cuts could not be guided, nor the alignment of the segments with respect to each other or in the mandible. Both these steps could benefit from visualising the VSP, which for aligning the segments would be like the visual alignment method described previously. However, it would be very difficult to create accurate replicas of the planned segments using this method. Therefore, it may be beneficial to output some numerical length and angle values for each segment when creating the VSP to allow the planned fibula cuts to be replicated more accurately in case of the guidance system failing.

5.3 Future Studies

The Phase One Cadaver Trial showed that using this system to guide all stages of mandibular reconstruction surgery is possible and indicated several areas within the system that should be further developed. The results also strengthen the hypothesis that using optical tracking to

perform an on-the-fly mandible reconstruction surgery greatly increases the flexibility of the procedure whilst improving accuracy and reducing ischemia time. Once these further developments are integrated into the system, two additional studies are planned, which are briefly outlined below. Full ethical approval was applied for and granted for both studies, as well as access to an additional 15 cadavers through the UBC Body Donation Program.

5.3.1 User Study Focused on Usability

The aim of the user study is to gain feedback on the usability of the system compared to the freehand and 3D-printed guide approach. Participants of this study will be residents, fellows and surgeons who took/take part in the Resident Plating Course, an annual educational event organised by Dr. Eitan Prisman. During this course, each participant completes two mandible reconstructions on artificial saw bones, one using the freehand method and one using the 3D-printed guide method. Post reconstruction CT scans of these two reconstructions are obtained along with user feedback in the form of a questionnaire. Participants from this course will be invited back to perform a third reconstruction using the image-guided system, again on artificial saw bones. These will also be CT scanned and an additional survey will be completed. This data, plus the questionnaires and CT scans obtained from the plating course, will allow a direct comparison of accuracy between the three reconstruction methods to be performed for each participant. Approximately 15 participants are expected. The questionnaires will also provide valuable useability feedback and ease of use comparison data between the three reconstruction methods and highlight where the image-guided system may need to be further developed.

5.3.2 Cadaver Trial Phase Two – Combined Assessment of Usability and Accuracy

After any updates have been made to the system following the user study, the system will be more extensively tested on cadavers. This study aims to further test the accuracy and usability of the system on a realistic model across a variety of simulated cases and additional participants. Approval had been granted for five ENT surgeons to perform three reconstructions each using the image-guided system on cadavers (15 total). The reconstructions will simulate three different types and sizes of resection to more robustly test the system. The same metrics will be recorded as in Phase One of the cadaver trial including time. Accuracy will again be measured using a postoperative CT scan. As three times the number of studies will be performed during this trial, statistical analysis should be possible.

5.4 Future Development and Testing

As mentioned above, this system is only in the initial stages of development. Based on the feedback from Phase One of the cadaver study in terms of usability and accuracy, there are few major improvements that should be made to the system before further testing the system. During these future studies, the reliability of the full system, as well as individual components, should be tested as this is part of the research objective but has not yet been evaluated.

The first proposed system improvement is to integrate the 3D Slicer system with the clinically used RDP based VSP generation system in Artisynth. This will allow a VSPs to be generated that better replicated the healthy mandible contour when using the image-guided system. This will also allow the image-guided system to benefit from any improvements made to this clinical VSP generation system as it is continually being developed by Dr Eitan Prisman's research team. This is also the software that the optimisation based VSP generation system is being developed in, so creating a link between Artisynth and 3D Slicer would allow image guided

reconstruction to utilise this advancement. Additionally, this is a much more reliable version of the VSP software than the module in 3D Slicer and should fix the issue with the updating of the VSP as well as remove the manual steps required to generate the VSP using 3D Slicer.

The ability to plan the placement of dental implant posts is in the process of being integrated into the VSP. Thus, it would also be beneficial to add the ability to guide the placement of these posts during surgery. Additionally, one of the big advantages of using image guidance is that theoretically it could be used for any donor bone. Therefore, the system should be updated to generalise the modules to allow this. A list of smaller updates suggested for the modules in outlined in Appendix E:.

In addition to the module updates, one of the major additional sources of error discovered during the cadaver trial was in digitising the actual cut planes. The reason for the higher-than-expected error should be investigated further. An alternative method may also be easier and quicker such as using a tracked flat plate to digitise the planes rather than the probe. Finally, as mentioned in section 4.1.4, a recommendation should be made by the system on whether the segment errors are high enough to warrant recalculating the VSP. However, these limits are not known. The effect of these errors on bony contact, structural integrity and potentially surgical outcomes would be beneficial to investigate to allow a more informed recommendation to be made and incorporated into the modules.

5.5 Concluding Remarks

Mandible reconstruction surgery is notoriously complex. The current surgical approach using a preoperative VSP to create patient-specific 3D-printed cutting guides goes a significant way to reducing this difficulty. However, this technique requires a lead time of up to four weeks. Additionally, once the guides are printed, the VSP cannot be altered as the guides are ridged,

so any required increase in mandible resection, or a change in the surgical plan cannot be accommodated for. This thesis aimed to develop a new surgical workflow and image guidance system to remove this lead in time by eliminating the need for printed cutting guides and generating the VSP intraoperatively. Specifically, this thesis outlines the software system developed for this workflow and verification testing performed.

The system utilises image guidance to move all steps into the operating room. The surgeon exposes the mandible, and using the onscreen visualisation, decides where the mandible should be resected. These cuts are then performed, and their location digitised so the system can generate a virtual surgical plan intraoperatively. To execute this plan, the image guidance system then guides the fibula osteotomies using an optically tracked cutting guide. The VSP can be continually updated throughout this process to account for any error or changes the surgeon might deem beneficial. Finally, the segments can first be guided into place with respect to each other and secured, then after the pedicle is cut this full reconstruction is guided into the mandible and secured.

The accuracy of how well the system can guide the fibula osteotomies was tested on artificial saw bone models. Although increasing the time per cut compared to the 3D-printed guide method, the accuracies achieved were comparable. The full system was then tested on five cadaver specimens to assess its accuracy, usability and efficiency on a more realistic model. Again, the accuracies of the final reconstruction for each metric measured were comparable to the printed cutting guide method, whilst an increase in overall surgical time was observed. However, this may be offset by the complete elimination of the lead in time. Additional studies are planned to further test the usability of the system across more participants as well as on additional cadaver specimens once noted developments are complete.

Although still in early stages of development, the testing performed as part of this thesis only increase the strength of the hypothesis that this system is a viable alternative to patient-specific cutting guides. Whilst allowing for all the benefits of using a VSP to be seen such as higher rates of bony contact and a better coherence with the native mandible contour, this system eliminates many of the issues seen with current surgical techniques such as the long lead in time and inflexibility of the system. The work down for his thesis has highlighted the potential this system has in mandibular reconstruction surgery and positioned the system in a promising position for potential clinical use in the future.

Bibliography

3D Slicer. (2021, August 9). https://www.slicer.org/

Bernstein, J. M., Daly, M. J., Chan, H., Qiu, J., Goldstein, D., Muhanna, N., De Almeida, J. R., & Irish, J. C. (2017). Accuracy and reproducibility of virtual cutting guides and 3D-navigation for osteotomies of the mandible and maxilla. *PLoS ONE*, *12*(3). https://doi.org/10.1371/JOURNAL.PONE.0173111

Breeland, G., Aktar, A., & Patel, B. C. (2021, June 18). *Anatomy, Head and Neck, Mandible*. StatPearls; StatPearls Publishing. https://www.ncbi.nlm.nih.gov/books/NBK532292/

Brown, A., Uneri, A., Silva, T., Manbachi, A., & Siewerdsen, J. (2018). Design and validation of an open-source library of dynamic reference frames for research and education in optical tracking. *Journal of Medical Imaging (Bellingham, Wash.)*, *5*(2), 1. https://doi.org/10.1117/1.JMI.5.2.021215

Chang, E. I., Jenkins, M. P., Patel, S. A., & Topham, N. S. (2016). Long-Term Operative Outcomes of Preoperative Computed Tomography-Guided Virtual Surgical Planning for Osteocutaneous Free Flap Mandible Reconstruction. *Plastic and Reconstructive Surgery*, *137*(2), 619–623. https://doi.org/10.1097/01.PRS.0000475796.61855.A7

Chang, S. Y., Huang, J. J., Tsao, C. K., Nguyen, A., Mittakanti, K., Lin, C. Y., & Cheng, M. H. (2010). Does ischemia time affect the outcome of free fibula flaps for head and neck reconstruction? A review of 116 cases. *Plastic and Reconstructive Surgery*, *126*(6), 1988–1995. https://doi.org/10.1097/PRS.0B013E3181F448C8

Chittaranjan, B., Tejasvi, M. A., Babu, B. B., & Geetha, P. (2014). Intramedullary Osteosarcoma of the Mandible: A Clinicoradiologic Perspective. *Journal of Clinical Imaging Science*, *4*(Suppl 2), 1–5. https://doi.org/10.4103/2156-7514.148273

Davies, J. C., Chan, H. H. L., Yao, C. M. K. L., Ziai, H., Dixon, P. R., Chepeha, D. B., Goldstein, D. P., Almeida, J. R. de, Gilbert, R. W., & Irish, J. C. (2021). Association of Plate Contouring With Hardware Complications Following Mandibular Reconstruction. *The Laryngoscope*. https://doi.org/10.1002/LARY.29706

Disa, J. J. (2009). Mandible Reconstruction. *Head and Neck Reconstruction*, 197–219. https://doi.org/10.1016/B978-0-7020-2926-4.50016-3

Dupret-Bories, A., Vergez, S., Meresse, T., Brouillet, F., & Bertrand, G. (2018). Contribution of 3D printing to mandibular reconstruction after cancer. *European Annals of Otorhinolaryngology, Head and Neck Diseases*, *135*(2), 133–136. https://doi.org/10.1016/j.anorl.2017.09.007

Fedorov, A., Beichel, R., Kalpathy-Cramer, J., Finet, J., Fillion-Robin, J.-C., Pujol, S., Bauer, C., Jennings, D., Fennessy, F., Sonka, M., Buatti, J., Aylward, S., Miller, J. V, Pieper, S., & Kikinis, R. (2012). 3D Slicer as an Image Computing Platform for the Quantitative Imaging Network. *Magnetic Resonance Imaging*, *30*(9), 1323–1341. https://doi.org/10.1016/j.mri.2012.05.001

Fernandes, R. (2007). An Easy Method for Predictable Osteotomies in the Vascularized Fibula Flap for Mandibular Reconstruction. *Journal of Oral and Maxillofacial Surgery*, *65*(9), 1874–

1875. https://doi.org/10.1016/J.JOMS.2006.10.051

Foley, B. D., Thayer, W. P., Honeybrook, A., McKenna, S., & Press, S. (2013). Mandibular Reconstruction Using Computer-Aided Design and Computer-Aided Manufacturing: An Analysis of Surgical Results. *Journal of Oral and Maxillofacial Surgery*, *71*(2), e111–e119. https://doi.org/10.1016/J.JOMS.2012.08.022

Grzybowski, G. (2021). *Development of an Image-Guided Surgical Workflow and Tracked Surgical Tools for Mandibular Reconstruction Surgery*. MASc Thesis, University of British Columbia.

Gürlek, A., Kroll, S. S., & Schusterman, M. A. (1997). Ischemic time and free flap success. *Annals of Plastic Surgery*, *38*(5), 503–505. https://doi.org/10.1097/00000637-199705000-00010

Hanasono, M. M., & Skoracki, R. J. (2013). Computer-assisted design and rapid prototype modeling in microvascular mandible reconstruction. *The Laryngoscope*, *123*(3), 597–604. https://doi.org/10.1002/LARY.23717

Hanken, H., Schablowsky, C., Smeets, R., Heiland, M., Sehner, S., Riecke, B., Nourwali, I., Vorwig, O., Gröbe, A., & Al-Dam, A. (2015). Virtual planning of complex head and neck reconstruction results in satisfactory match between real outcomes and virtual models. *Clinical Oral Investigations*, *19*(3), 647–656. https://doi.org/10.1007/S00784-014-1291-5

Hasan, W., Daly, M. J., Chan, H. H. L., Qiu, J., & Irish, J. C. (2020). Intraoperative cone-beam CT-guided osteotomy navigation in mandible and maxilla surgery. *The Laryngoscope*, *130*(5), 1166–1172. https://doi.org/10.1002/lary.28082

Hidalgo, D. A. (1989). Fibula Free Flap: A New Method of Mandible Reconstruction. *Plastic and Reconstructive Surgery*, *84*(1), 71–79. https://journals.lww.com/plasreconsurg/abstract/1989/07000/fibula_free_flap__a_new_method_of_mandible.14.aspx

Horowitz, G., Warshavsky, A., Fridman, O., Yanko, R., Raiser, V., Gur, E., Fliss, D., & Zaretski, A. (2019). Balsa wood for precise intra-operative bone contouring in fibula free-flap mandible reconstruction. *European Archives of Oto-Rhino-Laryngology : Official Journal of the European Federation of Oto-Rhino-Laryngological Societies (EUFOS) : Affiliated with the German Society for Oto-Rhino-Laryngology - Head and Neck Surgery*, *276*(8), 2339–2343. https://doi.org/10.1007/S00405-019-05496-4

Huang, J.-W., Shan, X.-F., Lu, X.-G., & Cai, Z.-G. (2015). Preliminary clinic study on computer assisted mandibular reconstruction: the positive role of surgical navigation technique. *Maxillofacial Plastic and Reconstructive Surgery 2015 37:1*, *37*(1), 1–7. https://doi.org/10.1186/S40902-015-0017-1

Kakarala, K., Shnayder, Y., Tsue, T. T., & Girod, D. A. (2018). Mandibular reconstruction. *Oral Oncology*. https://doi.org/10.1016/j.oraloncology.2017.12.020

Kazanjian, V. H. (1952). BONE TRANSPLANTING TO THE MANDIBLE. *American Journal of Surgery*.

Kirke, D. N., Owen, R. P., Carrao, V., Miles, B. A., & Kass, J. I. (2016). Using 3D computer planning for complex reconstruction of mandibular defects. *Cancer of the Head and Neck*, *1*(1), 17–17. https://doi.org/10.1186/s41199-016-0019-4

KLS Martin Group. (2019). *L1 ® Mandible ReconGuide* . Gebrüder Martin GmbH & Co. KG. www.klsmartin.com

Kokosis, G., Schmitz, R., Powers, D. B., & Erdmann, D. (2016). Mandibular Reconstruction Using the Free Vascularized Fibula Graft: An Overview of Different Modifications. *Archives of Plastic Surgery*, *43*(1), 3. https://doi.org/10.5999/APS.2016.43.1.3

Kral, F., Freysinger, W., Puschban, E. J., & Riechelmann, H. (2013). Comparison of optical and electromagnetic tracking for navigated lateral skull base surgery ARTICLE in INTERNATIONAL JOURNAL OF MEDICAL ROBOTICS AND COMPUTER ASSISTED SURGERY · JUNE 2013 Impact Factor: 1.53 Comparison of optical and electromagnetic tracki. *INTERNATIONAL JOURNAL OF MEDICAL ROBOTICS AND COMPUTER ASSISTED SURGERY*. https://doi.org/10.1002/rcs.1502

Kumar, B. P., Venkatesh, V., Kumar, K. A. J., Yadav, B. Y., & Mohan, S. R. (2016). Mandibular Reconstruction: Overview. *Journal of Maxillofacial & Oral Surgery*, *15*(4), 425. https://doi.org/10.1007/S12663-015-0766-5

Kumar, V., K, C., S, G., H, A., & A, A. (2017). Advent of Surgical Navigation in Oral and Maxillofacial Surgery and Application of Different Navigational Systems in Various Surgical Procedures: A Review. *JBR Journal of Interdisciplinary Medicine and Dental Science*, *06*(01), 1–5. https://doi.org/10.4172/2376-032x.1000225

Lasso, A., Heffter, T., Rankin, A., Pinter, C., Ungi, T., & Fichtinger, G. (2014). PLUS: Open-source toolkit for ultrasound-guided intervention systems. *IEEE Transactions on Biomedical Engineering*, *61*(10), 2527–2537. https://doi.org/10.1109/TBME.2014.2322864

Lin, P.-Y., Lin, K. C., & Jeng, S.-F. (2011). Oromandibular Reconstruction: The History, Operative Options and Strategies, and Our Experience. *ISRN Surgery*, *2011*, 1–10. https://doi.org/10.5402/2011/824251

Luu, K., Pakdel, A., Wang, E., & Prisman, E. (2018). In house virtual surgery and 3D complex head and neck reconstruction. *Journal of Otolaryngology - Head and Neck Surgery*, *47*(1), 75. https://doi.org/10.1186/s40463-018-0320-9

May, M. M., Howe, B. M., O'Byrne, T. J., Alexander, A. E., Morris, J. M., Moore, E. J., Kasperbauer, J. L., Janus, J. R., Abel, K. M. Van, Dickens, H. J., & Price, D. L. (2021). Short and long-term outcomes of three-dimensional printed surgical guides and virtual surgical planning versus conventional methods for fibula free flap reconstruction of the mandible: Decreased nonunion and complication rates. *Head & Neck*, *43*(8), 2342–2352. https://doi.org/10.1002/HED.26688

Meyer, S., Hirsch, J.-M., Leiggener, C. S., Msallem, B., Sigron, G. R., Kunz, C., & Thieringer, F. M. (2020). Fibula Graft Cutting Devices: Are 3D-Printed Cutting Guides More Precise Than a Universal, Reusable Osteotomy Jig? *Journal of Clinical Medicine*, *9*(4119), 4119. https://doi.org/10.3390/JCM9124119

Moro, A., Cannas, R., Boniello, R., Gasparini, G., & Pelo, S. (2009). Techniques on modeling the vascularized free fibula flap in mandibular reconstruction. *Journal of Craniofacial Surgery*, *20*(5), 1571–1573. https://doi.org/10.1097/SCS.0B013E3181B0DB5C

Nakayama, B., Kamei, Y., Ikuo, H., Hasegawa, Y., Kitano, H., & Torii, S. (2006). Free fibula bone wedge technique for mandible reconstruction using fibula osteocutaneous flaps. *Plastic and Reconstructive Surgery*, *117*(6), 1980–1985. https://doi.org/10.1097/01.PRS.0000210013.80850.27

Naujokat, H., Rohnen, M., Lichtenstein, J., Birkenfeld, F., Gerle, M., Flörke, C., & Wiltfang, J. (2017). Computer-assisted orthognathic surgery: evaluation of mandible registration accuracy and report of the first clinical cases of navigated sagittal split ramus osteotomy. *International Journal of Oral and Maxillofacial Surgery*, *46*(10), 1291–1297. https://doi.org/10.1016/j.ijom.2017.05.003

Northern Digital Inc. (2020). *Polaris Vega ST - NDI*. https://www.ndigital.com/products/polaris-vega/polaris-vega-st/

Northern Digital Inc. (2020). *Polaris Vega User Guide for ST , VT, and XT Models*. *5*.

Numajiri, T., Nakamura, H., Sowa, Y., & Nishino, K. (2016). Low-cost design and manufacturing of surgical guides for mandibular reconstruction using a fibula. *Plastic and Reconstructive Surgery - Global Open*, *4*(7). https://doi.org/10.1097/GOX.0000000000000682

Pietruski, P., Majak, M., Swiatek-Najwer, E., Popek, M., Szram, D., Zuk, M., & Jaworowski, J. (2016). Accuracy of experimental mandibular osteotomy using the image-guided sagittal saw. *International Journal of Oral and Maxillofacial Surgery*, *45*(6), 793–800. https://doi.org/10.1016/j.ijom.2015.12.018

Pietruski, P., Majak, M., Świątek-Najwer, E., Żuk, M., Popek, M., Mazurek, M., Świecka, M., & Jaworowski, J. (2019a). Navigation-guided fibula free flap for mandibular reconstruction: A proof of concept study. *Journal of Plastic, Reconstructive and Aesthetic Surgery*, *72*(4), 572–580. https://doi.org/10.1016/j.bjps.2019.01.026

Pietruski, P., Majak, M., Świątek-Najwer, E., Żuk, M., Popek, M., Mazurek, M., Świecka, M., & Jaworowski, J. (2019b). Supporting mandibular resection with intraoperative navigation utilizing augmented reality technology – A proof of concept study. *Journal of Cranio-Maxillofacial Surgery*, *47*(6), 854–859. https://doi.org/10.1016/j.jcms.2019.03.004

Pietruski, P., Majak, M., Świątek-Najwer, E., Żuk, M., Popek, M., Jaworowski, J., & Mazurek, M. (2019). Supporting fibula free flap harvest with augmented reality: A proof-of-concept study. *The Laryngoscope*, 1–7. https://doi.org/10.1002/lary.28090

Powcharoen, W., Yang, W. F., Yan Li, K., Zhu, W., & Su, Y. X. (2019). Computer-Assisted versus Conventional Freehand Mandibular Reconstruction with Fibula Free Flap: A Systematic Review and Meta-Analysis. *Plastic and Reconstructive Surgery*, *144*(6), 1417–1428. https://doi.org/10.1097/PRS.0000000000006261

Shan, X.-F., Chen, H.-M., Liang, J., Huang, J.-W., Zhang, L., Cai, Z.-G., Shan, X.-F., Chen, H.-M., Huang, J.-W., Cai, Z.-G., & Guo, C. (2016). Surgical navigation-assisted mandibular reconstruction with fibula flaps. *Int. J. Oral Maxillofac. Surg*, *45*, 448–453.

https://doi.org/10.1016/j.ijom.2015.08.1006

Shan, X. F., Chen, H. M., Liang, J., Huang, J. W., Zhang, L., Cai, Z. G., & Guo, C. (2015). Surgical navigation-assisted mandibular reconstruction with fibula flaps. *International Journal of Oral and Maxillofacial Surgery*, *45*(4), 448–453. https://doi.org/10.1016/j.ijom.2015.08.1006

Shenaq, D. S., & Matros, E. (2018). Virtual planning and navigational technology in reconstructive surgery. *Journal of Surgical Oncology*, *118*(5), 845–852. https://doi.org/10.1002/JSO.25255

Sorriento, A., Porfido, M., Mazzoleni, S., Calvosa, G., Tenucci, M., Ciuti, G., & Dario, P. (2020). Optical and Electromagnetic Tracking Systems for Biomedical Applications: A Critical Review on Potentialities and Limitations. *IEEE Reviews in Biomedical Engineering*, *13*, 212–232. https://doi.org/10.1109/RBME.2019.2939091

Strackee, S. D., Kroon, F. H. M., Spierings, P. T. J., & Jaspers, J. E. N. (2004). Development of a Modeling and Osteotomy Jig System for Reconstruction of the Mandible with a Free Vascularized Fibula Flap. *Plastic and Reconstructive Surgery*, *114*(7), 1851–1858. https://doi.org/10.1097/01.PRS.0000142766.26117.5B

Strackee, S., Kroon, F., Jaspers, J., & Bos, K. (2001). Modeling a fibula transplant in mandibular reconstructions: evaluation of the effects of a minimal number of osteotomies on the contour of the jaw. *Plastic and Reconstructive Surgery*, *108*(7), 1915–1921. https://doi.org/10.1097/00006534-200112000-00010

Succo, G., Berrone, M., Battiston, B., Tos, P., Goia, F., Appendino, P., & Crosetti, E. (2014). Step-by-step surgical technique for mandibular reconstruction with fibular free flap: application of digital technology in virtual surgical planning. *European Archives of Oto-Rhino-Laryngology 2014 272:6*, *272*(6), 1491–1501. https://doi.org/10.1007/S00405-014-3078-3

Tokuda, J., Fischer, G. S., Papademetris, X., Yaniv, Z., Ibanez, L., Cheng, P., Liu, H., Blevins, J., Arata, J., Golby, A. J., Kapur, T., Pieper, S., Burdette, E. C., Fichtinger, G., Tempany, C. M., & Hata, N. (2009). OpenIGTLink: an open network protocol for image-guided therapy environment. *The International Journal of Medical Robotics and Computer Assisted Surgery*, *5*(4), 423–434. https://doi.org/10.1002/RCS.274

Torroni, A., Marianetti, T. M. atte., Romandini, M., Gasparini, G., Cervelli, D., & Pelo, S. (2015). Mandibular reconstruction with different techniques. *The Journal of Craniofacial Surgery*, *26*(3), 885–890. https://doi.org/10.1097/SCS.0000000000001411

Ungi, T., Lasso, A., & Fichtinger, G. (2016). Open-source platforms for navigated image-guided interventions. *Medical Image Analysis*, *33*, 181–186. https://doi.org/10.1016/J.MEDIA.2016.06.011

Wang, E., Durham, J. S., Anderson, D. W., & Prisman, E. (2020). Clinical evaluation of an automated virtual surgical planning platform for mandibular reconstruction. *Head & Neck*, *42*(12), 3506–3514. https://doi.org/10.1002/HED.26404

Wang, W. H., Zhu, J., Deng, J. Y., Xia, B., & Xu, B. (2013). Three-dimensional virtual

technology in reconstruction of mandibular defect including condyle using double-barrel vascularized fibula flap. *Journal of Cranio-Maxillofacial Surgery*, *41*(5), 417–422. https://doi.org/10.1016/J.JCMS.2012.11.008

Wang, Y. Y., Zhang, H. Q., Fan, S., Zhang, D. M., Huang, Z. Q., Chen, W. L., Ye, J. T., & Li, J. S. (2016). Mandibular reconstruction with the vascularized fibula flap: comparison of virtual planning surgery and conventional surgery. *International Journal of Oral and Maxillofacial Surgery*, *45*(11), 1400–1405. https://doi.org/10.1016/J.IJOM.2016.06.015

Weitz, J., Bauer, F. J. M., Hapfelmeier, A., Rohleder, N. H., Wolff, K. D., & Kesting, M. R. (2016). Accuracy of mandibular reconstruction by three-dimensional guided vascularised fibular free flap after segmental mandibulectomy. *British Journal of Oral and Maxillofacial Surgery*, *54*(5), 506–510. https://doi.org/10.1016/J.BJOMS.2016.01.029

Wilde, F., Hanken, H., Probst, F., Schramm, A., Heiland, M., & Cornelius, C.-P. (2015). Multicenter study on the use of patient-specific CAD/CAM reconstruction plates for mandibular reconstruction. *International Journal of Computer Assisted Radiology and Surgery 2015 10:12*, *10*(12), 2035–2051. https://doi.org/10.1007/S11548-015-1193-2

Yaniv, Z. (2015). Which pivot calibration? *Medical Imaging 2015: Image-Guided Procedures, Robotic Interventions, and Modeling*, *9415*, 941527. https://doi.org/10.1117/12.2081348

Zavattero, E., Garzino-Demo, P., Fasolis, M., & Ramieri, G. (2015). To computer-aided design and manufacturing or not to computer-aided design and manufacturing? Free fibula flap with computer-aided technique for mandibular reconstruction. *The Journal of Craniofacial Surgery*, *26*(3), e206–e209. https://doi.org/10.1097/SCS.0000000000001431

Zhu, J. H., Deng, J., Liu, X. J., Wang, J., Guo, Y. X., & Guo, C. Bin. (2016). Prospects of Robot-Assisted Mandibular Reconstruction with Fibula Flap: Comparison with a Computer-Assisted Navigation System and Freehand Technique. *Journal of Reconstructive Microsurgery*, *32*(9), 661–669. https://doi.org/10.1055/s-0036-1584805

Appendices

Appendix A: Image-guided Surgery Surgical Steps

A.1 Tool Set Up

1) Using NDI Track Software, or the build in 3D Slicer Module, calibrate the NDI Probe via pivot calibration.
    a) Visually check calibration by pivoting the probe around its point and check the point of the probe model is the point of rotation.
2) Register Helping Hands and Cutting Guide (this step should only need to be performed once unless reference frames removed) using paired point registration.
    a) Place three corresponding fiducials on the virtual model and then on the Helping Hand Surface (Helping Hands were manufactured with specific divot on the surface to use as registration points).
    b) Visually check registration using probe to touch distinct points.
3) Perform saw calibration (if a guided saw is being used).
    a) Using the probe place three fiducials on the top surface of the saw blade and run the calibration algorithm in Mandible Reconstruction: Calibration and Registration Module

A.2 Mandible Set Up and Registration

4) Expose the mandible.
5) Attach the mandible fixator to either side of the mandible tumour leaving enough space for a mini plate to be attached to the native mandible after resection.
    a) Visually check the bone pins are engaged and secure on the surface of the mandible.
6) Position the fixator arms and lock the mandible fixator using the attached cam lock
7) Perform an initial mandible registration using paired point within the Mandible Reconstruction: Calibration and Registration Module

a) Place three corresponding fiducials on the virtual model and then on the mandible surface. (Ensure error is less than 10 mm)

8) Perform a surface mandible registration within the Mandible Reconstruction: Calibration and Registration Module.
   a) By drawing on the surface of the mandible with the probe, collect at least 75 surface points then run the surface registration algorithm. (Ensure error less than 1 mm)

A.3 Mandible Osteotomies

9) Move the probe over the surface of the mandible to visualise the preoperative CT and decides where the mandible osteotomies should be performed.
10) Using a surgical saw, make the mandible cuts in the desired locations and extract resected area.
11) Using the probe, digitise 3 points on each cut plane to calculate the cut plane location and angle using the Mandible Reconstruction: Mandible Osteotomies Module

A.4 Fibula Registration

12) Expose the fibula bone and elevate the viable fibula bone from the leg, leaving at least 5cm proximal and distal from the joints.
13) Attach the fibula bone clamp (and connected marker array) to the most proximal end of the viable fibula ensuring all pins are engaged with the fibula surface.
14) Perform an initial fibula registration using paired point within the Mandible Reconstruction: Calibration and Registration Module
   a) Place three corresponding fiducials on the virtual model and then on the fibula surface. (Ensure error is less than 10 mm)
15) Visually check the accuracy of the initial registration.

16) Perform a surface fibula registration within the Mandible Reconstruction: Calibration and Registration Module.
    a) By drawing on the surface of the fibula with the probe, collect at least 75 surface points then run the surface registration algorithm. (Ensure error less than 1 mm)
17) Visually check the final registration accuracy.

A.5 Generate VSP

18) Using the Mandible Reconstruction: Generate VSP Module, place a fiducial on the distal end of the viable fibula.
19) Adjust and surgical variables such as minimum segment length and maximum number of segments.
20) Generate the VSP

A.6 Fibula Osteotomies

21) Align the helping hands within their associated fibula segment using the visualisation and secure then place.
22) Align the cutting guide with the first fibula osteotomy plane, calculate the alignment accuracy and once sufficient, make the cut.
23) Once the first segment is fully cut, using the probe digitise three fiducials on each cut surface and the Mandible Reconstruction: Fibula Segment Creation Module will generate a model if the actual fibula segment.
24) The accuracy of this is outputted and if necessary, the VSP can be recalculated within the Mandible Reconstruction: Fibula Segment Creation Module
25) The above three steps are repeated until all fibula segments are created, and their actual models produced.

A.7 Segment Alignment

26) Roughly align the segments with respect to each other to ensure the position is suitable for guided alignment.
27) Using the visualisation created by the Mandible Reconstruction: Fibula Segment Alignment Module, align the fibula segments with respect to each other.
28) Once aligned, secure then together with mini plates
29) Remove all Helping Hands except Hand 2.
30) Swap the Hand 2 marker array position.
31) Cut the pedicle.
32) Move the fibula segment reconstruction up into the mandible workspace.
33) Using the visualisation created by the Mandible Reconstruction: Fibula Segment Alignment Module, align the full segment reconstruction with respect to the native mandible.
34) Secure the reconstruction to the mandible using miniplates.

Remove all hardware from the mandible reconstruction.

Appendix B: Workflow Testing Observations and Associated Module Updates

Observation	Added Function	Module Affected
Sometimes difficult to know if the marker arrays are visible	Warning banner appears when relevant marker arrays are not visible	All
Would be good to be able to change the contour before generating the VSP	Added a step in the module that shows the contour an allows it to be changed	Mandible Osteotomy
Difficult to align the fibula segments based on the segment model alone	An axis model was attached to each segment model	Fibula Segment Alignment
Fibula segments rotated with respect to each other	Added additional fiducials to the fibula modes to rotate the segments into alignment	VSP Generation
Difficult to keep fibula marker array in view when aligning segments with respect to each other	Changed to align segments to Hand 2 marker array instead of fibula marker array.	Fibula Segment Alignment
Difficult to ensure the probe continually remains on the bone surface when collecting surface points.	Add the ability to stop automatically collecting surface points.	Calibration and Registration
Errors made when cutting the fibula segments compound.	Update the VSP after each segment based on the actual fibula cuts.	Fibula Segment Creation
Placing the helping hand individually before osteotomies are mead is time consuming	Place all helping hands at the beginning and then make all the cuts.	Fibula Segment Creation
Many steps not clear how to interact with the module.	Additional instructions added to the user interface.	All

Observation	Added Function	Module Affected
Fiducial can be move one placed by accident	Lock all fiducials once placed.	All
Difficult to tell how off the cut plane is from the target.	Numerical calculation of this error added and displayed on user interface.	Fibula Segment Creation
Performing mandible registration directly followed by fibula registration could be problematic in terms of surgical workflow.	Change the module order so all mandible steps are completed before fibula registration.	Calibration and Registration Mandible Osteotomy
Accessing the fibula cut plane without moving the segment away from the mandible is very hard.	Place actual cut fiducials in terms of the hand marker array.	Fibula Segment Creation

Appendix C: Cadaver Trial Phase One Accuracy Results

C.1 General Accuracy Results

Accuracy Matric	Freehand		Guided		
Specimen Number	2554	2542	2540	2538	2539
Plan Updated	Yes	No	Yes	No	No
Plan Intercoronoid Width:	99.62	91.32	114.76	107.07	93.93
Actual Intercoronoid Width	101.18	90.33	113.92	105.77	95.00
Difference in Intercoronoid Width	1.56	-0.99	-0.84	-1.30	1.07
Plan Interangle Width	98.90	97.71	102.48	103.45	95.50
Actual Interangle Width	98.01	96.75	102.57	102.59	93.82
Difference in Interangle Width	-0.89	-0.97	0.09	-0.87	-1.68
Plan Mandible Projection	90.56	98.65	87.17	90.46	89.53
Actual Mandible Projection	89.95	100.03	85.72	93.19	88.33
Difference in Mandible Projection	-0.61	1.37	-1.45	2.73	-1.20
Distance Between Projection Points	3.97	7.87	3.69	5.01	3.89
Fiducial Registration Accuracy (Mand)	0.69	0.49	0.70	0.67	1.07
Fiducial Registration Accuracy (Fib)	2.71	3.36	1.28	2.35	2.53
ICP Accuracy	0.43	0.91	0.65	0.63	0.59

Accuracy Matric	Freehand		Guided		
Full Model Dice Score	0.87	0.69	0.90	0.83	0.72
Fib Model Dice Score (MandReg)	0.76	0.52	0.85	0.68	0.67
Fib Model Dice Score (FibReg)	0.81	0.69	0.88	0.87	0.80
Full Model 95 Hausdorff Distance	1.97	11.22	6.97	2.20	14.07
Full Model 50 Hausdorff Distance	0.62	1.99	1.19	0.80	2.83
Fib (MandReg) 95 Hausdorff Distance	2.87	6.76	1.75	3.62	3.28
Fib (MandReg) 50 Hausdorff Distance	1.25	2.55	0.78	1.55	1.47
Fib (FibReg) 95 Hausdorff Distance	2.35	3.80	1.62	2.03	2.18
Fib (FibReg) 50 Hausdorff Distance	0.93	1.60	0.62	0.65	0.91
Average Plate Distance	0.13	0.63	0.40	0.22	0.65
Minimum Plate Distance	0.02	0.20	0.06	0.00	0.11
Maximum Plate Distance	0.35	1.19	0.90	0.50	1.69
Mandible Cut 1 Offset	1.56	4.99	0.65	2.17	1.05
Mandible Cut 2 Offset	2.45	5.71	0.58	1.76	1.42
Mandible Cut 1 Angle Error	1.78	8.56	1.43	5.02	4.29
Mandible Cut 2 Angle Error	5.61	6.51	4.09	3.43	1.76

C.2 Fibula Osteotomy Accuracy Results

Freehand 1		Plan	Digitised	Actual	Plan/Actual	Digitised/Actual
Length	Seg1	36.54	35.94	30.41	-6.12	-5.53
	Seg2	24.90	28.63	27.80	2.91	-0.83
	Seg3	30.21	-	28.80	-1.41	-
	Average				0.75	-0.83
Angle	Seg1	161.06	154.81	155.93	5.13	1.12
	Seg2	135.13	139.20	141.87	6.74	2.67
	Seg3	142.48	-	139.33	3.15	-
	Average				4.94	2.67
	Cut 1	158.19	160.45	173.98	15.78	13.53
	Cut 2	24.57	33.64	27.10	2.52	6.54
	Cut 3	165.17	168.49	168.54	3.37	0.05
	Cut 4	30.19	29.29	26.68	3.52	2.61
	Cut 5	148.43	-	145.64	2.78	-
	Cut 6	8.64	-	11.66	3.02	-
	Average				3.04	5.69

Freehand 2		Plan	Digitised	Actual	Plan/Actual	Digitised/Actual
Length	Seg1	45.04	45.21	44.51	-0.53	-0.71
	Seg2	31.69	32.80	30.98	-0.71	-1.82
	Seg3	41.89	41.74	41.21	-0.68	-0.53
	Average				**-0.70**	**-1.17**
Angle	Seg1	151.13	149.27	147.89	3.24	1.38
	Seg2	120.08	123.79	121.56	1.48	2.24
	Seg3	148.14	140.96	147.38	0.76	6.42
	Average				**1.12**	**4.33**
	Cut 1	159.60	163.45	164.20	4.61	0.75
	Cut 2	31.92	28.49	35.03	3.11	6.54
	Cut 3	147.07	143.16	146.29	0.79	3.12
	Cut 4	27.01	20.34	25.58	1.44	5.24
	Cut 5	151.52	143.84	151.94	0.43	8.10
	Cut 6	8.84	10.67	4.69	4.15	5.99
	Average				**1.98**	**5.80**

Guided 1		Plan	Digitised	Actual	Plan/Actual	Digitised/Actual
Length	Seg1	32.60	31.47	33.47	0.87	2.00
	Seg2	49.65	44.56	47.37	-2.28	2.81
	Seg3	-	-	-	-	-
	Average				-0.71	2.40
Angle	Seg1	139.98	138.11	141.71	1.73	3.60
	Seg2	101.23	97.99	97.38	3.85	0.61
	Seg3	-	-	-	-	-
	Average				2.79	2.10
	Cut 1	165.90	164.87	166.47	0.57	1.60
	Cut 2	25.94	27.03	24.76	1.17	2.27
	Cut 3	127.71	126.15	125.31	2.40	0.84
	Cut 4	27.55	28.86	28.93	1.38	0.07
	Cut 5	-	-	-	-	-
	Cut 6	-	-	-	-	-
	Average				1.38	1.20

Guided 2		Plan	Digitised	Actual	Plan/Actual	Digitised/Actual
Length	Seg1	34.77	33.62	33.47	-1.30	-0.15
	Seg2	28.32	30.15	27.27	-1.05	-2.88
	Seg3	39.82	41.41	38.86	-0.95	-2.55
	Average				-1.10	-1.86
Angle	Seg1	138.89	-	142.74	3.85	-
	Seg2	126.88	136.32	128.36	1.48	7.97
	Seg3	158.06	162.81	160.59	2.54	2.22
	Average				2.62	5.09
	Cut 1	171.15	-	174.64	3.49	-
	Cut 2	33.22	-	32.30	0.91	-
	Cut 3	147.54	146.32	147.38	0.16	1.06
	Cut 4	20.87	11.44	19.35	1.52	7.91
	Cut 5	161.50	162.99	161.29	0.22	1.71
	Cut 6	8.94	5.55	5.29	3.65	0.25
	Average				1.66	2.73

Trial Run		Plan	Actual	Plan/Actual
Length	Seg1	26.15	23.74	-2.41
	Seg2	27.33	27.27	-0.05
	Seg3	33.38	33.68	0.30
	Average			0.12
Angle	Seg1	142.90	162.43	19.53
	Seg2	128.44	129.48	1.05
	Seg3	141.03	137.08	3.95
	Average			2.50
	Cut 1	162.39	167.83	5.44
	Cut 2	19.58	10.85	8.72
	Cut 3	157.83	159.46	1.63
	Cut 4	30.16	31.84	1.68
	Cut 5	150.29	148.53	1.76
	Cut 6	9.31	11.56	2.25
	Average			3.21

Appendix D: Detailed Time Map of New and Existing Surgical Workflows

D.1 Average Cadaver Study Time Map

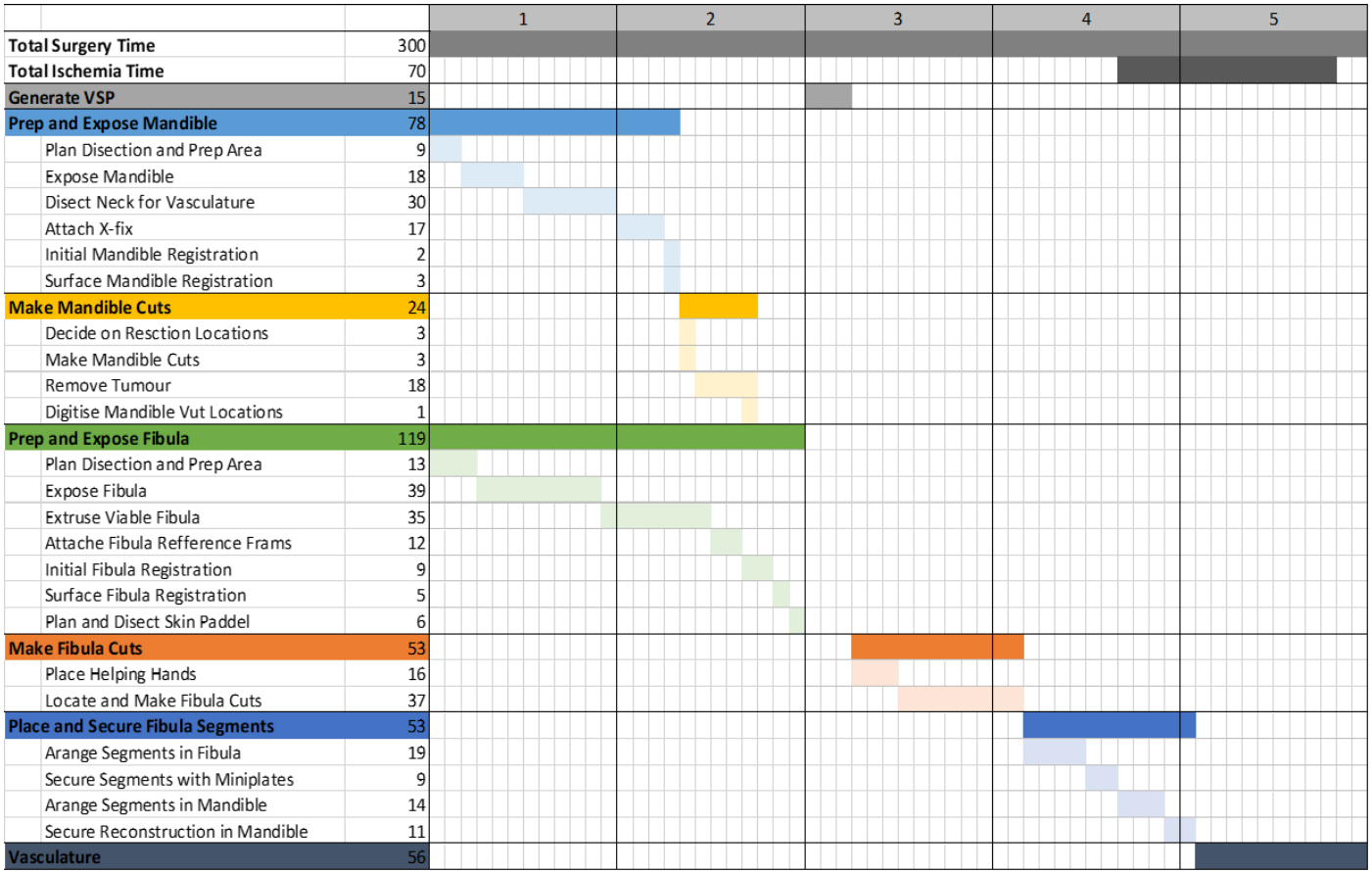

D.2 Shortest Time Cadaver Study Time Map

		1	2	3	4
Total Surgery Time	184				
Total Ischemia Time	60				
Generate VSP	15				
Prep and Expose Mandible	63				
Plan Disection and Prep Area	9				
Expose Mandible	18				
Disect Neck for Vasculature	30				
Attach X-fix	4				
Initial Mandible Registration	1				
Surface Mandible Registration	1				
Make Mandible Cuts	22				
Decide on Resction Locations	2				
Make Mandible Cuts	1				
Remove Tumour	18				
Digitise Mandible Vut Locations	1				
Prep and Expose Fibula	106				
Plan Disection and Prep Area	13				
Expose Fibula	39				
Extruse Viable Fibula	35				
Attache Fibula Refference Frams	6				
Initial Fibula Registration	5				
Surface Fibula Registration	2				
Plan and Disect Skin Paddel	6				
Make Fibula Cuts	22				
Place Helping Hands	11				
Locate and Make Fibula Cuts	11				
Place and Secure Fibula Segments	53				
Arange Segments in Fibula	7				
Secure Segments with Miniplates	4				
Arange Segments in Mandible	11				
Secure Reconstruction in Mandible	7				
Vasculature	56				

D.3 Patient-Specific Guide Time Map

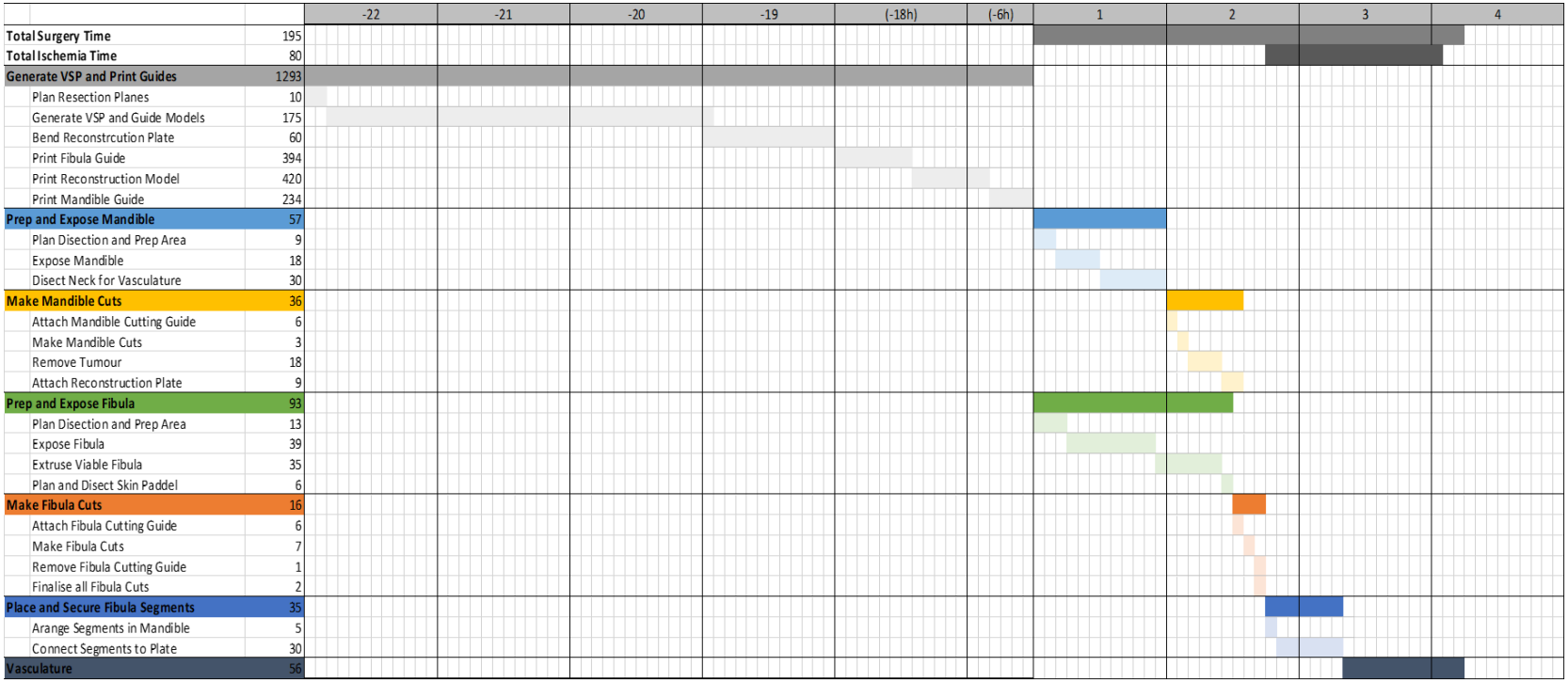

Appendix E: Suggested Module Updates

1. Show error of angle/displacement live in each anatomical plane (may not be needed based on user feedback from cadaver study)
2. When aligning at fibula show the mandible model for context and to help gauge deviating from plan
3. Update planned segments in mandible to reflect how segments were placed in fibula
4. Guide placement of helping hands
5. Add bin icon to delete last fid or hold to delete all fids in list
6. Add button to check angle and length deviation guiding segment placement
7. Stop the CT rotating on the red slice when looking on the mandible
8. Add rules of thumb to hand placement module
9. Add additional instructions to registration steps